The International Journal of Advanced Manufacturing Technology (2024) 131:3113–3164
https://doi.org/10.1007/s00170-022-10767-2

APPLICATION

Nanofluids application in machining: a comprehensive review

Xiaoming Wang[1] · Yuxiang Song[1] · Changhe Li[1] · Yanbin Zhang[2] · Hafiz Muhammad Ali[3] · Shubham Sharma[4] · Runze Li[5] · Min Yang[1] · Teng Gao[1] · Mingzheng Liu[1] · Xin Cui[1] · Zafar Said[6] · Zongming Zhou[7]

Received: 14 November 2022 / Accepted: 22 December 2022 / Published online: 4 January 2023

Abstract

Nanofluids are efficient heat transfer media that have been developed over the past 27 years and have been widely used in the electronic microchannel, engine, spacecraft, nuclear, and solar energy fields. With the high demand for efficient lubricants in manufacturing, the application of nanofluids in machining has become a hot topic in academia and industry. However, in the context of the huge amount of literature in the past decade, existing review cannot be used as a technical manual for industrial applications. There are many technical difficulties in establishing a mature production system, which hinder the large-scale application of nanofluids in industrial production. The physicochemical mechanism underlying the application of nanofluids in machining remains unclear. This paper is a complete review of the process, device, and mechanism, especially the unique mechanism of nanofluid minimum quantity lubrication under different processing modes. In this paper, the preparation, fluid, thermal, and tribological properties of nanofluids are reviewed. The performance of nanofluids in machining is clarified. Typically, in friction and wear tests, the coefficient of friction of jatropha oil-based alumina nanofluids is reduced by 85% compared with dry conditions. The cutting fluid based on alumina nanoparticles improves the tool life by 177–230% in hard milling. The addition of carbon nanotube nanoparticles increases the convective heat transfer coefficient of normal saline by 145.06%. Furthermore, the innovative equipment used in the supply of nanofluids is reviewed, and the atomization mechanisms under different boundary conditions are analyzed. The technical problem of parameterized controllable supply system is solved. In addition, the performance of nanofluids in turning, milling, and grinding is discussed. The mapping relationship between the nanofluid parameters and the machining performance is clarified. The flow field distribution and lubricant wetting behavior under different tool-workpiece boundaries are investigated. Finally, the application prospects of nanofluids in machining are discussed. This review includes a report on recent progress in academia and industry as well as a roadmap for future development.

Keywords Nanofluids · Machining · Turning · Milling · Grinding · Minimum quantity lubrication

Abbreviations

MQL	Minimum quantity lubrication
NMQL	Nanofluid minimum quantity lubrication
SEM	Scanning electron microscopy
EDS	Energy dispersive spectrometer
SDBS	Sodium dodecyl benzene sulphonate
GA	Gum Arabic
SDS	Sodium dodecyl sulfate
TX100	Triton X100
CTAB	Cetyltrimethylammonium bromide

✉ Changhe Li
sy_lichanghe@163.com

✉ Yanbin Zhang
zhangyanbin1_qdlg@163.com

[1] School of Mechanical and Automotive Engineering, Qingdao University of Technology, Qingdao 266520, China

[2] State Key Laboratory of Ultra-Precision Machining Technology, Department of Industrial and Systems Engineering, The Hong Kong Polytechnic University, Hong Kong, China

[3] Mechanical Engineering Department, King Fahd University of Petroleum and Minerals, Dhahran 31261, Saudi Arabia

[4] Department of Mechanical Engineering, IK Gujral Punjab Technical University, Punjab 144603, India

[5] Department of Biomedical Engineering, University of Southern California, Los Angeles, CA 90089–1111, USA

[6] College of Engineering, University of Sharjah, 27272 Sharjah, United Arab Emirates

[7] Hanergy (Qingdao) Lubrication Technology Co., Ltd., Qingdao 266100, China

COF Coefficient of friction
CHTC Convective heat transfer coefficient

1 Introduction

In the context of energy shortages, it is imperative to increase the research and development of advanced energy-saving and environmental protection technologies. Influenced by the laws and policies of green development and the growing concept of sustainability, traditional cutting manufacturing must be transformed [1–3]. Low-carbon manufacturing and clean production facing the transformation of old and new kinetic energy and global sustainable development are imperative [4, 5]. Sustainable cutting technology based on cutting fluid reduction has been proposed [6, 7]. Implement a strategy of sustainable manufacturing to ensure that the manufacturing cycle is critical for the effective use of available resources [8]. Furthermore, human health is widely concerned [9]. However, more than 85% of the cutting fluids in the manufacturing industry are mineral-based oils, which have high carcinogenicity, resulting in a contradiction between human health and the improvement of lubrication efficiency. As shown in Fig. 1, there are many defects in traditional machining, such as environmental pollution, human health threats, and high cost. With the enhancement of environmental protection awareness, the traditional flooding cooling and lubrication method of metal cutting fluids is strictly restricted by laws and policies [10]. The cheap advantage of cutting fluid no longer exists with further research on new sustainable cutting technologies [11]. Therefore, the use of large amounts of cutting fluid has become an obstacle to the development of the manufacturing industry and sustainable manufacturing.

In the 1990s, dry cutting technology was widely used in academia and industry [12]. The application of dry cutting in machining provides new prospects for sustainable technology. This process eliminates the use and treatment cost of the cutting fluid because of the rejection of the lubrication medium in the processing process [13–15]. Dry cutting technology has gradually been promoted as a processing technology to realize clean production. However, new and higher requirements have been proposed for cutting tools, machining parameters, and the rigidity and precision of machine tools [16–18]. Owing to the lack of cooling and lubricating media in the cutting area, tools are easy to wear along with high-temperature, high-pressure, and high-speed solid friction at the interface of the tool-workpiece and tool-chip [19, 20]. Even the machined workpiece material adheres to the tool surface, thereby reducing the surface quality of the machined parts [21]. Therefore, dry cutting cannot guarantee the geometric tolerance and surface integrity of parts in the machining of some efficient machining parameters and difficult materials. Moreover, it is difficult to ensure machining efficiency owing to the strict constraints in the engineering manufacturing cycle. Cryogenic cooling technology is a processing method that sprays a cryogenic medium to the cutting area to provide a cooling effect [22]. The effective area and temperature difference of the heat dissipation expands. Thus, the temperature of the cutting zone is reduced, and the tool life is increased [23]. Cryogenic cooling is a green-machining method. A self-lubricating tool means that the tool has antifriction, wear resistance, and lubrication functions [24]. It can achieve low-wear cutting without the addition of an additional lubricant. A solid lubricant is coated and combined on the tool surface to form a solid lubricating film, which can play a lubricating role. The application of self-lubricating tools can save cooling and lubricating systems, reduce investment in equipment, and avoid environmental pollution from the cutting fluid.

Minimum quantity lubrication (MQL) is a sustainable cutting lubrication method in which a small amount of liquid lubrication medium (usually less than 100 mL/h) is atomized by a certain pressure of gas into micrometer droplets and then transported to the cutting zone through a nozzle. Consequently, the tool-workpiece and tool-chip friction interfaces are fully lubricated under the motion of the microdroplets [25–27]. Therefore, the tool friction and wear and the temperature of the cutting zone are significantly reduced, and the production cost of the parts is reduced. Researchers have

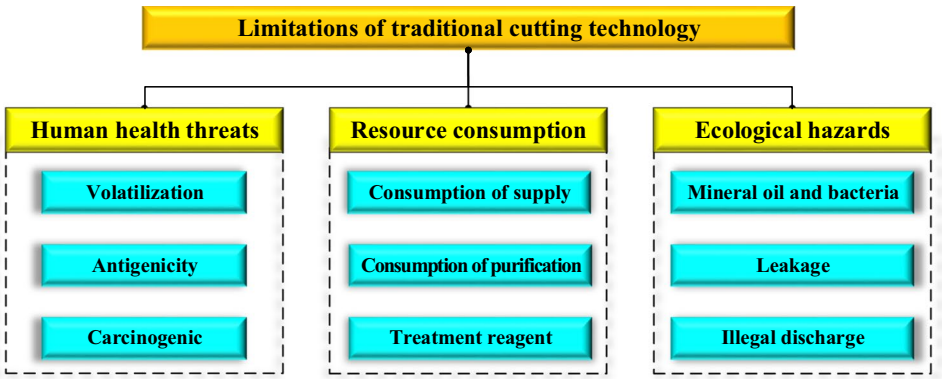

Fig. 1 Defects of the traditional cutting method

attempted to use vegetable oil as a lubricant to spray the friction interface [28, 29]. Effective lubrication of the friction interface in the cutting area is ensured, and adverse effects on the environment and human health are eliminated [30]. The lubrication medium consumed by MQL is less than 10% of the traditional cutting fluid supply and ensures the finish of the tool and workpiece surface after cutting. The MQL supply device can be flexibly arranged near the cutting machine tool and is suitable for various cutting conditions. However, under the condition of a small lubricant, the imperious demands for an efficient lubricant in the manufacturing process have gradually emerged.

Nanotechnology was proposed in the late 1950s [31, 32]. Nanotechnology is science, engineering, and technology performed at the nanoscale (1–100 nm). Nanofluids were created in the 1990s in response to the rise of nanotechnology. The concept of nanofluids was first proposed in 1995 by Choi at the Argonne Laboratory in the USA [33]. Previously, micron particles were added to the base fluid to increase its heat transfer performance [34–36]. However, problems such as particle deposition and blockage of microchannels have prevented this technology from being adopted by industry. The use of nanoparticles instead of micron sized particles can help overcome these limitations. Therefore, as a new heat conduction medium, nanofluids have very broad application prospects in the increasingly tense energy situation in the world [37]. Significant research interest has been generated in both academia and industry. Nanofluids are widely used in electronic microchannels, engines, spacecraft, nuclear energy, and solar energy. Nanoparticles exceed the macroscopic size of particles owing to their surface-to-volume ratios and other significant physical, chemical, and biological properties.

Nanofluid minimum quantity lubrication (NMQL) is an efficient and clean precision lubrication method aimed at overcoming the bottleneck of heat-transfer technology in MQL applications [38, 39]. Numerous studies have found that the presence of solid nanoparticles effectively improves the thermal conductivity of the lubricating medium [40–42]. Meanwhile, the ball effect, film-forming effect, filling effect, and polishing effect are accompanied by the anti-wear and anti-friction synergistic behaviors of the tool-chip and tool-workpiece interfaces [43, 44]. Therefore, the cutting force in machining is effectively reduced, and the surface integrity of the workpiece is significantly improved. NMQL has all the advantages of MQL. Therefore, it has great potential as a new sustainable industrial cutting technology. Table 1 presents a comparative evaluation of the different machining lubrication conditions.

In conclusion, the application of nanofluids in manufacturing has gone through three stages: the disorderly use of traditional oil-based cutting fluid, the tentative development of dry cutting, and the research and development of plant oil-based cutting fluid reduction technology. In contrast to existing reviews, this paper focuses on the characteristics of nanofluids that are widely used in the manufacturing field and their unique mechanisms under different processing methods. As shown in Fig. 2, this article reveals a new process, new device, and new mechanism of nanofluids in manufacturing. First, the preparation, fluid, thermal, and tribological properties of the nanofluids are revealed. The

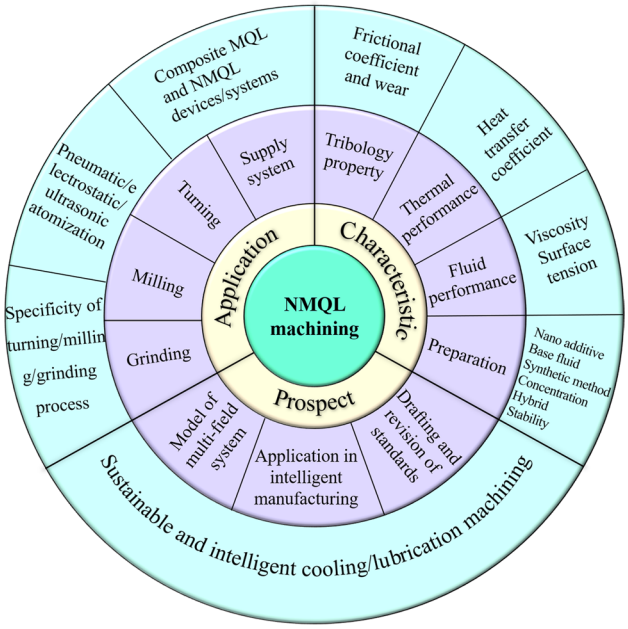

Fig. 2 Paper structure

Table 1 Evaluation of different machining conditions

Machining condition	Cost	Sustainability	Simplicity of system	Cooling effect	Lubrication effect
Flooding	☆	☆	☆☆☆	☆☆☆☆☆	☆☆☆☆
Dry	☆☆☆☆☆	☆☆☆☆☆	☆☆☆☆☆	☆	☆
Self-lubrication tool	☆☆☆☆	☆☆☆☆	☆☆☆☆	☆☆☆	☆☆☆☆
Cryogenic	☆☆☆☆	☆☆☆☆☆	☆☆☆☆	☆☆☆☆☆	☆
MQL	☆☆☆☆	☆☆☆☆☆	☆☆☆☆	☆☆☆	☆☆☆☆
NMQL	☆☆☆☆	☆☆☆☆☆	☆☆☆☆	☆☆☆☆	☆☆☆☆☆

☆Better performance

performance of nanofluids in machining is clarified. Furthermore, the innovative equipment used in the supply of nanofluids is reviewed, and the atomization mechanisms under different boundary conditions are analyzed. The technical problem of a parameterized controllable supply system is solved. Furthermore, the performance of nanofluids in turning, milling, and grinding is discussed. The mapping relationship between the nanofluid parameters and the machining performance is clarified. The flow field distribution and lubricant wetting behavior under different tool-workpiece boundaries are investigated. Finally, the application prospects of nanofluids in machining are discussed. This article includes a report on recent progress in academia and industry as well as a roadmap for future development.

2 Characteristics of nanofluids

2.1 Preparation

The preparation of nanofluids has laid the foundation for subsequent research and application. Nanofluids that can be stored for a long time and maintain excellent application performance have been investigated by researchers. High-performance nanofluids are affected by the nanoparticles, substrate solution, preparation process, concentration, and dispersion characteristics. This section summarizes and guides the preparation of nanofluids for application in manufacturing processes.

2.1.1 Nano additive phase

The fundamental problem of nanophase addition is the material characteristics. The specific heat capacity, thermal conductivity, hardness, density, and structural characteristics will have a significant impact on the nanofluid. Nanoparticles can be divided into zero dimension, one dimension, and two dimensions according to their size characteristics.

1. Performance comparison

The use of nanofluids to improve the machining performance of base fluids has been widely demonstrated. In an earlier study, Shen et al. [45] studied the grinding performance of cast iron under different lubrication conditions. A higher G ratio (less wheel wear), lower grinding force, and better surface finish are obtained under NMQL conditions. Scholars have performed lateral comparisons of the properties of different nanoadded phases using different processing methods and materials.

Cui et al. [46] studied the tribological properties of graphene nanofluids using friction and wear tests. In the experiments, 3 vol % nanofluids were prepared using palm oil mixed with graphene nanoparticles. As shown in Fig. 3, layered nanoparticles (MoS_2, MoO_3 and hBN) were used as controls. The results show that the coefficient of friction (COF), error, and scratch area of the graphene nanofluids are smaller. Scanning electron microscopy (SEM) and energy dispersive spectrometry (EDS) images of the scratched surface also verified this conclusion. The sheet structure can make the lubricating oil effectively fill the pits on the workpiece surface to increase the surface smoothness, thereby improving lubrication performance. Graphene has small intermolecular forces compared with other materials, which facilitates sliding between the molecular layers and improves lubrication properties. The layered molecular structure of graphene is difficult to deform under large loads during lubrication, thus enabling the protection of lubrication and guaranteeing sliding between layers.

In the turning process, Das et al. [47] discussed the properties of different nanofluids in AISI 4340 steel during hard turning. Three groups of nanofluids were prepared: Al_2O_3, CuO, and Fe_2O_3. The CuO nanofluid showed excellent performance, followed by the Fe_2O_3 nanofluid and Al_2O_3 nanofluid. In subsequent studies, Das et al. [48] analyzed the influence of fluid properties such as thermal conductivity, viscosity, surface tension, and contact angle. Different nanofluids were prepared by dispersing ZnO, CuO, Fe_2O_3 and Al_2O_3 nanoparticles in deionized water. In the process of hard turning, the cutting force of the Al_2O_3 nanofluid was the largest, whereas that of the CuO nanofluid was the smallest. Compared with the other three nanofluids, the CuO nanofluid exhibited the least surface wear and fine structure. This may be because the CuO-based nanofluid has a stronger heat-carrying capacity than the other two nanofluids, leading to smaller changes in the microstructure. The CuO nanofluid exhibited the lowest residual stress. Compared with other nanofluids, the CuO nanofluid can obtain the lowest microhardness, better surface texture, and lowest surface roughness. Kumar et al. [49] described the application of water-based Al_2O_3 and TiO_2 nanofluids as coolants in the hard-turning operations of AISI D2 steel. The results show that the TiO_2 nanofluid enhances the machinability compared with Al_2O_3 nanofluids. Because of the higher lubrication characteristics of TiO_2, the tool-chip friction is significantly reduced, which reduces the heat. When the concentration of TiO_2 is 0.01 wt %, compared with the same concentration of Al_2O_3 nanofluid, the tool surface wear is reduced by 29%, the cutting temperature is reduced by 9.7%, and the surface roughness is reduced by 14.3%.

In the milling process, Bai et al. [50] evaluated the lubrication properties of different nanofluids in Ti-6Al-4 V milling through experiments. Six nanofluids were selected: Al_2O_3, SiO_2, MoS_2, CNTs, SiC, and graphene. Cottonseed oil was used as the base. The experimental results show that Al_2O_3 nanoparticles achieve the minimum milling force, followed by SiO_2 nanoparticles. The surface roughness value of the Al_2O_3 nanofluid is the smallest, whereas

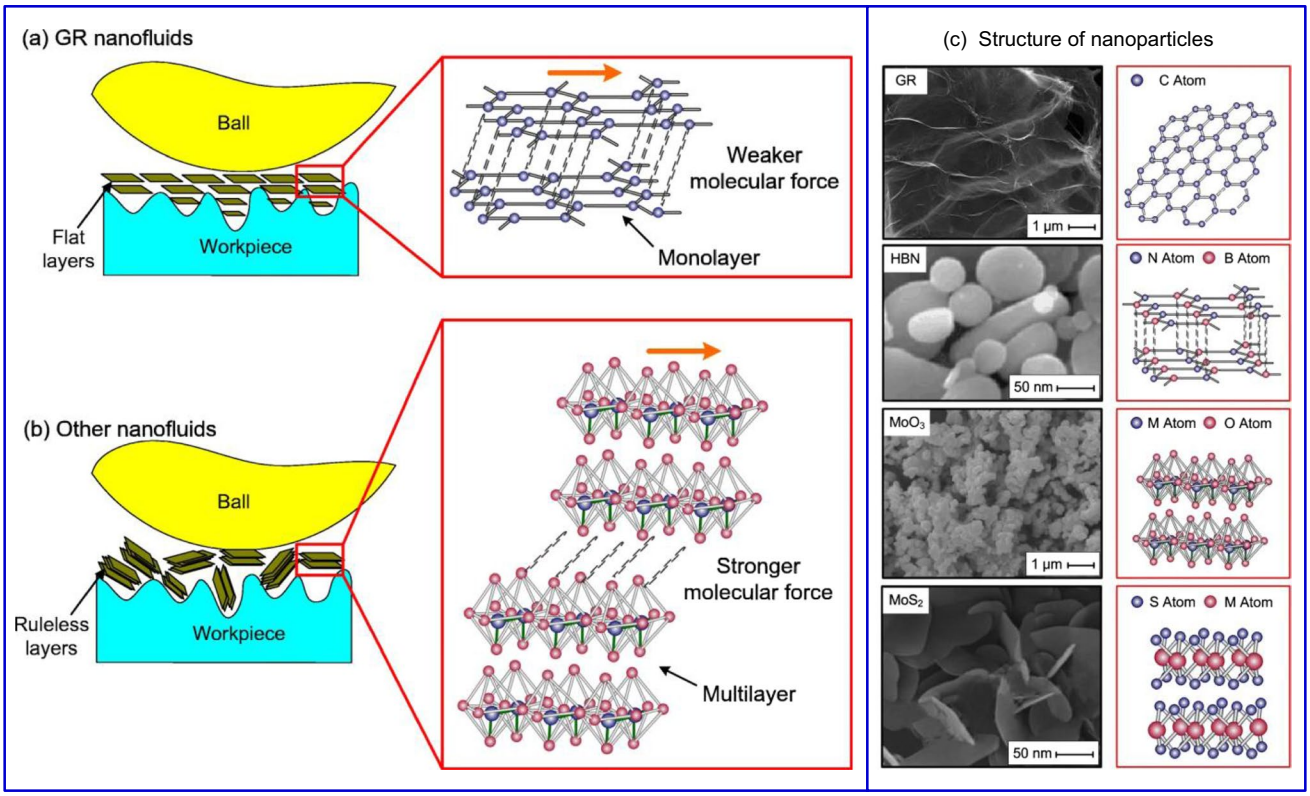

Fig. 3 Lubrication mechanism of stratiform nanoparticles [46]

that of the MQL is the largest. The surface roughness values of the six nanofluids are in the following order: $Al_2O_3 < SiO_2 < MoS_2 < CNTs < graphite < SiC$. Yuan et al. [51] prepared nanofluids by mixing four types of nanoparticles (Cu, graphene, MoS_2, and Al_2O_3) at two concentrations (1% and 2%) with native − 77 vegetable oil. During MQL milling of the Ti-6Al-4 V alloy, the nanofluid machining performance was evaluated in terms of cutting force and surface roughness reduction. From the analysis, it can be seen that Cu and graphite nanoparticles have a greater effect in reducing the cutting force and surface roughness. Confirmation tests revealed that Cu nanofluids reduced the cutting force and surface roughness by 8.84% and 14.74%, respectively. The graphite nanofluid reduced the cutting force and surface roughness by 5.51% and 21.96%, respectively. Yin et al. [52] conducted an experimental study on the milling of Ti-6Al-4 V. The results show that Al_2O_3 nanoparticles exhibit high hardness, which is beneficial for reducing milling force. SiO_2 nanofluids exhibit high viscosity, which can improve the surface quality of the workpiece. Figure 4 shows that the Al content on the workpiece surface under Al_2O_3 NMQL milling is 3.93% higher than that under MQL milling. Therefore, a large number of Al_2O_3 NMQL and Al_2O_3 nanoparticles deposited on the workpiece surface during processing are conducive to the formation of lubrication films. On the workpiece surface, aluminum forms a deposition of elements used to form the lubrication film, thus improving lubrication performance. In contrast, the S content on the workpiece surface is relatively low under MoS_2 NMQL. Under SiO_2 and SiC NMQL, the Si contents on the workpiece are 0.31% and 0.09%, respectively. These results indicate that the nanoparticles cannot be stably deposited on the workpiece surface under these working conditions. The best workpiece surface quality was obtained by milling SiO_2 NMQL, which indicates a better lubrication performance of the SiO_2 NMQL. However, the formed lubrication film cannot stably adhere to the workpiece surface. The carbon content of the workpiece surface under CNT and graphite NMQL reaches 4.72% and 5.31%, respectively, but the quality of the workpiece surface is poor.

In the grinding process, Li et al. [53] studied the effect of different palm oil-based NMQL on the surface grinding temperature of nickel-based alloys. Six types of nanoparticles, namely MoS_2, ZnO, CNTs, ND, Al_2O_3, and SiO_2, were used to prepare the nanofluids. The results show that the lowest grinding temperature of the CNT NMQL is 110.7 ℃. Lee et al. [54] studied the characteristics of the NMQL microgrinding process through numerous experiments. A series of experiments with a CBN wheel and tool steel workpiece were conducted in a miniaturized table

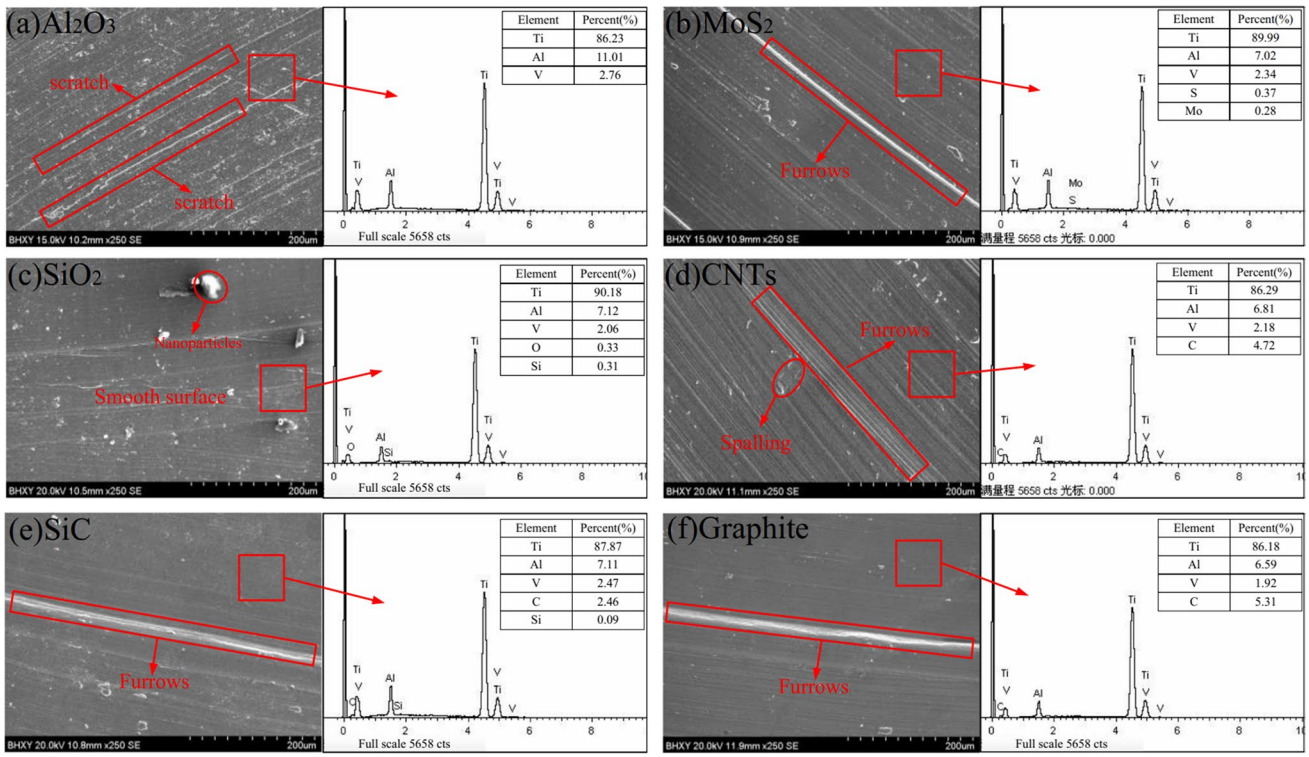

Fig. 4 Workpiece surfaces under different working conditions [52]

grinding machine system. The results show that ND nanoparticles can reduce the grinding force more effectively than Al_2O_3 nanoparticles. Moreover, the study also shows that Al_2O_3 nanoparticles seem to be more effective than ND particles in reducing the surface roughness, especially at larger sizes. This may be because the hardness of the Al_2O_3 nanoparticles is lower than that of the ND particles.

For other machining methods, Ni et al. [55] conducted an experimental comparison of the processing properties of three sesame oil-based nanofluids containing Fe_3O_4, Al_2O_3, and carbon nanoparticles. Broach AISI 1045 steel under MQL lubrication was used. The results show that the carbon nanofluid exhibits the best lubrication effect. The average broaching load peak value and load valley value are reduced by 725 N and 614 N, which are 115.7% and 118.5% lower than those of the commercial cutting fluid, respectively. The root mean square error of the broach vibration signal is 36.15% lower than that of the commercial cutting fluid. Moreover, the best surface quality is obtained. Pal et al. [56] compared the performance of Al_2O_3, MoS_2, SiO_2, CuO, and graphene nanoparticles in drilling AISI 321 steel. Among the nanofluids mentioned above, Al_2O_3 NMQL provides excellent cooling lubrication and enhanced machining performance, followed by MoS_2, SiO_2, CuO, and graphene.

2. Shape and size

Nanofluids play a crucial role in frictional interfaces during machining. Therefore, there is a consensus on the shape of the nanoparticles. Even with different mechanisms, spherical nanoparticles always behave well. Pal et al. [56] showed that the Al_2O_3 nanoparticle rolling or ball bearing mechanism improves the drilling processing performance. The experimental results of Virdi et al. [57] for Inconel-718 grinding also verified this statement. Musavi et al. [58] also found that the surface quality of superalloys obtained by NMQL processing using spherical CuO nanoparticles is better. As shown in Fig. 5, Tevet et al. [59] studied the tribological characteristics of layered-structured nanoparticles. The results show that the nanoparticles exhibit rolling, sliding, and peeling behaviors under boundary lubrication conditions. It is suggested that the viscosity and wear behavior of the friction interface can be improved by increasing the sphericity of the nanoparticles. Similarly, Fan et al. [60] experimentally characterized and analyzed that spherical nanoparticles can significantly reduce friction and wear. Kao and Lin [61] studied the tribological characteristics of TiO_2 nanofluids in cast iron. The results show that the COF obtained with nanofluids is always lower than that obtained without nanoparticle oil, even though viscosity loss is caused by the temperature increase. Nanoparticles provide a rolling function and surface repair and add more viscosity as a lubricant. Spherical TiO_2 nanoparticles are suitable as

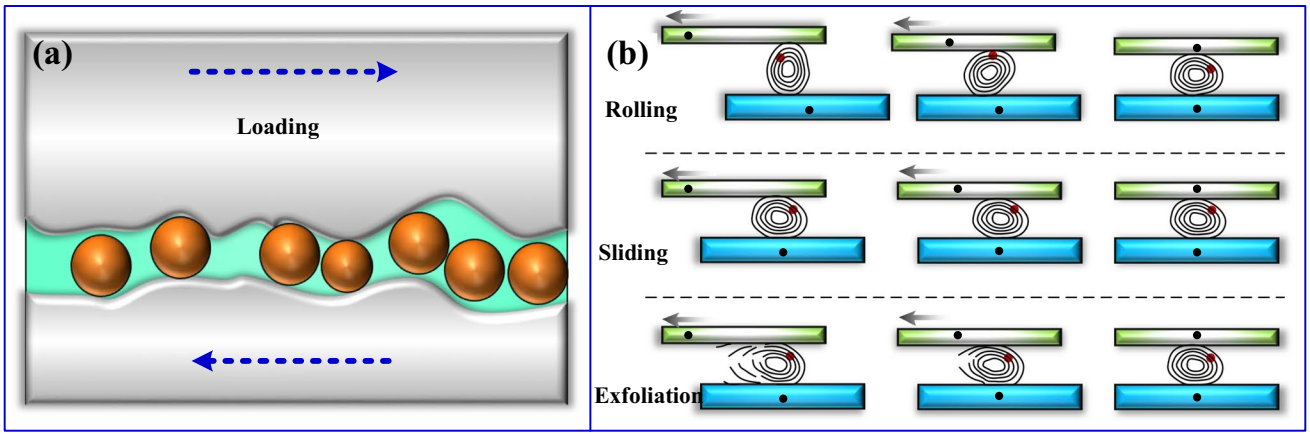

Fig. 5 Contact behavior of nanoparticles at the friction interface

suspensions for tribological and lubrication applications in the mechanical industry. Moreover, an experimental study of Ti-6Al-4 V milling by Yin et al. [52] specifically showed that spherical Al_2O_3 and SiO_2 nanoparticles improved the lubrication effect of the base oil.

Regarding the size of the nanoparticles, there are some contradictions in the current research. It is agreed that the processability of nanometer solid particles is better than that of micron solid particles. However, the size of nanoparticles has been debated. Compared with traditional micron-scale mixed fluids, nanofluids have the following advantages [62]. First, the specific surface area of the nanoparticles is larger, and the heat transfer performance is better. Second, they are more stable and difficult to settle. Then, they reduce the blockage of the supply system and promote the miniaturization of the system. The small size of the nanoparticles contributes to the transfer of heat energy during the cutting process [63]. In a recent study, a theoretical model of the grinding temperature field established by Yang et al. [64] confirmed this point of view. A study by Khajehzadeh et al. [65] on turning AISI 4140 hardened steel with a water-based TiO_2 nanofluid showed that the average reduction in tool side wear decreased from 46.2 to 34.8% as the nanoparticle size increased from 10 to 50 nm. Dubey et al. [66] used two different particle sizes in the nanofluid configuration to turn AISI 304 steel. The experimental results show that the surface roughness obtained from the 40 nm Al_2O_3 particle size is lower than that of the 30 nm alumina particle size. Lee et al. [54] suggested that the nanoparticle size is more critical than the bulk concentration for the surface roughness. In the case of nanofluid MQL, smaller nanoparticles can be more effective for producing smoother surfaces.

In another set of studies, conclusions were dialectical. Mao et al. [67] found that when the diameter of the nanoparticles increased, the tangential grinding force decreased slightly, and the peak grinding temperatures were similar. However, as the nanoparticle diameter increased, the surface finish deteriorated. Yuan et al. [68] considered that large nanoparticles make the contact surface relatively flat and generate a low cutting force. In this respect, the larger nanoparticles reduce the cutting force more effectively. For soybean oil- and rapeseed oil-based nanofluids, nanoparticles with a smaller size (SiC) are preferred to obtain better surface quality. Because of the large size of the high-hardness diamond combined with the low viscosity of the base fluid, the scraping effect on the workpiece surface is greater. However, when the viscosity of the base oil is sufficient, such as in natural oil 77, the size effect is significantly reduced. When combined with a high-viscosity base fluid, large nanoparticles are surrounded by oil molecules, which weaken the adverse size effect of the nanoparticles. In general, nanoparticles with a larger size can achieve a lower cutting force but poorer surface quality. To reduce the adverse size effect of nanoparticles in the MQL processing of nanofluids, base fluids with high viscosity should be selected to cooperate with larger-sized nanoparticles. Lee et al. [69] studied the machining performance of nanofluid airflow-assisted electrostatic atomization lubrication for titanium alloy microgrinding. The results show that larger nanodiamond particles (80 nm) are more conducive for enhancing the performance of nanofluids during grinding. In conclusion, nanoparticles of different sizes have different mechanisms of action at the frictional interface. The orientation of the machining results should be evaluated before selecting the size of the nanoparticles. As shown in Fig. 6, when the size of the nanodiamond particles is small (35 nm), owing to the high surface roughness of the workpiece, they may not effectively penetrate the contact area between the workpiece and grinding tool grit. As a result, they do not provide a sufficient ball-bearing effect for the contact area, which may be worse at low weight concentrations. Therefore, there was no substantial improvement in the friction behavior of the

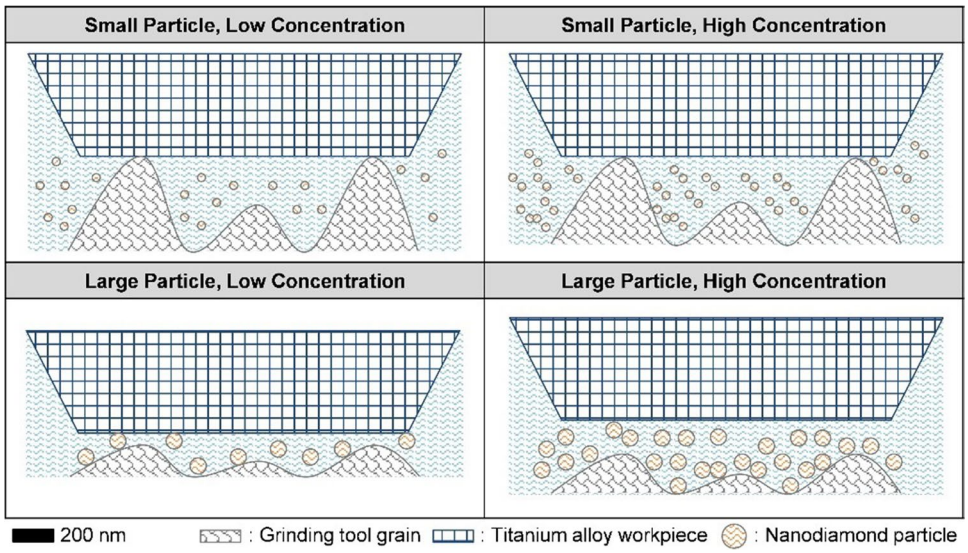

Fig. 6 Interface between workpiece and tool using different size nanoparticles [69]

contact area. On the other hand, larger nanodiamond particles (80 nm) can stay in the contact area more effectively and provide a sufficient ball bearing effect. In other words, the size of nanodiamond particles should be sufficiently large to match the surface roughness of the workpiece to ensure the positive impact of nanofluids. However, if the larger nanodiamond particles exceed the optimal amount at a high weight concentration, they may cause a scratch effect, and the ground may become slightly rough.

3. Special requirements

Some special properties also make the selection of materials for nanoparticles fascinating. For example, Fe_3O_4 nanoparticles can be directed by applying a magnetic field, which allows precise control of the region of action. Magnetic fluids are stable colloidal systems composed of magnetic nanoparticles coated with surfactants that are dispersed in a carrier liquid. By applying an external magnetic field, fluids can be confined, positioned, shaped, and controlled at the desired locations. The load capacity of the magnetofluid lubrication film can also be increased using an appropriate magnetic field. The distribution of the magnetic field intensity on the friction surface significantly affects the tribological properties of the magnetofluid. The experimental results show that compared with the carrier liquid, the magnetofluid has better anti-friction performance in the presence of an external magnetic field, and the life of the friction parts can be greatly improved [70]. Xu et al. [71] used a magnetic fluid as a lubricant to improve the operation performance of ball bearings under the condition of lack of lubrication. The diffusion resistance of the lubricant on the bearing was evaluated via centrifugation. Preliminary experiments showed that magnetic fluids can be used to reduce lubricant loss under appropriate magnetic fields.

Lv et al. [72] proposed a new lubrication strategy for magnetic MQL using a water-based Fe_3O_4 nanofluid as the cutting fluid. The effects of different magnetic inductions on the dynamic viscosity and atomization properties of the nanofluid were studied. The results show that the water-based Fe_3O_4 nanofluid has a higher dynamic viscosity and larger droplet size at a higher magnetic induction intensity. Water-based Fe_3O_4 NMQL with magnetic induction of 60 to 100 mT shows lower PM10 and PM2.5, tool wear, milling forces, and surface roughness values than LB-2000 vegetable oils applied in MQL. Guo et al. [73] superimposed an external magnetic field on a microtextured tool to facilitate the infiltration of magnetic nanofluids into the microtextured tool-chip interface. As shown in Fig. 7, the effects of different magnetic field parameters on the machining characteristics of microtextured tools under magnetic nanofluid lubrication were studied. The results show that magnetic nanofluids can effectively migrate to the microtextured tool-chip interface under an applied magnetic field. Thus, the derivative cutting degree caused by the microtextured tool can be effectively suppressed. The machining characteristics of the textured tool gradually improved as the magnetic field strength increased from 300 to 1200. Moreover, the permeability mechanism of magnetic nanofluids at the microtextured tool-chip interface under different magnetic field parameters is also discussed.

To summarize, the boundary conditions of the machining process must be considered. At high temperatures, high pressures, and high-speed boundaries, lubrication and heat transfer requirements need to be considered. Therefore, nanoparticles as an excellent heat transfer medium and superhard particles are recommended for use under severe friction conditions. Solid lubricant-type nanoparticles with multilayer structures that can effectively transfer the friction state of frictional interface components are recommended for other interfaces.

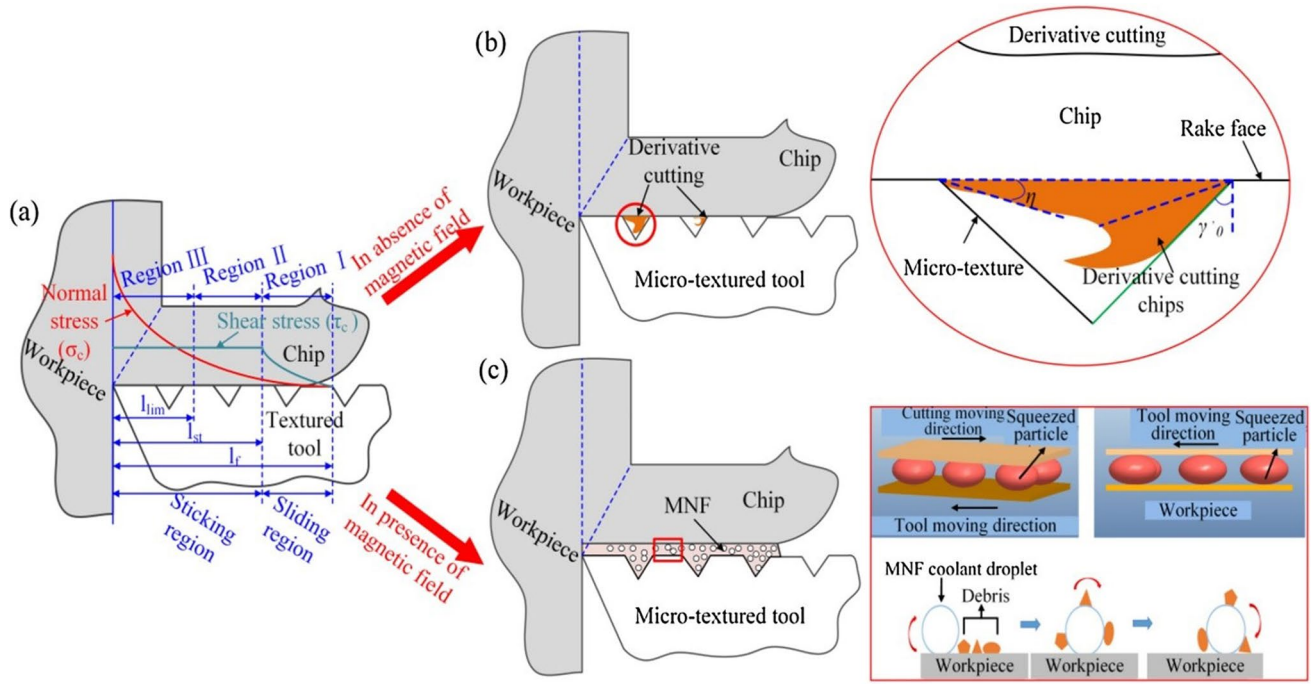

Fig. 7 Tool chip interface under magnetic field [73]

2.1.2 Base fluid

In the preparation of nanofluids, water, ethylene glycol, and oil are excellent solvents for dispersing nanoparticles. For machining-oriented nanofluids, water- and oil-based nanofluids coexist. Oil-based nanofluids have the advantage of ensuring lubrication, whereas water-based nanofluids improve the availability of nanofluids because water is readily available and inexpensive. Mao et al. [67] systematically analyzed the influence of nanofluid parameters on grinding performance. The experimental results show that the lubrication performance of water-based nanofluids is worse than that of oil-based nanofluids, but the cooling effect is the opposite. First, water-based nanofluids are not suitable for processing rusty parts. Second, the use of water-based nanoparticles alone cannot satisfy the lubrication requirements at the interface of intense friction. Najiha et al. [74] stated that the use of water-based nanofluids, with the help of water cooling and nanoparticle lubrication, can achieve oil-based MQL cutting of aluminum alloy materials. However, the lubrication performance of oil-based MQL can be further improved by adding a nanoreinforced phase.

Water-based nanofluids have been widely used in electrostatic atomization MQL. Lv et al. [75] found that the oil mist concentration of graphene water-based nanofluids was lower than that of oil-based electrostatic atomization MQL. The deposition performance of the charged droplets was improved in the presence of graphene. Moreover, Xu et al. found that water-based Al_2O_3 and SiO_2 nanofluids have a strong charging capacity, exhibit lower surface tension and contact angle, and better oil mist inhibition ability [75, 76]. Some scholars have also carried out research on the electrostatic atomization of vegetable oil [77–79]. Lee et al. [69] considered that diamond nanofluid droplets can be injected into the grinding wheel–workpiece contact area more effectively and stably, and this technology improves the surface roughness of the workpiece. In this study, the base fluid was a mixture of vegetable oil and isopropyl alcohol. Lv et al. [80] considered that the superior performance of graphene nanofluid lubricant by electrostatic atomization was due to the enhanced penetration and deposition of the nanofluid at the frictional interface by electrostatic atomization. In this study, LB-2000 vegetable oil was used as the base fluid. End milling of Inconel 718 by Shokrani et al. [81] showed that charged WS_2 nanofluids increased tool life by 10% and significantly improved surface integrity. From existing research, oil-based nanofluids have higher requirements for charging voltage, which has raised the requirements for device stability.

In traditional ultrasonic atomization, the low viscosity and surface tension of water-based fluids make them easier to break into droplets. Huang et al. carried out ultrasonic atomization processing of water-based nanofluids and successively optimized the process parameters of grinding and micromilling [82–85]. It has been shown that nanographene has excellent thermal conductivity, and the heat in the cutting/grinding zone is carried out by the nanofluid, which reduces thermal damage to the tool and thereby reduces tool

wear. Ultrasonic atomization effectively disperses nanoparticles in the nanofluid and maximizes the heat transfer performance. In recent studies, Hadad et al. [86] and Lefebure et al. [87] developed novel devices to overcome these defects. Hadad et al. [86] developed an ultrasonic atomization MQL nozzle that used the Venturi effect to generate primary atomization and enhanced secondary atomization by high-frequency vibration of the resonant surface of the nozzle tip. Therefore, compared with the traditional aerosolized MQL system, the particle size of the vegetable oil droplets is smaller, and the distribution is more uniform. Lefebure et al. [87] carried out a study on the atomization performance of biodegradable biolubricants with ultrasonic atomization MQL. The results show that the size distribution of the atomized droplets is affected by the mesh size, driving voltage, and lubricant viscosity. The droplet size decreases with an increase in voltage. At low voltages, viscosity had no effect on the average droplet diameter, but there was a significant positive correlation at high voltages. The droplet size will be greatly increased significantly with an increase in the vibration net aperture. There are few reports on the application of ultrasonic atomization to vegetable oil nanofluids during processing. However, with the help of new devices, this technology will be studied further in the near future.

Oil-based nanofluids can be divided into vegetable and mineral oil-based nanofluids. The discussion on vegetable and mineral oils has been clarified by Zhang et al. [88] and Wang et al. [62] in a previous review. Mineral oils are not recommended for further use, whereas vegetable oils have broad application prospects. Gaurav et al. [89] investigated the performance of a Jojoba oil-based MoS_2 nanofluid in Ti-6Al-4 V turning. The results show that jojoba oil also acts as a strong and sustainable alternative to commercial mineral oil in turning under pure oil and nanofluid conditions. The long-chain fatty acid structure, excellent thermal oxidation stability, high viscosity index, and layered structure reduce the cutting force, surface roughness, and tool wear by 35–47%. Padmini et al. [90] compared MoS_2 nanofluids with three plant-based oils (coconut, sesame, and rapeseed) for turning AISI 1040 steel. The results show that the coconut oil-based nanofluid has the best processing performance. Compared with rapeseed oil-based nanofluid, tool wear was reduced by 31.58%. Su et al. [91] studied the effect of vegetable oil- and ester oil-based nanofluids on the cutting force and temperature in AISI 1045 turning. Graphite-LB2000 and graphite-Prieco6000 nanofluids were prepared using a two-step method. The experimental results show that the cutting force and temperature are significantly reduced using graphite-based nanofluids. Compared to PriEco6000 unsaturated polyol esters, LB2000 vegetable oil is the best base oil for graphite-based nanofluid processing. Yuan et al. [68] selected nanoparticles with different hardnesses and vegetable oils with different viscosities as nanofluids for the milling of aviation aluminum alloy 7050. The results show that, compared with the dry processing conditions, the cutting force of rapeseed oil-based NMQL is the lowest, while the surface roughness of natural 77 oil-based diamond nanofluid is the lowest, which decreases by 10.71% and 14.92%, respectively. Yin et al. [92, 93] systematically revealed the lubrication mechanisms of different vegetable oils with different physicochemical properties at the tool-workpiece interface. To verify the interfacial lubrication characteristics of different vegetable oils, MQL milling experiments were performed on AISI 1045 using five vegetable oils: cottonseed, palm, castor, soybean, and peanut oils. The experimental results show that palm oil obtains the lowest milling force, COF, and surface roughness values and the smoothest workpiece surface. SEM images of the workpiece surfaces under different conditions are shown in Fig. 8. Moreover, the physicochemical properties (composition, molecular structure, viscosity, surface tension, and contact angle) of vegetable oil were analyzed. Palm oil with a high saturated fatty acid content, high viscosity, and small contact angle formed a lubricating film with the highest strength and largest diffusion area at the tool-workpiece interface. Therefore, palm oil can achieve the best lubrication effect. Dong et al. [94] studied the milling temperature of 45 steel using cottonseed, palm, castor, soybean, and peanut oils as base oils. The results demonstrate the advantages of biological lubricants as base oils, especially cottonseed oil, palm oil, and castor oil, which can be used as base oils for milling. Zhang et al. [95] compared the processing performance of different oils based on grinding 45 steel and discussed the lubricating performance of soybean oil, palm oil, and rapeseed oil as base oils and liquid paraffin. The experimental results show that palm oil-based nanofluids generate the best lubrication performance under MQL conditions because of the high saturated fatty acids and high film-forming properties of the carboxyl groups in palm oil. Because viscosity has different effects on lubrication and heat transfer properties, high-viscosity nanofluids significantly reduce the heat transfer performance while improving the lubrication properties. Considering the lubrication and heat transfer performance, soybean oil with the lowest viscosity is the best choice for the base oil. Moreover, Zhang et al. [96] used the COF, specific friction energy, total heat flux, and grinding peak temperature as evaluation parameters to comprehensively analyze the influence of the physical properties (viscosity and surface tension) of vegetable oil on the cooling effect. Vegetable oil nanofluids exhibit better cooling properties than mineral oils because of their beneficial effects on fatty acid molecules. Moreover, the influence mechanism of viscosity and surface tension on the cooling properties of nanofluids is also discussed. Vegetable oils with a low viscosity and surface tension exhibit good cooling properties, whereas those with a high viscosity and surface tension

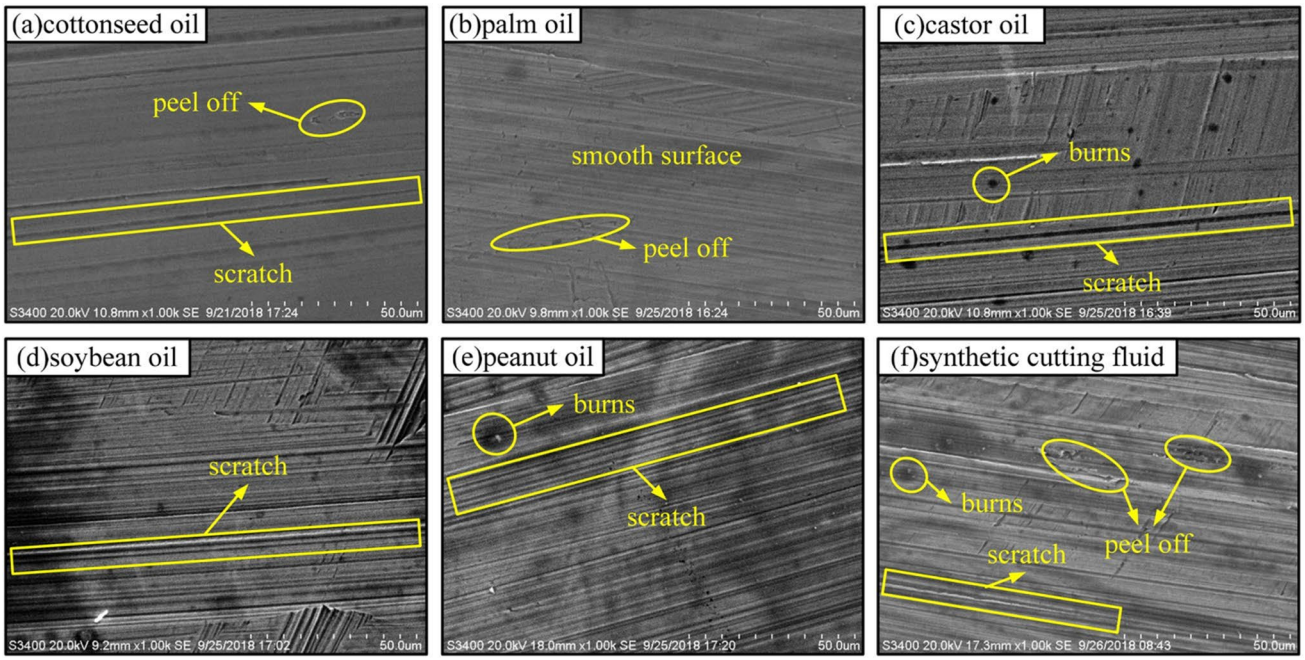

Fig. 8 SEM images of the workpiece surfaces under different conditions [92]

exhibit good lubrication properties. As a result, palm oil nanofluids with high viscosity and surface tension achieved the lowest COF, specific friction energy, and peak grinding temperature and exhibited superior grinding performance compared to other products. Wang et al. [97] used seven typical vegetable oils (soybean, peanut, corn, rapeseed, palm, castor, and sunflower oil) as the base fluid to experimentally evaluate the friction characteristics of the grinding wheel–workpiece interface in the grinding of nickel-based alloy GH4169. The experimental results show that MQL grinding using vegetable oil achieves a lower COF, specific grinding energy, and grinding wheel wear than the flooding condition. Castor oil achieves the best lubrication performance and workpiece surface quality. The COF and specific grinding energy of castor oil decrease by 50.1% and 49.4%, respectively, compared to flood conditions. Corn oil had the highest G ratio (29.15).

In this study, the application of blended vegetable oil in processing is presented. Guo et al. [98] used castor oil as the base oil and mixed it in a 1:1 ratio with six types of vegetable oils (soybean, corn, peanut, sunflower, palm, and rapeseed oil). GH4169 was used as the workpiece to evaluate the lubrication performance in the grinding zone. The results show that the comprehensive lubrication performance of the mixed oil is better than that of castor oil, and soybean/castor oil shows the best performance. As shown in Fig. 9, compared to castor oil, the specific grinding force and specific normal grinding force decreased by 27.03% and 23.15%, respectively. The workpiece surface profile curves obtained under four working conditions (castor oil, castor/soybean oil, castor/corn oil, and castor/palm oil) were analyzed. The amplitude of the surface profile curve of castor/soybean oil was larger, and the correlation coefficient was higher than those of the other mixed oils. Consequently, the workpiece exhibited the best surface quality. Guo et al. [99] also prepared seven castor/soybean oil mixtures with volume ratios of 1:0.5 and 1:4 for MQL grinding of nickel-based alloys. The viscosity and tribological behavior of the blended oil were compared with those of pure castor oil. The results show that the optimal castor/soybean volume ratios are 1:0.5, 1:1, 1:1.5, and 1:2. The maximum fractal dimension and minimum scale coefficient are realized when the volume ratio is 1:2. Thus, the optimal volume ratio is determined.

The polar groups in the molecular structure of vegetable oil can form an adsorption film on the metal surface during the lubrication process, which has a good lubrication effect. However, the oxidation of vegetable oil limits its lubrication performance. The main components of most vegetable oils are fatty acid glycerides, and the type of fatty acid has a significant impact on the properties of vegetable oils. The existence of unsaturated double bonds in the carbon chains of fatty acids leads to poor oxidation stability. Improving the antioxidation of vegetable oil has always been a hot issue in the food and industrial fields, and the addition of antioxidants is undoubtedly the most direct method for enhancing the oxidation stability of vegetable oil. For example, vitamin E is used as an antioxidant [99]. Chemical modification is another method to improve the antioxidant properties of

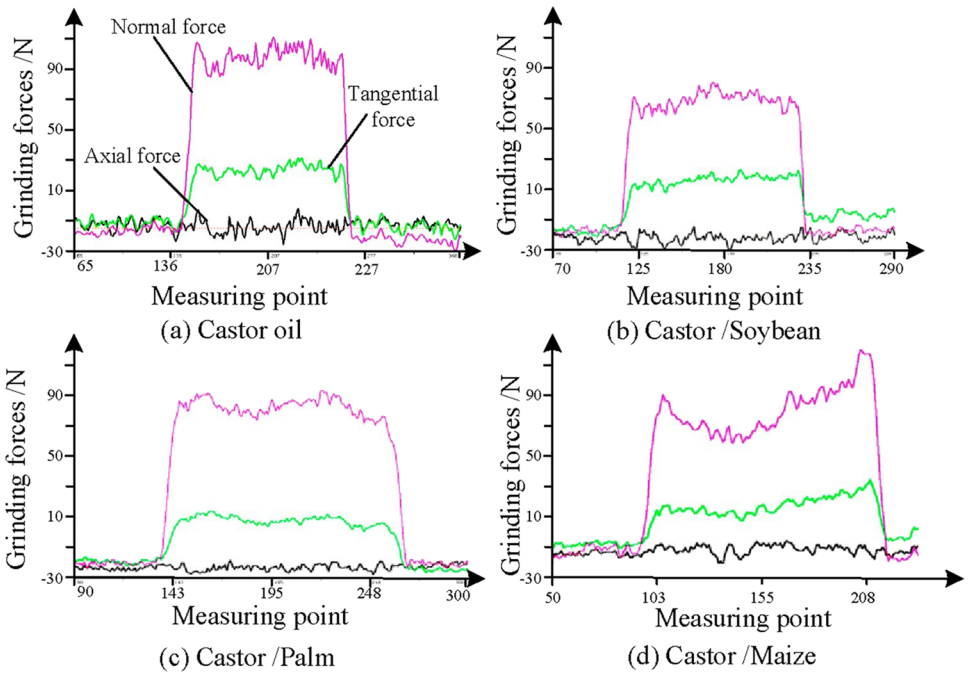

Fig. 9 Grinding force measuring signal images of four different lubrications [98]

vegetable oils. This method focuses on the chemical reaction of the carboxyl and carbon chains of unsaturated fatty acids to change the unsaturated degree, carbon chain length, and branch of vegetable oil fatty acids to improve the thermal oxidation stability of vegetable oil. Common modification methods include hydrogenation, esterification, vulcanization, epoxidation, and isomerization [100].

Therefore, water- and oil-based nanofluids are determined based on the manufacturing boundary conditions. When lubrication is urgently needed, the application of oil-based nanofluids is necessary. Subsequently, the selection of the base fluid should match the supply mode. When electrostatic and ultrasonic atomization is used, further comprehensive evaluation is needed, including equipment and processing requirements.

2.1.3 Synthetic method

Stable suspension of nanofluids is necessary for machining. Nanofluids can be prepared using both single- and two-step methods. In the single-step method, the preparation process of nanoparticles and dispersion of nanoparticles in the base liquid are completed simultaneously [37]. Nanoparticles are prepared using physical or chemical methods and are directly miscible with the base fluid. As shown in Fig. 10, the two-step method involves the preparation and dispersion of nanofluids in two steps [101]. First, nanoparticles are prepared by vapor deposition, chemical reduction, or mechanical grinding and then dispersed into the base liquid by mechanical stirring, ultrasonic vibration, and the addition of dispersants. Although the two-step method tends to accumulate nanoparticles during the preparation process, it is more economical. The advantages and disadvantages of the two-step method are also discussed. In this method, stirring and ultrasonic treatment can reduce the aggregation of particles, which is a challenge in nanofluid preparation. Moreover, dispersants were added to enhance the stability of the nanofluids. Another feature of the two-step process is that it is well suited for the large-scale production of nanofluids. Notably, the two-step process is the most cost-effective method for preparing nanofluids.

The convenience of this two-step method determines its wide applicability. The two-step method is widely used for the preparation of machining-oriented nanofluids. Because the stability of nanofluids prepared by the one-step method decreases owing to the long-term transport and storage process, it is difficult to accept. The two-step method has been widely adopted. With the rapid development of nanotechnology, there is an urgent need to further reduce the cost of nanoparticles.

2.1.4 Concentration

The performance characteristics that vary with the concentration of nanofluids are well known. At low concentrations, the performance improves with an increase in the nanofluid concentration. However, after reaching a certain concentration, the processing performance does not continue to improve. Therefore, the unresolved question of the optimal nanofluid concentration has been extensively studied. The instability of the nanofluids became apparent when the concentration is increased.

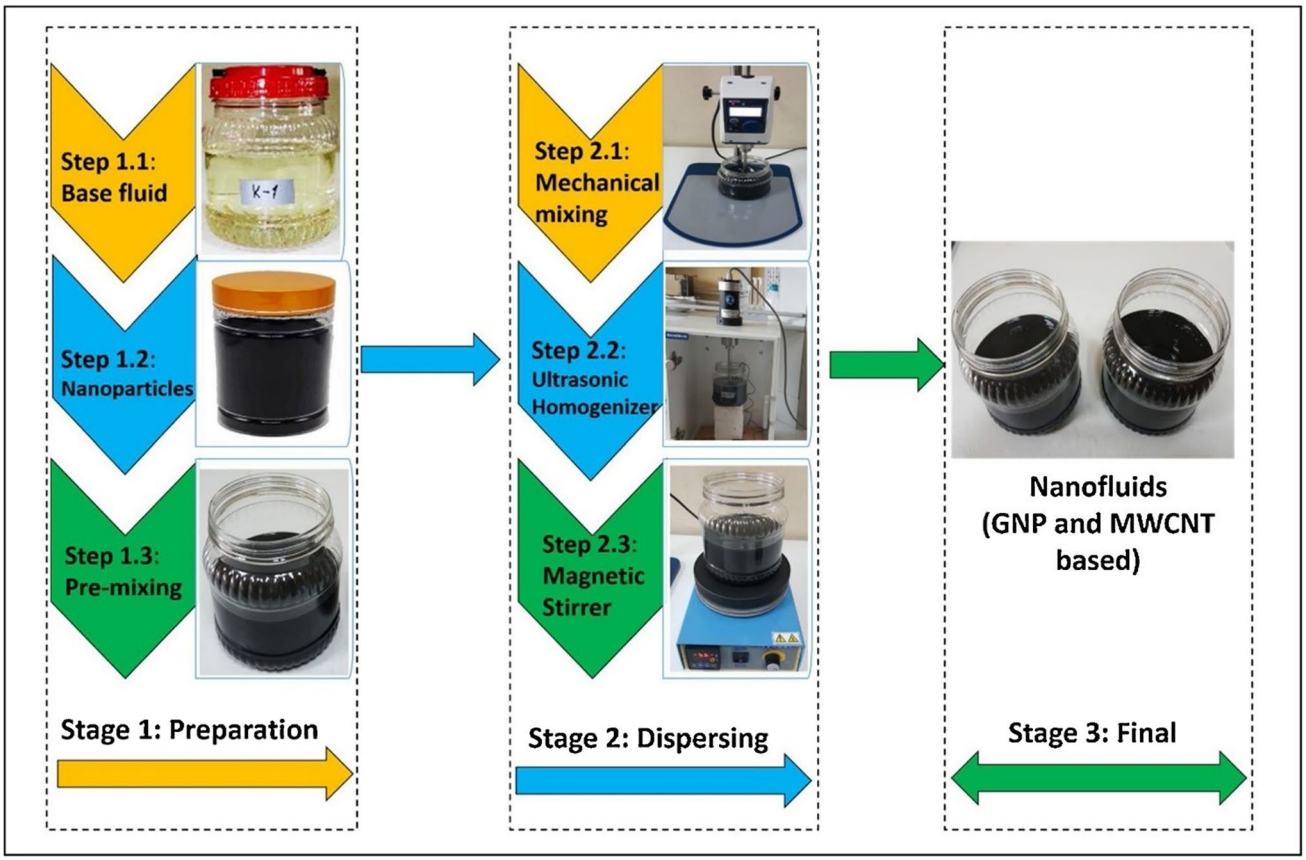

Fig. 10 Two-step preparation method [101]

From a tribological perspective, Talib et al. [102] suggested that hBN particles with low concentrations provided a thin lubricating film, which transformed the particles from sliding friction to rolling friction. As shown in Fig. 11, at low concentrations, the presence of hBN particles provides lubricating elements that allow them to move parallel to each other on their own and slide over other particles with relative ease. The hBN particles filled the valley at the contact interface, creating a lubricating film that reduced friction and prevented wear formation, thereby reducing the COF. A high concentration of hBN particles significantly increases the COF. This is because the stress concentration gradually increases with an increase in the hBN concentration. Too many particles were trapped in the rough valley, restricting the movement of nearby particles and generating more force. Compared to 0.05 wt %, 0.1 wt % and 0.5 wt % hBN particles are considered abrasive, and when it slides along the contact surface, it creates more damage areas, resulting in abrasive wear. From the perspective of heat transfer, Li et al. [103] used CNT nanoparticles to prepare 8 types of palm oil-based nanofluids with volume fractions of 0.5–4% for MQL grinding experiments of nickel-based alloys. The

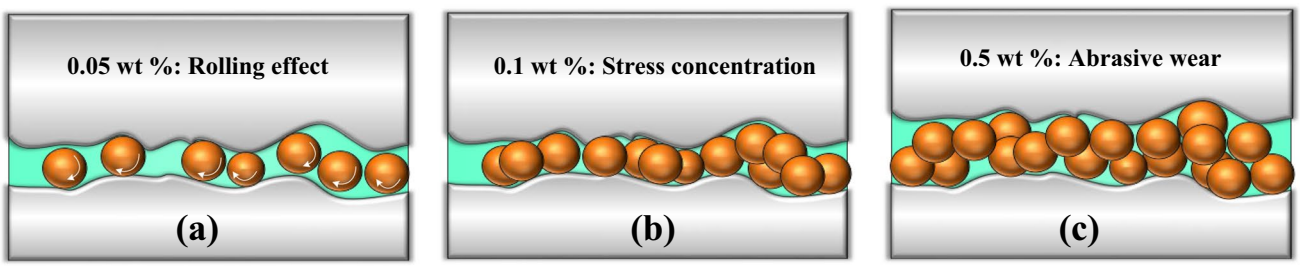

Fig. 11 Lubrication films with various concentrations of hBN particles

2 vol % nanofluid reached 21.93 N grinding force, the lowest grinding temperature was 109.8 ℃, and the lowest proportion factor was 42.7%. Therefore, the 2 vol % nanofluid achieved the best lubrication and heat-transfer performance. From the perspective of the cutting force and surface quality, Zhang et al. [104] experimentally studied the influence of nanoparticle concentration on the lubricating properties of NMQL grinding. Nanofluids with different concentrations of MoS_2, CNTs, and the hybrid (MoS_2-CNTs) were prepared. The effects of the nanofluid mass fraction on the grinding force ratio and workpiece surface quality were investigated using a nickel-based alloy as the workpiece. The results show that 8% MoS_2-CNTs is the best concentration of NMQL. Sen et al. [105] mixed Al_2O_3 nanoparticles at different concentrations (0.5–5%) with palm oil for Inconel 690 machining. The performance was evaluated in terms of the surface roughness, specific cutting energy, tool wear, and cutting temperature. A model based on a fuzzy interference system was developed to determine the optimal concentration of Al_2O_3 nanoparticles. The optimum concentration of Al_2O_3 in MQL milling was 2.5%.

It is noteworthy that some studies have shown that two key concentration values to improve machining performance. Duan et al. [106] studied the effect of cottonseed oil-based Al_2O_3 nanofluid concentration on milling force and workpiece surface quality. NMQL milling experiments were performed on cottonseed oil-based Al_2O_3 nanofluids with different mass fractions using 45 steel. The results show that the minimum milling force is obtained at a concentration of 0.2 wt %. At a concentration of 0.5 wt %, the minimum surface roughness value is obtained, and the micromorphology of the workpiece/chip is the best. Roushan et al. [107] used water-based CuO nanofluids for the microend milling of Ti-6Al-4 V. The results show that at a low concentration (0.25 vol %), the surface roughness of the workpiece is the smallest, and at a higher concentration (1 vol %), the tool wear and stacking edge formation are reduced. Virdi et al. [57] studied the working grinding of Inconel-718 using plant oil-based Al_2O_3 nanofluids. It can be seen from the results that the surface roughness value is better when the concentration of nanoparticles is 0.5 wt %. However, compared with overflow cooling, the G ratio, grinding energy, and tangential force increased with a 1 wt % concentration of nanoparticles in the NMQL condition.

In general, as the concentration of nanoparticles continues to increase, the instability of nanofluids becomes very obvious, and the academic community has a strong consensus on this [58, 108–114]. However, the optimal concentrations obtained in different studies are different. The stable suspension gradually undergoes flocculation, condensation, precipitation, and phase separation. In the field of machining, the optimal concentration is influenced by many factors, such as the processing parameters, properties of the nanoparticles and base solution, and storage environment. An analysis of existing research shows that there are probably two key concentrations that require attention. Scholars in the field of recommendation have jointly promoted the establishment of databases to provide the latest concentration recommendation tables for engineering applications.

2.1.5 Hybrid nanofluids

Researchers have a positive attitude toward hybrid nanofluids owing to their excellent thermal and tribological properties [115, 116]. Singh et al. [117] developed hybrid nanofluids with better thermal and tribological properties by mixing Al_2O_3-based nanofluids with graphene nanosheets at volume concentrations of 0.25, 0.75, and 1.25 vol %. As the nanoparticle concentration increased, the thermal conductivity and viscosity increased. The thermal conductivity of the hybrid nanofluids is lower than that of its composition, and the viscosity is between that of its composition. Tribological tests confirmed that the wear decreased with increasing nanoparticle concentration, and the hybrid nanofluid produced the smallest amount of wear. Compared with Al_2O_3 nanofluids and base fluids, hybrid nanofluids exhibit better wettability. Sharma et al. [118] found that compared with Al_2O_3 nanofluids, the cutting force, feed force, thrust force, and surface roughness of an Al_2O_3/MoS_2 hybrid nanocutting fluid were significantly reduced. Sharma et al. [119] tested the thermophysical properties of the prepared hybrid nanofluids. The tribological behavior and spreadability of all the nanofluid samples were investigated using needle disk tests and contact angle measurements. The results show that an increase in the concentration of nanoparticles in the cutting fluid reduces wear, and the hybrid nanofluids have the lowest wear. Junankar et al. [120] found that compared with CuO and ZnO nanofluids, the surface roughness of hybrid nanofluids was reduced by 65% and 60%, respectively. Moreover, under the hybrid nanofluids condition, the cutting temperature is reduced by 11% and 13%, respectively, compared with CuO and ZnO nanofluids. Thakur et al. [121] found that MQL based on an Al_2O_3-CuO hybrid nanofluid could significantly improve the surface quality and reduce the cutting temperature and cutting force. Dubey et al. [122] conducted an NMQL turning experiment on AISI 304 steel. The results show that the use of hybrid nanomaterials (Al_2O_3/graphene) results in an approximately 13% reduction in force, a 31% reduction in surface roughness, and a 14% reduction in temperature compared with the Al_2O_3 nanofluid.

In addition, some innovative research needs attention. Sirin et al. [123] studied the machining properties of an Inconel X-750 superalloy using hBN, graphene, and MoS_2 nanoparticles with different shapes and properties. According to the experimental results, the hBN/graphene hybrid nanofluids are superior to the hBN/MoS_2 and graphene/

MoS_2 conditions in all performance criteria. The tool life of hBN/graphene nanofluids was improved by 36.17% and 6.08% compared with graphene/MoS_2 and hBN/MoS_2 nanofluids, respectively. Safiei et al. [124] attempted to improve the processing performance using a combination of SiO_2-Al_2O_3-ZrO_2 tri-hybrid nanofluids and MQL technology. Tri-hybrid nanofluids produce a high-quality surface finish and reduce the cutting temperature using optimal machining parameters. In this process, the surface roughness value is reduced by 28–75% compared with other lubrication techniques. Zhang et al. [125] studied the performance of Al_2O_3/SiC hybrid NMQL grinding of nickel-based alloys. The results show that, owing to the physical synergistic effect, the surface roughness obtained by the hybrid nanofluid consisting of Al_2O_3 and SiC is lower. Based on these findings, an optimal mixing ratio is determined. As shown in Fig. 12, the Al_2O_3/SiC (2:1) nanofluid had the lowest specific grinding energy, indicating the best lubrication performance. Zhang et al. [126] optimized the size ratio of hybrid nanoparticles to improve the lubrication performance of MQL grinding. The experimental results show that the effects of different Al_2O_3/SiC mixed-particle sizes on the grinding performance of NMQL are different. When the size ratio of the Al_2O_3/SiC mixture is 70:30, the highest removal rate and lowest R_{Sm} of the workpiece are achieved. The lowest R_a value is obtained at 50:30. The best morphology and largest droplet wetting area are obtained at 30:70. Moreover, the cross-correlation function curve of the workpiece surface profile at 30:70 has the shortest period, largest amplitude, and largest number of correlations (0.67), indicating that the workpiece surface quality is the best. Therefore, 30:70 is the optimal size ratio for the Al_2O_3/SiC mixed nanofluids.

The excellent performance of hybrid nanofluids has been repeatedly demonstrated. According to the mechanism of different nanoparticles in processing, multifunctional and comprehensive nanofluids can be realized. The scientific collocation of different nanoparticles is a problem that needs to be solved. First, machining-oriented requirements should be better summarized, such as which materials and processing parameters require lubrication as the main factor and which are oriented by cooling requirements. Furthermore, unlike hybrid nanofluids, core–shell nanoparticles can combine different materials in a single nanoparticle. Core–shell nanoparticles are a new research direction. For example, core–shell nanoparticles of iron oxide and other film layers can not only realize a magnetic field-controlled fluid but also complete the functional application of the film layer at the friction interface. These studies may not be applicable to industry in the short term, but they provide a new way to solve the problem. There may also be new phenomena that promote technological innovation and progress.

2.1.6 Stability

The stability of nanofluids is a key factor that affects the machining performance. Figure 13 shows the agglomeration of nanoparticles. Winding and agglomeration limit the tribological properties of nanofluids. These limitations can be addressed mechanically and chemically, with the exception of controlling the concentration of the nanoadded phase.

1. Mechanical and ultrasonic methods

The mechanical dispersion method involves dispersing nanoparticles in a liquid medium by means of mechanical energy, such as shear force or collision force, such as ball milling and mechanical stirring. The ultrasonic dispersion method involves placing the nanofluid directly in an ultrasonic field and using the appropriate frequency of ultrasonic waves to vibrate the nanoparticles. Thus, the mutual attraction between nanoparticles can be overcome, and the balance between particles in the original particle

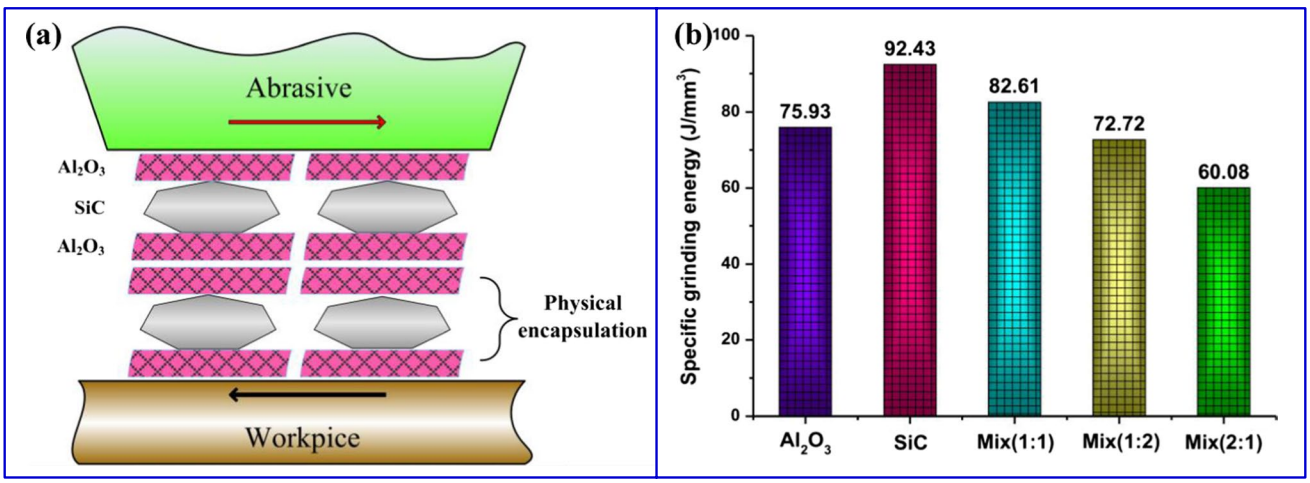

Fig. 12 Properties and mechanism of hybrid nanofluids [125]

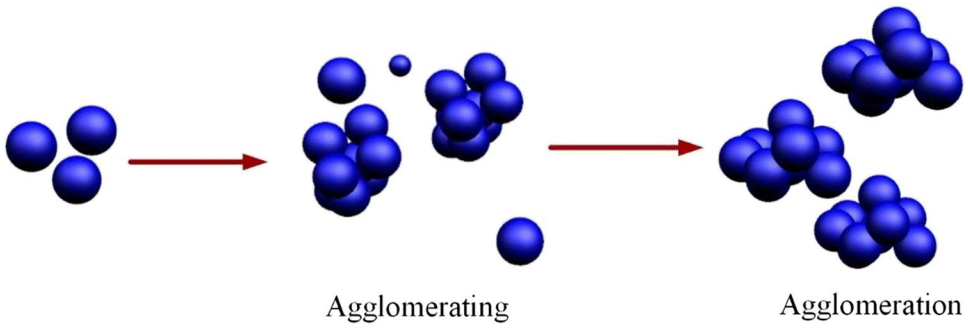

Fig. 13 The agglomeration of nanoparticles [106]

cluster and between particles and the base liquid molecules can be destroyed so that the nanoparticles can be dispersed into the base liquid. Homogenization of nanofluid suspensions by ultrasonic vibration is widely used in the field of manufacturing. Acoustic cavitation caused by ultrasonic treatment generates a strong shear force that decomposes agglomerates. In general, acoustic cavitation in a liquid can improve the diffusion rate and produce highly concentrated and uniform dispersions of materials with micron or nanometer sizes in the base liquid. Noroozi et al. [127] found that using a more powerful ultrasound probe can improve the thermal diffusivity and stability of nanofluids compared with bath ultrasound. Mondragon et al. [128] believed that one of the required conditions for the production of stable SiO_2 nanofluids with a certain solid content was a 5-min high-energy treatment with an ultrasonic probe. Mahbubul et al. [129] reported the application of ultrasonic conditions to the dispersion of Al_2O_3 nanoparticles in water using a two-step method. The prepared samples were treated with an ultrasonic horn for 1–5 h with amplitudes of 25% and 50%. The results show that when the amplitude is 50%, the maximum ultrasonic energy is obtained when the nanoparticles last for 3 h. When the sonar power is 50%, the particle dispersion is good. When the amplitude is 50% and 25%, the optimal durations are 3 h and 5 h, respectively. Mao et al. [130] found that the suspension stability of nanofluids is poor under short-term ultrasonic vibrations. When the ultrasonic vibration time exceeds 0.5 h, nanofluids with good suspension stability can be obtained.

2. Dispersant

Figure 14 shows that the surfactant disperses the nanoparticles appropriately through hydrophobic surface forces or electrostatic repulsion forces [131]. Mao et al. [130] found that when the sodium dodecyl benzene sulfonate (SDBS) concentration was low, higher SDBS concentrations led to better suspension stability of the nanofluid. However, when the concentration of SDBS exceeded 0.5%, supersaturated adsorption occurred on the nanoparticle surface. As a result, the suspension stability of the nanofluid deteriorated with an increase in SDBS concentration. When the pH value is lower than 7, the suspension stability of the nanofluid is significantly improved with increasing pH value. When the pH was higher than 7, sedimentation appeared clearly in the dispersed system. The morphology of the Al_2O_3 nanoparticles in the dispersion system was analyzed by scanning electron microscopy. It was found that some large aggregates

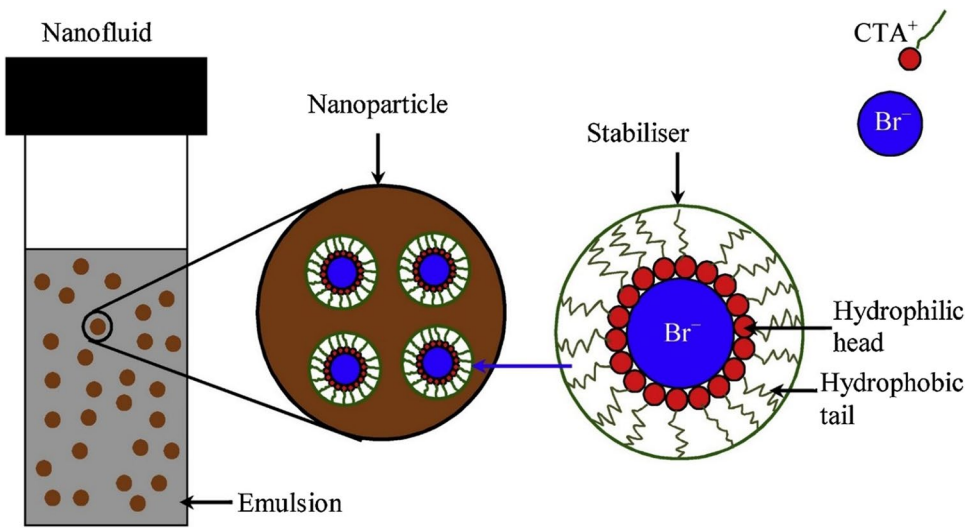

Fig. 14 Nanofluids and stabilizers [131]

appeared in the dispersive system without dispersant application. Moreover, Al_2O_3 nanoparticles were uniformly dispersed in the dispersion system with the addition of a dispersant. Shabgard et al. [132] showed that the application of 1 vol% gum Arabic (GA) as a surfactant provided significant suspension stability for a long time, even without ultrasonic homogenization. Shukla et al. [133] investigated the effects of MoO_3/water nanofluids mixed with six different surfactants on the tribological and machining properties of AISI 304 steel during turning. The optimum values of the mixture ratio and volume concentration were obtained by zeta potential and thermal conductivity tests. The results show that the SPAN20 surfactant provides the best machining performance at mixing ratios of 3:2 and 0.45 vol %. The mean cutting force and tool wear are significantly reduced by 32.05% and 53%, respectively, and the minimum surface roughness is 1.21 µm. Musavi et al. [58] evaluated the performance of nanofluids in superalloy machining by using surfactants as additive elements. Nanofluid solutions were prepared using nanosized CuO and nanosized SiO_2 nanoparticles with different volume fractions. Sodium dodecyl sulfate (SDS) was selected as a suitable surfactant for polar fluids. Compared to nanofluids without surfactants and conventional fluids, enhanced nanofluids can significantly improve the cutting mechanism. The main reason for this phenomenon can be attributed to the high ability of the surfactant to disperse nanoparticles in the fluid and to prevent the aggregation of nanoparticles. After a short time, the nanoparticles in the nanofluid have no surfactant attached to other particles, forming a large mass (nanoparticle aggregation) and resulting in rapid nanoparticle sedimentation. Through nanoparticle deposition, the environment becomes nanoparticle free and has properties and capabilities that are similar to those of conventional fluids. Behera et al. [134] studied the spreading behavior and correlation between the surface tension and surface energy of Al_2O_3 nanofluids with different surfactants on tungsten carbide cutting blades and Inconel 718. The results show that the diffusion parameters of the nanofluid vary linearly with the surface tension of the cutting tool. The processing results obtained in this study were interpreted in terms of the spreading coefficient, and the best wetting behavior was observed when a nonionic surfactant was used to add the nanofluids. Therefore, the Inconel 718 machining experiments using the nanofluids described above showed the lowest COF, tool wear, and chip curl radius.

To compare the performance of different dispersants, Amrita et al. [135] measured the thermal conductivity of graphene-dispersed emulsified oil by varying the surfactant type. Based on the surfactant used, the thermal conductivity of 0.1 wt % graphene dispersed emulsifier oil was found to be Triton X100 (TX100) > GA > SO > SDBS > cetyltrimethylammonium bromide (CTAB). Gao et al. [136] analyzed the dispersion mechanism of different surfactants and evaluated the dispersion stability and tribological properties of palm oil-based CNTs nanofluids. The results show that the nanofluid containing APE-10 has the highest viscosity, lowest COF, smallest roughness value, and good surface morphology, indicating its excellent dispersion stability and friction properties. Moreover, APE-10 proved to be the best dispersant for CNT nanofluids under various experimental conditions. Sirin et al. [137] investigated the effects of dry, base fluid, single fluid, and mixed nanofluid cooling and lubrication conditions on the drilling performance of nickel-based alloys. Two dispersants, SDS and GA, were used for the performance comparison experiments with two nanoparticles, including graphene nanoplates and hBN. The results show that the cutting force, hole quality, burr height, and tool wear are the best when SDS is added to the hBN/graphene hybrid nanofluid. The evaluation of surfactants added to nanofluids shows that SDS outperforms GA in terms of machining properties.

In general, the stability of nanofluids is affected by several conditions. It is also necessary to use physical dispersion, as well as a dispersion medium, for the preparation of nanofluids. Therefore, new highly stable nanofluidic solvents need to be developed. Physical methods are widely used in manufacturing; however, the use of dispersants is relatively obscure. Some scholars have not used dispersants in their research, while others have used them irrationally. Special selection manuals or labels should be provided for the production of special dispersants. Therefore, practitioners in the machining field do not need to study the chemical composition of the dispersant in depth, and the appropriate dispersant medium can be selected through the label. This will be of great help to enhance the performance of nanofluids and avoid the waste of resources.

2.2 Fluid performance

The rheological properties of nanofluids directly affect their ability to enter the cutting zone and their performance in the processing zone. Viscosity is the ratio of the shear stress to the shear rate. It is defined as the exchange of energy owing to molecular adhesion forces and irregular motion in the cutting fluid. Viscosity is a measure of the resistance of a liquid to flow. The viscosity of the cutting fluid is an important factor that affects lubrication. During workpiece machining, the relative motion of the workpiece and tool creates shear stress in the cutting fluid at the tool-workpiece interface and thus internal friction in the cutting fluid.

A surface layer is formed at the contact between the liquid and gas, where mutual attraction or surface tension occurs. Surface tension helps the liquid surface automatically contract and maintain its spherical shape. Surface tension is caused by the cohesion between the liquid molecules. Fewer

molecules are present on the surface than in the liquid. The molecules are subjected to a force directed at the liquid, which causes the surface layer to shrink, thereby minimizing the surface area of the liquid.

2.2.1 Viscosity

A high viscosity reflects greater internal friction. Viscosity influences the formation of lubricant films. It is difficult for a cutting fluid with a small viscosity to form a thick and strong lubricating film on a high-temperature friction surface. Because of its low strength and thickness, the bearing capacity of the lubricating film is very small. It is easily destroyed by friction at the tool-workpiece interface, thereby reducing the lubrication effect and increasing the friction between the tool and workpiece. Therefore, it is important to study the effects of different base oil viscosities on the processing properties for the selection of nanofluids. Vegetable oils have different viscosity values owing to the molecular structure of fatty acids. With an increase in viscosity, the COF of the corresponding base oil decreases [97]. This trend is particularly pronounced in castor oil, which has a much higher viscosity than other base oils. Therefore, the COF of castor oil is low [98]. High-viscosity fluids exhibit superior anti-friction and anti-wear effects. Gaurav et al. [89] attributed the improvement in the performance of jojoba oil to the structure of long-chain fatty acids, excellent thermal oxidation stability, and high viscosity index. Cui et al. [46] studied the tribological properties of graphene nanofluids at the grinding wheel–workpiece interface through friction and wear tests. Graphene nanoparticles have a larger specific surface area, which improves the viscosity of the nanofluid and lubrication performance. Yin et al. [52] conducted an experimental study on Ti-6Al-4 V milling to explore the lubrication properties of different nanofluids. The tribological properties of several nanoparticles (Al_2O_3, MoS_2, SiO_2, CNTs, SiC, and graphite) were studied using cottonseed oil as the base oil. The results show that the surface quality of the workpiece can be significantly improved owing to the high viscosity of SiO_2 nanofluids. In another study, Das et al. [138] prepared four groups of nanofluids using ZnO, CuO, Fe_2O_3, and Al_2O_3 nanoparticles for the hard turning of AISI 4340 steels. Among the four nanofluids, Al_2O_3 and CuO had the highest and lowest viscosities, respectively. When comparing the four nanofluids used, the CuO nanofluids showed the best performance, while the Al_2O_3 nanofluid ranked last. This is negatively correlated with the viscosities of different fluids. This indicates that viscosity is not the only contributing factor in machining.

Viscosity also affects the infiltration ability of nanofluids. The nanofluid droplets enter the cutting zone at a certain speed and angle. The permeability of the droplets affects the heat exchange efficiency and thus the heat exchange ability of the nanofluids. Viscosity is one of the factors that affect the infiltration ability of nanofluids. Owing to inertia, the droplets continue to flow forward after entering the tool-workpiece interface. However, as shown in Fig. 15, the viscosity force on the contact surface between the nanofluids and workpiece impedes the displacement of the droplets. Consequently, high-viscosity fluids have poor fluidity and short flow distances, making it difficult to penetrate the clearance of the cutting zone [96]. In contrast, low-viscosity lapping fluids can effectively penetrate these gaps. Therefore, a low viscosity results in high permeability of the liquid.

The literature shows that the addition of nanoparticles to the base fluid results in an increase in the dynamic viscosity of the nanofluid. Nwoguh et al. [139] introduced the experimental research results of using Al_2O_3, MoS_2, and TiO_2 nanoparticles to form nanofluids to enhance the viscosity and thermal conductivity of high-oleic acid soybean vegetable oil for machining hard-cutting metals. The results show that the viscosity of high-oleic acid soybean oil increases with increasing nanoparticle concentration, but the suspension stability of the nanofluid decreases. The thickening and entanglement mechanisms of nanoparticles are responsible for the viscosity behavior of nanofluids. In the machining of Inconel-718, lower oil flow rates can be applied because of the increased viscosity for optimal performance, reduced power consumption, and reduced negative impact on the environment. Zhang et al. [95] used nanofluids to grind 45 steel workpieces. The effect of adding MoS_2 nanoparticles with a size of 50 nm was studied. The experimental results show that high-viscosity nanofluids significantly reduce the

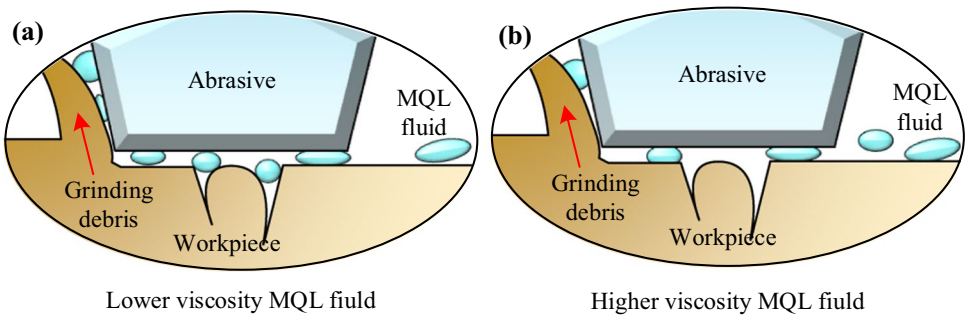

Fig. 15 Influence of viscosity on infiltration [96]

heat transfer performance while improving the lubrication performance. Considering the lubrication and heat transfer performance, soybean oil with the lowest viscosity is the best choice for the base oil. With an increase in the fraction of MoS_2 in soybean oil, an increase in the viscosity of nanofluids leads to an improvement in lubrication properties. However, a fraction that is too high can cause nanoparticles to agglomerate and destroy the lubrication properties. In the experiment, 6 wt % was determined to be the best concentration of MoS_2 nanoparticles.

Moreover, the viscosity of the nanofluids decreases with increasing temperature [139, 140]. The main reason for this decrease is that as the temperature increases, the interactions between the fluid molecules weaken. Bertolini et al. [140] selected graphene as a nanoadditive phase to prepare nanofluids. As shown in Fig. 16, the results show that the viscosity of pure oil can be improved by the addition of graphene at different temperatures. Meanwhile, the viscosity decreases with increasing temperature. Therefore, the viscosity index is another nanofluid index to be considered. The viscosity index indicates the degree to which the viscosity of a fluid varies with the temperature. A higher viscosity index is desirable because it indicates little variation in viscosity over a wide range of temperatures. Conversely, a lower value of the viscosity index indicates greater viscosity variation over a wide range of temperatures. This implies that the lubrication film becomes extremely thin at high temperatures and extremely thick at low temperatures. Talib et al. [102] found that the presence of hBN in base oil significantly increased the viscosity index by 2–14% compared to samples without hBN nanoparticles. The viscosity index value increased significantly with increasing hBN concentration. A high viscosity index ensures stable lubrication over a wide range of operating temperatures.

2.2.2 Surface tension

The contact angle is the angle between the tangent line of the gas−liquid interface and the solid−liquid boundary. The tangent line of the gas−liquid interface is drawn based on the intersection of the gas, liquid, and solid. A small contact angle of the droplets represents a large penetration area. The area of penetration is called the effective lubrication area of the nanofluids. A large and effective lubrication area yields a better lubrication effect. When the contact angle of the droplets is too large, the effective lubrication area of the cutting fluid is too small to provide sufficient lubrication. In the majority of current literature, nanofluids are injected into the cutting area in the form of a mist through a nozzle. Surface tension is an important parameter that affects droplet breakage and tearing. Therefore, the state of droplets on the workpiece determines the lubrication effect. In general, the surface tension has a significant effect on the boiling heat transfer process, wetting behavior, and spray characteristics of nanofluids. Das et al. [141] measured the surface tension of nanofluids. They found that the addition of nanoparticles to the base fluid reduced the surface tension.

1. Effect of surface tension on wettability

Wettability describes the ability of fluids to diffuse, permeate, and cover tools and artifacts. The smaller the contact angle is, the better the wettability of the fluid. Wettability is the ability of a liquid to maintain its contact with a solid surface. Therefore, wettability is an effective parameter for evaluating lubrication and cooling. The surface tension controls the wettability of a surface. The adhesive force between the liquid and solid causes droplets to spread onto the surface. Cohesion within the liquid prevents the droplet from coming into contact with the surface. When the contact angle is large, a less wet surface is obtained. As the droplet spreads on the solid surface, the contact angle decreases. Thus, a well-wetted surface shows a lower contact angle, whereas a poorly wetted surface shows a higher contact angle [62]. Most liquids are fully wetted by high-energy surfaces such as metals, glass, and ceramics. The lubrication/cooling performance of the fluid is mainly affected by its penetration into a large number of capillaries in the tool-chip contact area during machining. The cutting fluid penetrates into the cutting area through the capillary tube and generates adsorption or chemical reaction on the contact surface of the tool, chip, and workpiece, forming a lubrication film

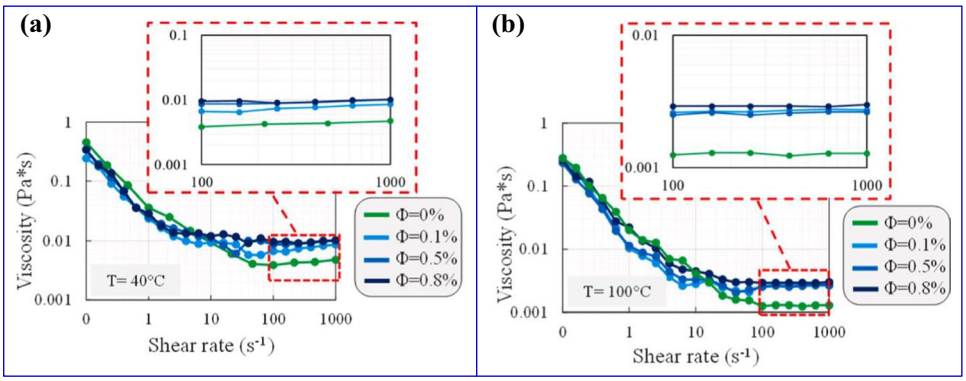

Fig. 16 Viscosity of nanofluids at different temperatures [140]

and playing a lubrication role [142]. The heat generated by plastic deformation in the first deformation zone and friction in the second deformation zone are reduced, which is the indirect cooling effect produced by lubrication. Moreover, the cutting fluid penetrates the cutting area, and through conduction, convection, and vaporization, the cutting tool, workpiece, and chip on the cutting tropics go, reducing the temperature of the cutting area, which is a direct cooling effect. Therefore, the process of cutting fluid penetration into the cutting zone directly affects lubrication and cooling.

2. Effect of surface tension on atomization performance

In the atomization process, the nozzle structure, jet parameters, and physical properties of the nanofluids affect the atomization effect. As shown in Fig. 17, the surface tension is an important parameter that affects the atomization effect of nanofluids. The smaller the surface tension is, the easier the droplet breakage and the better the atomization effect. When the nanofluid is ejected from the nozzle to the cutting zone, the lower the surface tension of the nanofluid is, the smaller the droplets that are atomized. The smaller the droplet, the easier it is to obtain between the friction interfaces because of the smaller cutting area. Therefore, different droplet sizes resulted in different cooling and lubrication effects of the nanofluids in the cutting zone. Su et al. [91] found that the surface tension of an LB2000-based nanofluid was lower than that of a Prieco6000-based nanofluid under the same mass fraction of graphite nanoparticles. Therefore, LB2000 nanofluids can obtain smaller droplets during atomization than Prieco6000-based nanofluids. Therefore, the penetration ability of the LB2000 nanofluid MQL fog is better than that of the Prieco6000 nanofluid. Jia et al. [79] believed that according to liquid atomization theory, reducing the liquid surface tension is beneficial for improving the atomization characteristics. Therefore, the utilization rate and migration permeability of the lubricant can be further improved.

3. Effect of surface tension on heat transfer

Zhang et al. [143] analyzed the influence of the contact angle on the effect of MQL grinding. They found that the contact angle significantly affects the surface quality of the workpiece. A small contact angle leads to a low surface roughness of the workpiece. It can also produce good cooling and lubrication effects, as small contact angles representing large permeation areas and contact angles of nanofluid droplets completely cooled and lubricated by MQL grinding fluid can significantly affect the lubrication and cooling [95]. For boiling heat transfer, this effect is manifested in the wettability of the droplet. High-contact-angle surfaces tend to reduce the heat-transfer coefficient compared to surfaces with lower contact angles. Liquids with lower surface tension are more effective in heat transfer, whereas liquids with greater surface tension are ineffective in heat transfer. As the contact angle decreases, the droplet becomes thinner, and the contact area becomes larger. Liquids have lower surface tension and are well spread, thus covering more of the surface area for heat transfer. Fluids with higher surface tensions exhibit the opposite result [138]. The surface tension of nanofluids is negatively correlated with boiling heat transfer. Moreover, surface tension plays an important role in boiling heat transfer, particularly during bubble formation, expansion, separation, and motion. The low surface tension of the nanofluids indicates that the binding force on bubble formation and expansion is weak. Therefore, there are many bubbles and a highly active boiling heat transfer.

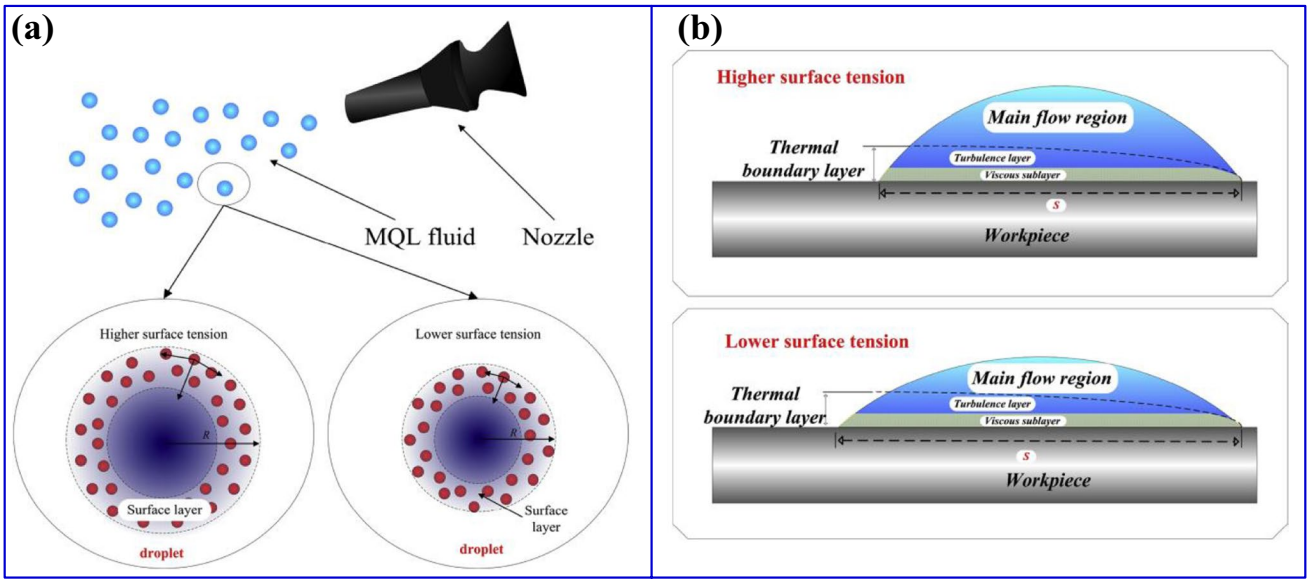

Fig. 17 Effect of surface tension on atomization and heat transfer [96]

The presence of more bubbles and high boiling heat transfer activity are conducive to obtaining excellent performance, such as reducing the temperature in the grinding zone, avoiding workpiece combustion, and improving the machining quality of the workpiece [53].

Furthermore, according to the theory of thermal convection, the droplets in the process of thermal convection can be divided into a thermal boundary layer and a mainstream zone. The thickness of the thermal boundary layer remains the same. However, the fluid in the main flow zone moves quickly from the cutting zone before it absorbs sufficient heat. In other words, the fluid in the mainstream region does not provide a satisfactory heat exchange effect. As shown in Fig. 17, when the surface tension decreases, the thermal boundary layer expands, and the proportion of abrasive fluid in the main flow area decreases [96]. This result explains why the MQL droplets with smaller contact angles have a high cooling efficiency.

2.3 Thermal performance

In the machining process, the high heat flux in the grinding and cutting zones causes the workpiece and tool to generate heat, resulting in adhesion or wear. Therefore, the thermal properties of nanofluids are important factors that affect the processing results. The heat transfer coefficient refers to the surface convective heat transfer coefficient (CHTC) characterizing the performance of convective heat transfer between a fluid and a solid surface [144, 145]. Scholars and engineers agree that nanofluids can significantly improve heat transfer coefficients [146–148]. Here, we mainly focus on the process of processing the heat transfer coefficient. Mao et al. [149] divided four different stages according to the heat transfer mechanism of liquid droplets at different surface temperatures: the nonboiling heat transfer area, nucleating boiling heat transfer area, transitional boiling heat transfer area, and stable film boiling heat transfer area. Moreover, a relevant mathematical model of the heat transfer in the grinding zone was established. The simulation results for the surface temperature in the grinding process agree well with the experimental results, which show that the theory of the surface heat transfer coefficient is reliable. Mao et al. also showed four stages of boiling heat transfer of the lubricating medium with respect to temperature change: nonboiling heat transfer, nucleate boiling, transition boiling, and stable film boiling. In the nonboiling zone, the heat-transfer coefficient remained unchanged. In the nucleate boiling region, the heat transfer coefficient increases rapidly with increasing temperature, and the heat transfer coefficient is at its maximum when the critical heat flux density is reached. In the transition boiling zone and stable film boiling zone, the heat transfer coefficient decreases with an increase in temperature. The transition boiling region was significantly reduced, but the stable film boiling region tended to be moderated. Li et al. [53] found that CNT nanofluids with high thermal conductivity exhibit good heat transfer performance. The energy ratio coefficient of heat transferred to the workpiece by MQL grinding was 40.1%. This implies that approximately 60% of the heat generated by the CNT nanoparticles was not transferred to the workpiece. Moreover, a mathematical model of the CHTC is established based on boundary layer theory. The model calculation shows that CNT nanofluids have the highest heat transfer coefficient of 1.3×10^4 W/(m^2 K), which explains the excellent heat transfer performance of CNT nanofluids. Cui et al. [150] used a calculation formula for the energy ratio coefficient of the cooling medium to characterize the heat transfer performance. The results show that the energy ratio coefficient can be increased by 36.4% by using a temperature nanolubricant. Because of its high viscosity, the low-temperature nanolubricant shows excellent abrasive performance, and the convective heat transfer ability is significantly improved. The critical cutting depth and plastic stacking were significantly reduced, thus reducing the surface defects.

The modeling of convective heat transfer behavior in MQL processing has been extensively studied. Shen et al. [151] found that the average CHTC in the contact zone of pouring grinding was estimated to be 4.2×10^5 W/(m^2 K), and the average CHTC in MQL grinding was estimated to be 2.5×10^4 W/(m^2 K). Hadad and Sadeghi [152] considered the effects of conventional fluid parameters and MQL techniques (such as air pressure, oil mist velocity, and oil droplet characteristics) to predict the fluid convection coefficient. Using this analysis program, the surface heat flux and subsurface temperature distributions in the grinding area can be calculated according to the grinding process parameters. The average CHTC estimated and measured in the grinding contact zone was approximately 3.7×10^4–4.3×10^4 W/(m^2 K).

Regarding the convective heat transfer behavior of NMQL, Yang et al. [64] discussed the influence of nanoparticle size on heat convection in the cooling method. Nanofluids using 30 nm nanoparticles exhibited the greatest thermal convection coefficient and the lowest mean surface temperature. The results confirmed a positive correlation between the average surface temperature of the workpiece and the size of the nanoparticles. In subsequent studies, Yang et al. [153] analyzed the atomization mechanism of nanofluid aerosol cooling, revealed the influence of jet parameters on spray boundaries, and performed a statistical analysis of the probability density of the droplet size in the grinding zone. Based on an analysis of the heat transfer coefficient of a single nanofluid droplet, a theoretical model of the cooling convection heat transfer coefficient of nanofluid aerosols is established. Moreover, a new method is proposed to measure the convection heat transfer coefficient of aerosol cooling. Figure 18 shows

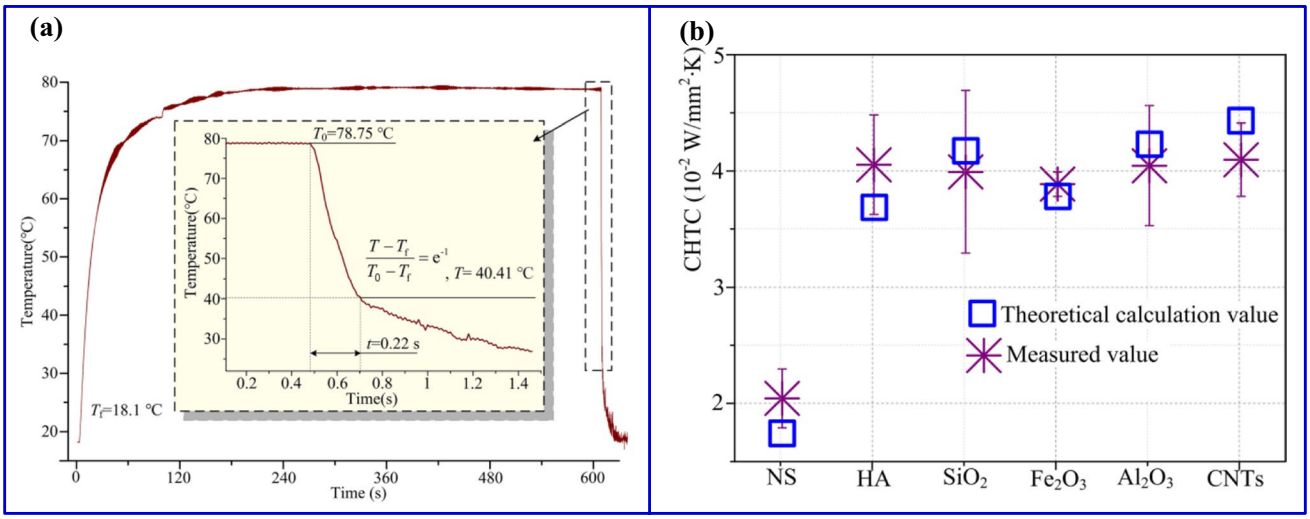

Fig. 18 CHTC of nanofluids [153]

the theoretical calculation and measured CHTC of pure normal saline aerosol cooling and nanofluid aerosol cooling using HA, SiO_2, Fe_2O_3, Al_2O_3, and CNT nanoparticles. The CHTC of nanofluid aerosol cooling using HA, SiO_2, Fe_2O_3, Al_2O_3, and CNT nanoparticles increases by 141.98%, 137.65%, 130.25%, 141.36%, and 145.06%, respectively, compared to the CHTC of pure normal saline aerosol (1.62×10^{-2} W/mm^2 K). The theoretical calculation value of CHTC is also consistent with the actual measurement value, and the model error is 7.26%, which verifies the correctness of the theoretical model.

Moreover, some scholars have analyzed the heat transfer behavior under the coupling effect of low temperature and NMQL. Zhang et al. [154] simulated the temperature field in a grinding zone under different cooling conditions. The results show that the composite process of cold air and NMQL has the best cooling effect, followed by low-temperature cold air and NMQL. Furthermore, Zhang et al. [155] established a CHTC model of cold air nanofluids in vortex tubes based on boiling heat transfer conduction theory and conducted numerical simulations of the finite difference and temperature field in the grinding zone under different cold air fractions in vortex tubes. The simulation results show that with an increase in the cold air fraction, the maximum temperature initially decreases and then increases. The effectiveness of the CHTC model was verified through an experiment on Ti-6Al-4 V.

In conclusion, the high heat transfer coefficient of the nanofluid reduces the thermal damage to the workpiece. When the low-temperature medium was coupled, the heat-transfer coefficient was further improved. Therefore, nanofluids are recommended for machining low- and medium-cutting parameters and for easily cutting materials. In the case of high-efficiency parameters and difficult materials, the idea of solving the large heat flux is to adopt the coupling process of a low-temperature medium and nanofluids.

2.4 Tribology performance

Under the effects of high temperature and high stress, the tool rake face chip and tool flank face workpiece produce strong friction. Wear is divided into mechanical and thermal wear. The wear caused by the intense friction between the elastic deformation of the rake face chip and flank face-workpiece machining surface is called mechanical wear. When the heat flux is not too high, mechanical abrasion caused by this friction is the main cause of tool wear [156, 157]. Owing to the intense plastic deformation of the metal and friction generated by the cutting heat, the hardness of the blade is reduced, and the loss of cutting performance is caused by wear, which is called thermal wear.

2.4.1 Coefficient of friction

For nanoparticles with high surface energy, the nanoparticles penetrate the space between the contact surfaces and gradually deposit on the friction surface, finally forming a thin friction film [158, 159]. The friction-reduction mechanism of nanoparticles with different characteristics at the friction interface is diverse. Influenced by external loads, high contact pressures are created between friction pairs, and nanoparticles with high hardness can roll on the friction surface, such as bearings, and transform sliding direct friction into rolling indirect friction [35, 160]. Near-spherical nanoparticles can change the friction patterns between the friction pairs, reducing friction and causing a ball effect. Another type of nanoparticle that can be used as a solid lubrication medium can form a layer of lubricating oil film

on the friction surface, thereby causing a certain anti-friction effect. Owing to the looseness, flexibility, and malleability of the nanoparticles, the film shed during sliding can be replenished and quickly renewed by subsequent adsorption, thus easing friction. Cui et al. [46] verified the reduction in the COF using a frictional wear experiment, as shown in Fig. 19.

Mao et al. [161] studied the role of NMQL in the grinding process using friction and wear experiments. The results show that the nanoparticles added to the base body fluid, especially Al_2O_3, exhibit obvious friction reduction and anti-wear properties. Compared to pure deionized water, the COF was reduced by 34.2% after adding Al_2O_3 nanoparticles to deionized water. Akincioglu et al. [162] studied the influence of hBN nanofluid on the COF and wear resistance of AISI 316 L stainless steel. HBN nanoparticles were added to 0.50 vol % vegetable oil, and the nanofluids were prepared by a two-step method. The results show that the COFs of oil and hBN nanofluid tests are 72.46% and 77.64% lower than those of dry tests under an 8 N load, respectively. Kumar et al. [163] investigated the friction and wear characteristics of water-based nanofluids. Al_2O_3, hBN, MoS_2, and WS_2 nanoparticles were used to prepare deionized water-based nanofluids, and a tribological study of the nanofluids was carried out on a spherical tribometer in MQL mode on the Ti-6Al4 V workpiece. The influence of different velocities of nanofluids on the COF of the workpiece has been reported. Compared to other nanofluids, Al_2O_3 nanofluids exhibit excellent friction and wear properties. Compared with dry conditions, the COF of Al_2O_3 nanofluids in MQL mode was reduced by 53.89%. Singh et al. [164] dispersed Al_2O_3 and ZrO nanoparticles in jatropha oil to develop biodegradable nanofluids. The tribological properties of the nanofluids were investigated using Hastelloy C-276 and tungsten carbide pin wear tests. The experimental results show that the COF decreases significantly. Compared to dry conditions, jatropha oil, Al_2O_3 nanofluid, ZrO nanofluid, and hybrid nanofluid decreases by 83.3%, 85%, 80%, and 81.6%, respectively.

Kulandaivel et al. [165] investigated the machinability of a Monel K500 alloy using graphene oxide-based jojoba oil as the biolubricant. Experiments were conducted under dry, submerged, MQL, and NMQL conditions. The results show that NMQL reduces the COF by 0.051 under extreme wear conditions, and the lubrication state is enhanced. Yin et al. [166] evaluated the milling properties of 45 steels under different lubrication conditions (dry, flooding, MQL, and NMQL). The results show that compared with other lubrication conditions, NMQL achieves the minimum milling force peak value and COF. Li et al. [167] evaluated the tribological properties of NMQL grinding. The results show that, compared with dry grinding, the coefficients of friction of MQL grinding, NMQL grinding, and flooding grinding are reduced by 11.22%, 29.21%, and 32.18%, respectively. Jia et al. [168] demonstrated the lubrication properties of nanoparticles during surface grinding. The results show that, compared with dry grinding, the tangential grinding forces of MQL grinding, NMQL grinding, and flood grinding decreased by 45.88%, 62.34%, and 69.33%, respectively. Wu et al. [169] used YG8 to perform surface grinding experiments under four working conditions (dry, flooded, MQL, and NMQL) to verify the effectiveness of NMQL grinding. The results show that the minimum specific grinding force, COF (0.21), and specific grinding energy are obtained by NMQL grinding. Singh et al. [170] found that 1.5 wt % graphene in rapeseed oil-based NMQL resulted in 16.9%, 22.1%, 33.83%, and 15.1% reductions in surface roughness,

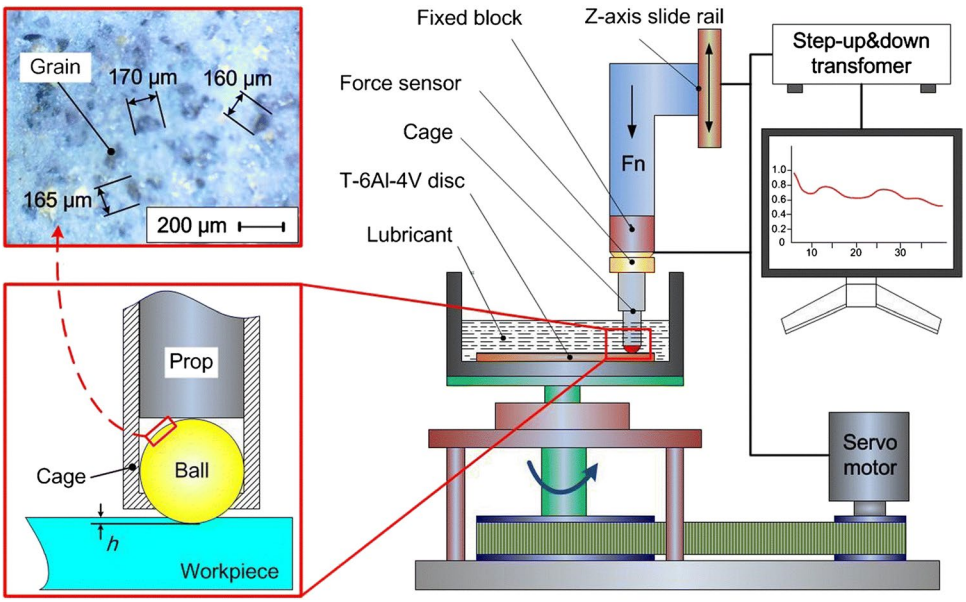

Fig. 19 Friction and wear test system [46]

grinding force, specific grinding energy, and COF, respectively, compared to conventional overflow cooling. Pal et al. [171] compared the abrasive properties of AISI 202 stainless steel under various lubrication conditions. The results show that the performance of NMQL lapping using vegetable oil is much better than that of dry, wet, and pure MQL processing. Under the condition of a 1.0 wt % concentration of MoS_2 nanoparticles, the minimum normal force and tangential force under MQL lashing conditions are 9.2 N/mm and 0.76 N/mm, respectively. Compared with dry conditions, 43% and 33% less, respectively. Zhang et al. [172] studied the machining of carbide YG8 under four grinding conditions (dry, flooding, MQL, and NMQL slip). The minimum COF was 0.385 under NMQL.

It is noteworthy that the antiwear and antifriction effects of nanofluids can be further enhanced by external devices. As shown in Fig. 20, Guo et al. [173] designed a textured tool based on bionics that was used to enhance the machining performance of intermittent cutting together with nanofluids. The results show that the integration of bionics-based NMQL with the tool surface microstructure results in lower values of the COF, cutting force, tool temperature, tool wear, and surface roughness. Furthermore, ultrasonic vibration machining changes the material removal mechanism owing to intermittent cutting behavior [174–177]. A typical study showed that grinding forces and temperatures in UVG can be reduced by 41% and 40%, respectively [178]. Rabiei et al. [179] studied the tribological properties of ultrasonic vibration-assisted grinding using NMQL. The results show that the combination of NMQL and ultrasonic-assisted grinding reduces the COF to 27.3% compared to dry grinding. Moreover, the shiny surface is free of any thermal damage and combustion compared to the dark and charred surfaces obtained by dry grinding.

Nanofluids greatly reduce the friction at the interface. The reduction in friction force not only reduces the mechanical and thermal loads but also changes the friction angle during the material removal process, thus changing the shear angle in the material shear zone. Therefore, the application of nanofluids in processing can alter the material removal mechanism. The interface friction behavior under the effects of nanofluids must be further quantitatively characterized to establish analytical mathematical models of the cutting forces. Behera et al. [180] studied the prediction of machining force under minimal lubrication by considering the contact length and chip thickness. The double contact zone theory (viscous sliding) was used to simulate the friction force during MQL processing. A model of the local COF was developed as a function of the cutting conditions and MQL parameters. The model predicted the cutting force, contact length, and chip thickness in MQL with reasonable accuracy, which was also verified by experimental work. To further improve the model, it is necessary to consider the effect of nanofluids on the friction interface.

2.4.2 Interface wear

The nanoparticles in the lubricant migrated to the surface of the friction pair. They were then deposited on the friction surface to form a deposition film, thereby reducing friction and wear. The instantaneous high temperatures during sliding melted the nanoparticles and simultaneously repaired the damaged surface. Moreover, during the friction process, some high-hardness nanoparticles are used for precision

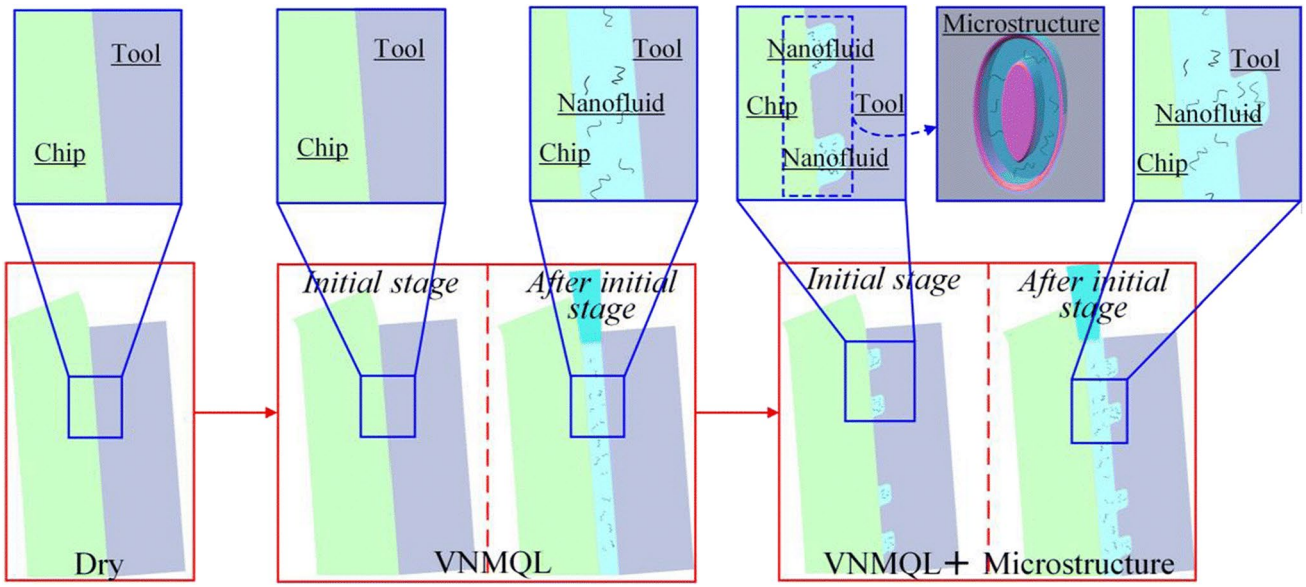

Fig. 20 Friction interface between the textured tool and the workpiece [173]

polishing. After polishing, the roughness of the friction pair was reduced. The contact area increased, thereby reducing the COF. Furthermore, the compressive stress on the contact surface is also reduced, which increases the bearing capacity of the lubricant; this is known as the nanoparticle polishing mechanism.

The addition of nanofluids can significantly reduce the wear. Mao et al. [161] studied the role of nanofluids in the MQL grinding process using friction and wear experiments. The results show that compared with pure deionized water, the wear weight is reduced by 43.4% after adding Al_2O_3 nanoparticles to deionized water. Nunez et al. [181] used MQL spray lubrication mixed with TiO_2 in the turning process of AISI 304 steel to improve the surface quality and reduce cutting tool wear. The results show that vegetable oil containing $0._{5\%\ TiO2}$ increases the surface roughness by 50% and reduces the tool flank surface wear by 25%. Yin et al. [166] performed a spectral analysis of milling force. Spectral analysis of the milling forces shows that NMQL obtains the lowest milling force and amplitude in the mid-frequency region, thus indicating the least tool wear loss.

The form of tool damage at the friction interface also changed. Roushan et al. [107] used water and CuO nanofluids for micromilling Ti-6Al-4 V. The results show that at a low concentration (0.25 vol %), the surface roughness of the CuO nanofluids for WC tools coated with AlTiN is minimal, whereas at a higher concentration (1 vol %) of water-based CuO nanofluids, the tool wear and accumulation edge formation are reduced. Yucel et al. [182] processed AA 2024 T3 with different cooling/lubrication strategies and analyzed the main tool wear mechanism under MQL of a mineral oil-based MoS_2 nanofluid. Under dry cutting conditions, the cutting tool produced dense built-up edges and layer formations. However, the formation of the built-up edge was significantly eliminated by the nanofluid. As shown in Fig. 21, there is less cutting-edge damage when machining aluminum alloys under NMQL compared to dry cutting and MQL environments. Gunan et al. [183] added Al_2O_3 nanoparticles to plant-based cutting fluids to prepare nanocutting fluids with different volume concentrations (0.5, 1.0, and 1.5 vol %). The prepared nanofluids were used in MQL systems during the milling of Hastelloy C276. According to tool wear analysis, a low percentage diameter reduction and stacked edge formation were observed in uncoated WC micro end mills under 1 vol % CuO NMQL. The high concentration of the CuO nanofluid in the cutting zone emits high heat dissipation. Meanwhile, lower and upper milling burr widths were measured in all cutting environments, and it was observed that coated cutters with 0.25 vol % CuO NMQL performed better and produced lower burr widths.

Reduced wear results in an improved tool life. Minh et al. [184] investigated the potential properties of Al_2O_3 nanoparticle-based cutting fluids in hard milling under various lubrication conditions. With Al_2O_3 nanofluids, the tool life was improved by nearly 177–230% with MQL owing to better tribological behavior and cooling effects. Sirin and Kivak [123] studied the machining properties of an Inconel X-750 superalloy using hBN, graphite, and MoS_2

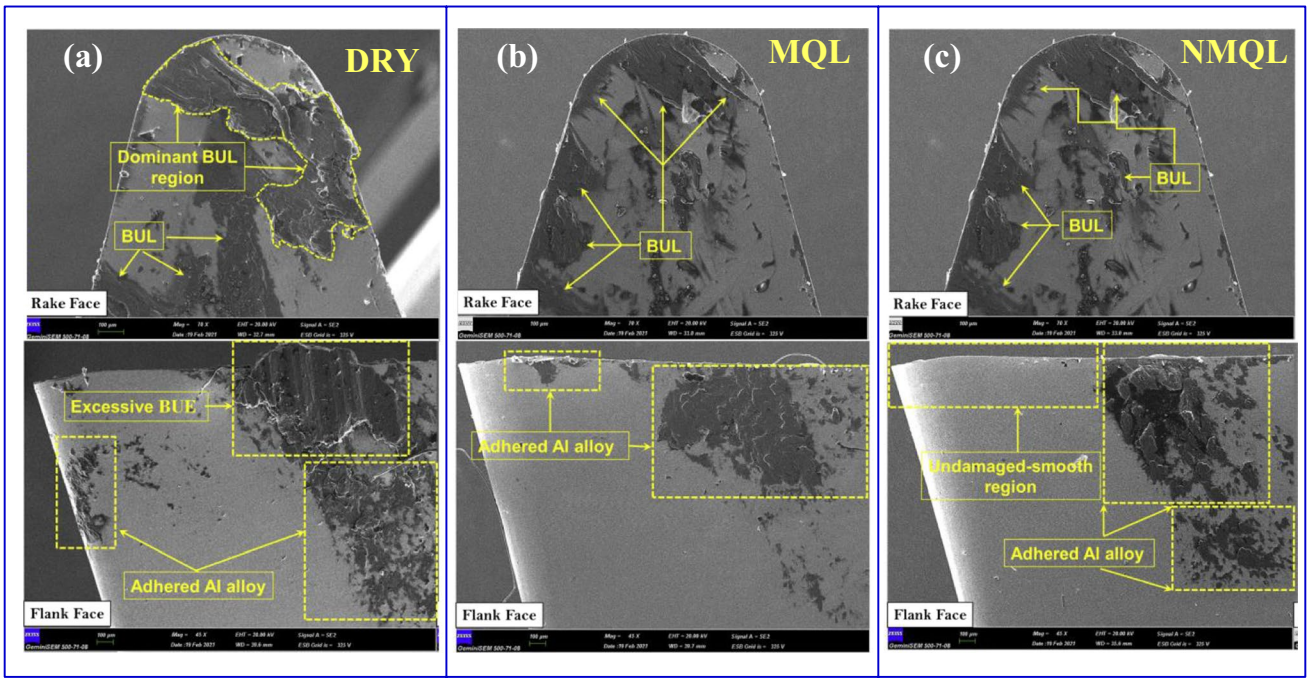

Fig. 21 Tool wear under different conditions [182]

nanoparticles with different shapes and properties. According to the experimental results, it can be seen that hBN/graphene mixed nanofluids are superior to hBN/MoS_2 and graphene/MoS_2 among all performance criteria. Compared with graphene/MoS_2 and hBN/MoS_2 nanofluids, the tool life of hBN/graphene hybrid nanofluids was increased by 36.17% and 6.08%, respectively. Kumar et al. [49] found that the tool life of TiO_2 nanofluids with 0.01 wt% concentration was 154 min at the rear tool surface wear standard of 0.3 mm, which was 2.52 times higher than that obtained in dry cutting and 1.47 times higher than that obtained under the impact of air−water spraying. This phenomenon is caused by the excellent wettability, lubricity, and heat dissipation of TiO_2 nanofluids.

It should be noted that not all the conditions of the nanofluid performance were satisfactory. Kivak et al. [101] processed Ni-hard 4 with a coated ceramic tool and found that tool wear mainly occurred at the front end of the cutting blade. As shown in Fig. 22, under pure MQL cutting conditions, the minimum nasal wear during the turning process was 0.171 mm, followed by the graphene NMQL (0.33 mm) and CNT NMQL (0.416 mm). Compared with dry cutting (0.552 mm), the reductions in nose wear were approximately 69%, 40.2%, and 24.6%, respectively. Thus, pure MQL showed the best results in significantly reducing the nose wear of coated ceramic tools. The nanofluids used did not show the expected improvement in tool wear compared with pure MQL.

Owing to the high-performance heat transfer characteristics of nanofluids, the cutting temperature can be significantly reduced during the machining process. Consequently, the thermal adhesion points generated by the friction interface are reduced. Meanwhile, the temperature reduces the thermal load of the friction interface and the thermal stress of the friction pair. Residual tensile stress and microcrack formation were inhibited, and the fatigue damage resistance of the workpiece was enhanced. Moreover, the reduction in friction also reduces the tangential force load, the stripping phenomenon between the interference bumps at the interface of the friction pair, and the mechanical wear.

3 Applications in machining

3.1 Supply system

Nanofluids must be transported to friction and heat production areas, and several feeding and atomizing devices are continually being developed. Atomizing nozzles include conventional pneumatic, electrostatic, and ultrasonic atomizing nozzles.

3.1.1 Devices

1. Nozzle

The typical structure of conventional pneumatic atomizing nozzles is shown in Fig. 23. The lubricant was torn and broken using compressed air to achieve droplet ejection. Bangma [185] developed an MQL system using exhaust gas. Except for a mixture of atomized lubricant droplets, the exhaust airflow can blow chips off the tool/metal interface. Li et al. [186] developed an internal/external intelligent cooling lubrication nozzle system and method. The real-time milling depth of the workpiece was obtained by the vision system and sent to the lubrication mode controller for processing. The control-reversing device operates according to the set milling depth threshold and the data obtained from the vision system to adjust the switch to the internal or external cooling system. Guo et al. [187] invented the structure, separation, recovery mechanism, and system of the MQL

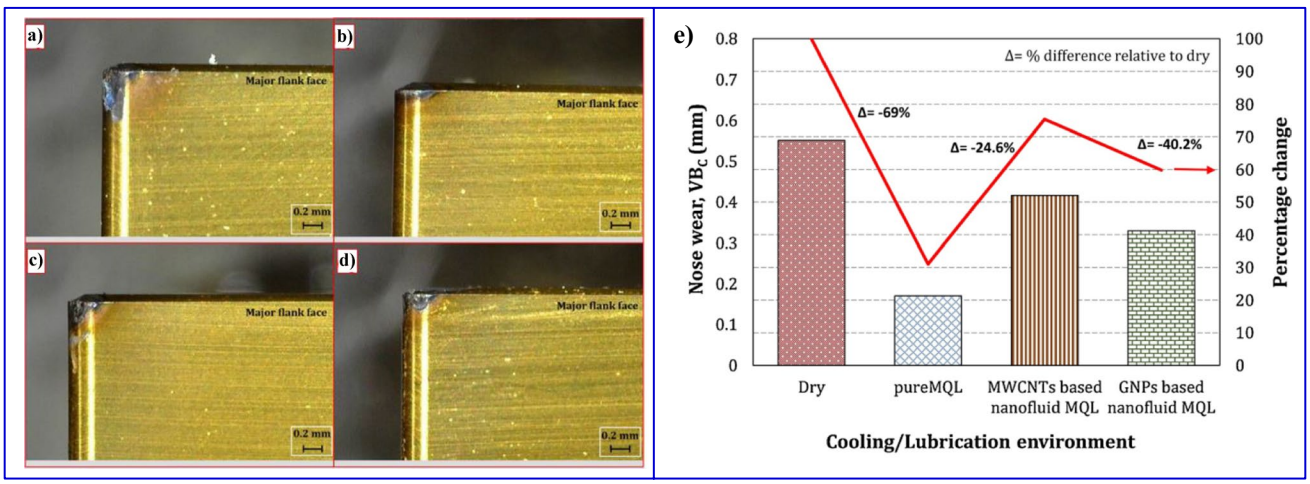

Fig. 22 Wear of ceramic tools with different lubrication modes [101]

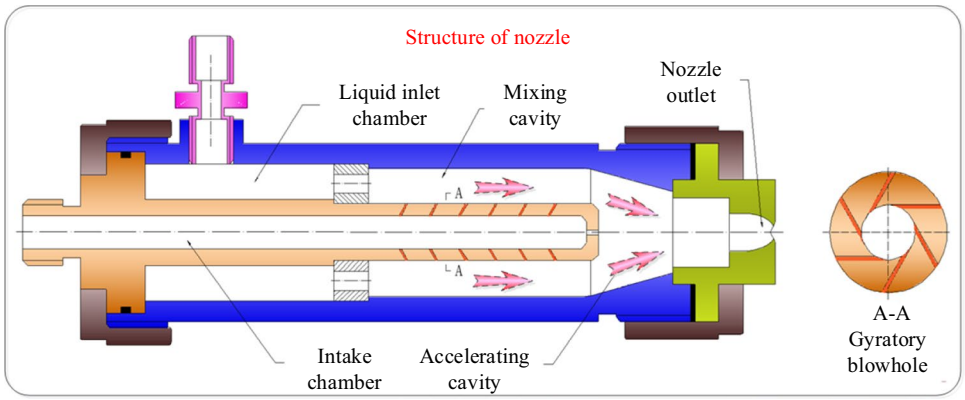

Fig. 23 Pneumatic atomizing nozzle structure

liquid supply nozzle in high-speed milling. The setting of the box can effectively avoid the splashing of the chip and fog droplets, reduce the processing process to the environment, and reduce the harm caused by the operator. Meanwhile, it can effectively realize the separation of lubricants, chips, and gases and reduce pollution to the environment.

A typical electrostatic atomization device is shown in Fig. 24 [77]. The lubricating medium was charged by applying a high voltage. The atomization and infiltration characteristics of the charged lubricant were improved. In the development of an electrostatic atomization nozzle, Yang et al. [188] developed an electrostatic atomization internal cold grinding head, including an electrostatic atomization film-forming part and an internal cold grinding part. It can not only fully atomize the coolant and control the distribution of the coolant drops to effectively reduce the temperature of the grinding area but also spray the medical auxiliary materials to the wound surface after grinding through the electrostatic atomization film-forming device during bone grinding. Jia et al. [189] developed an electrostatic nozzle including a nozzle core and nozzle body. A free space is formed between the upper nozzle body and nozzle core to store compressed air. A gas–liquid mixing chamber, acceleration chamber, and nozzle outlet were arranged inside the nozzle core from top to bottom. A microconvex texture was evenly arranged on the wall of the acceleration chamber. Su et al. [190] developed a method and device for controlling nanofluid droplet spray cutting. The cutting tool was connected to the positive output end of the adjustable high-voltage electrostatic generator through the wire and grounded, and the electrostatic nozzle was connected to the negative output end of the adjustable high-voltage electrostatic generator through the high-voltage cable. The rear end of the charging nozzle was connected to a microinjection pump through a silicone rubber tube, which delivered a nanofluid to the charging nozzle. The adjustable high-voltage electrostatic generator provides a negative high voltage to the charging nozzle and induces a positive charge on the tool surface with polarity opposite to that of the charging nozzle. Xu et al. [191] invented a charged aerosol U-shaped nozzle including a U-shaped shell, aerosol tube, and high-voltage electrostatic transmission wire. One end of the high-voltage

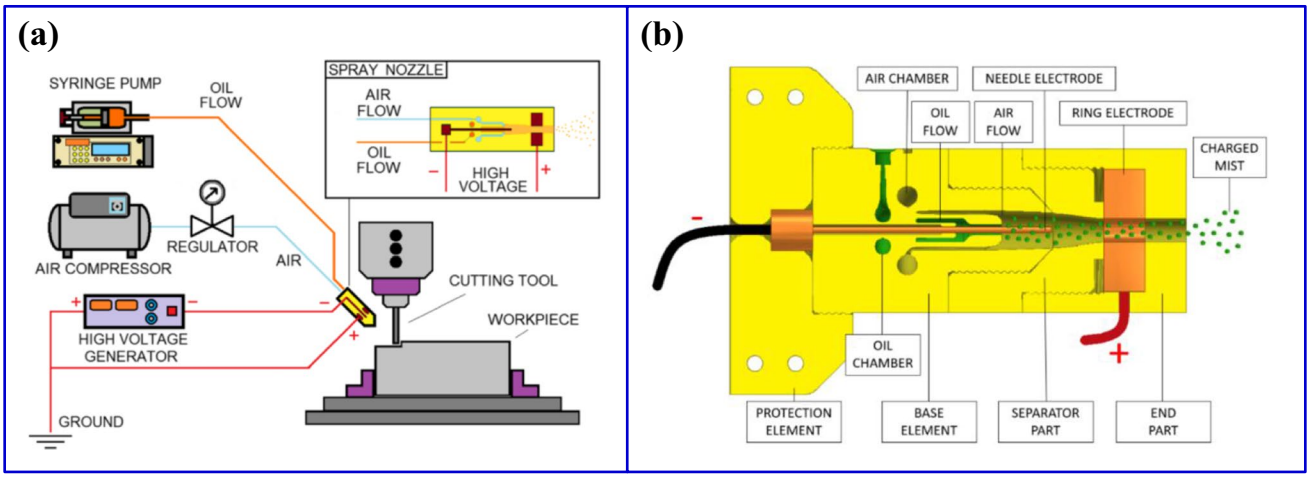

Fig. 24 Electrostatic atomizing nozzle [77]

electrostatic transmission wire was passed through the middle channel of the U-shaped housing. After the high-voltage electrostatic transmission wire enters the U-shaped shell, it is divided in two ways, and each end of the two methods is provided with a charged electrode. The two charged electrodes charged the aerosols in the aerosol tube on both sides. The aerosol exits were arranged on both sides of the U-shaped shell. Furthermore, Xu et al. [192] and Yang et al. [193] combined an MQL device with an electrostatic atomization system. An electrostatic atomization MQL transport device has been developed, which has the characteristics of a compact structure, high integration, and convenient installation.

For the development of an ultrasonic atomization nozzle, Yang et al. [194] developed an ultrasonic focusing auxiliary atomization cooling device. The medical nanofluids after pneumatic-ultrasonic-electrostatic tertiary atomization are broken into droplets. Using the focusing effect of ultrasonic atomization, microdroplets are introduced into the grinding tool-bone wedge space constraints. Li et al. proposed a new structure for a longitude-bend conversion ultrasonic atomization system composed of a longitudinal vibration system and bending vibration disc [195] and further proposed a spherical focused ultrasound-assisted vapor fog cooling system [196]. Based on ultrasonic atomization technology, focused ultrasound was used to focus microdroplets in the cutting/grinding zone. The grinding experiments show that focused ultrasound is helpful in strengthening the heat transfer of steam and fog in the central area and further improves the heat transfer capacity. Zhao et al. [197] developed a type of ultrasonic vibration-atomizing rotary-jet cooling device. The ultrasonic atomized droplets are driven from the nozzle unit to the machining area by high-pressure gas blown into the high-pressure air intake unit in the form of a rotating jet. As shown in Fig. 25, Hadad et al. [86] developed an ultrasonic atomizing MQL nozzle that utilized the Venturi effect to generate primary atomization and enhanced secondary atomization by high-frequency vibrations on the resonant surface of the nozzle tip.

2. Feeding devices

The transport of microdroplets with MQL can be divided into single and double-channel systems according to different pipelines. A single-channel system atomizes the lubricating medium into microdroplets and stores them in a container. Then, the microdroplets in the container were transported to the cutting area through a pipeline and conventional nozzle using differential pressure. The liquid phase was broken into microdroplets through an atomizing nozzle and sprayed directly onto the friction interface of the cut area. The single-channel system is simple in structure and easy to maintain; however, it requires a transport channel. The transport of droplet groups in a single-channel system is easily affected by droplet collision condensation, pipeline droplet rupture, pipeline inner-wall oil film formation, pipeline inner-wall oil film rupture, etc. The single-channel MQL system is simpler to implement [198]. They are typically used for external transportation. In a single-channel system, there are two common methods for generating droplets: the metering pump method and the pressurized tank method. In the metering pump method, lubricating oil is supplied to the air flow by a pneumatic positive-displacement micropump connected to an in-line air nozzle. The

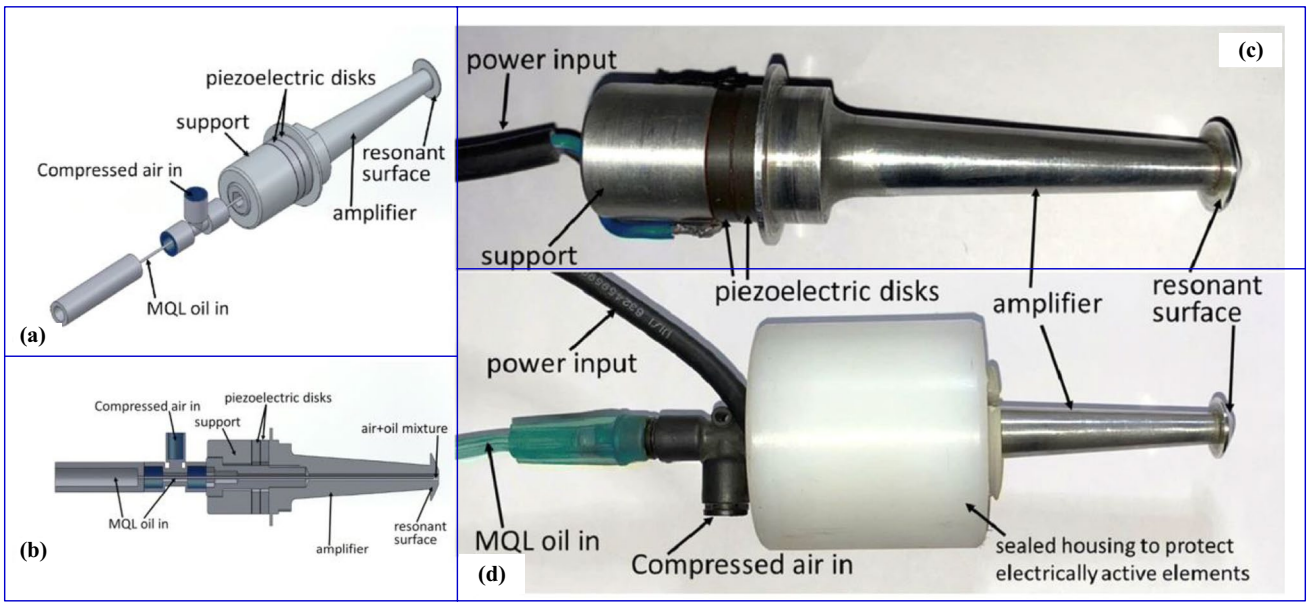

Fig. 25 Ultrasonic atomizing nozzle [86]

quantity of oil generated by the fog supply was adjusted by controlling the speed of the pump. In the pressurized tank method (Fig. 26), the lubricant tank is pressurized, and oil and compressed air are mixed in a Venturi nozzle or similar device to produce droplets. The oil supply was adjusted by adjusting the oil supply pressure setting and throttling element in the pipe. If the air pressure, lubricating oil pressure, and lubricating oil volume can be adjusted separately, then the best control effect can be achieved. This method produces finer fog that becomes more uniform over time. In the two-channel system, oil and air are delivered to the nozzle and mixed near the nozzle tip. A typical two-channel MQL supply device is shown in Fig. 26. The use of a two-channel system is more convenient, less restrictive, and has fewer requirements for transport pipelines. Moreover, according to the liquid-phase transport mode of the double-channel system, it can be divided into pump and no-pump types. The pump-free type uses the Venturi effect to control liquid flow, whereas the pumped type uses a precision lubrication pump to control MQL medium flow [95]. In this system, the flow rate of the compressed air and lubricating medium can be adjusted separately and mixed in a special nozzle to spray atomized microdroplets through the compressed air to the cutting/grinding zone. Compared with other lubrication medium supply methods, a continuous supply of precision lubrication pump transport can achieve accurate control of the atomization performance.

Many new supply devices have been developed. Kapoor et al. [200] developed an atomized cutting fluid system. The system includes a common chamber terminating at a forming droplet nozzle and a nozzle portion immediately behind the forming droplet nozzle. The atomizer produced a spray directly behind the nozzle section in a communal room. Xiong [201] developed an MQL supply system for externally and internally cooled high-speed machine tools. The system adopts a single-channel system supply mode. The lubricating medium entered the atomizing chamber through a microatomizing nozzle. The lubricant was transported to the cutting zone after passing through the primary and secondary settling chambers. Xiong et al. [202] developed a high-pressure pneumatic pulse MQL oil-mist supply system. The pulsed working mode can provide sufficient oil mist, which is conducive to lubrication and chip removal in deep hole processing. Yao et al. [203] developed an electronically controlled precision-adjustable micropump including a liquid container, solenoid valve, controller, and pump body. It is used to solve the disadvantages of traditional mechanical micropumps, such as low adjustment precision, narrow controllable adjustment range, complex structure, and high-precision requirements of accessories. Yuan et al. [204] developed an MQL feeding system. Using a spherical micropump, the lubricant flow in the transmission pipeline of the MQL system can be precisely controlled. Therefore, the lubricant could be accurately and quantitatively obtained from the liquid storage cavity to the nozzle. The atomization method involves pneumatic atomization. Li et al. [205] developed a continuous-feeding precision MQL pump. The pump was driven by a stepping motor to realize intelligent switching under various lubrication conditions. The mixing ratio and flow rate of the oil, water, and gas can be adjusted intelligently. Accurate and continuous filling of the lubricant in the machining area, improving the cooling and lubrication effect, improving the workpiece surface quality, and providing equipment support for the intelligent filling of trace lubricating oil. Jochen et al. [206] developed a machine tool or handheld work tool to dispense lubricating fluids for material processing operations. This technology utilizes capillary action to supply lubricant.

3.1.2 Atomization characteristics

The influence of the atomization supply parameters on the droplet transport of nanofluids has been studied extensively. Rahim et al. [207] compared the atomization performance of MQL with different nozzle outlet diameters. The larger the nozzle outlet diameter is, the larger the atomization cone angle, and the lower the Sault mean diameter, which can be obtained under higher pressure. Obikawa et al. [208]

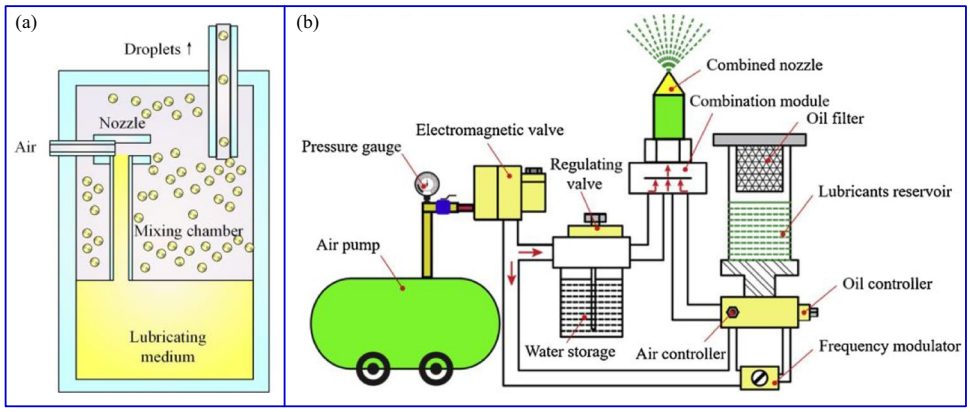

Fig. 26 Atomization feeding system [199]

compared the performance of three types of internal cold tool handles in finishing machining: conventional nozzle, direct injection of the cover plate, and oblique injection of the cover plate. Fluid dynamics analysis showed that the internal cold tool shank with oblique spray had the maximum oil mist transfer rate, and the cutting performance comparison experiment verified the simulation analysis. Alberdi et al. [209] studied the influence of the nozzle structure on the velocity and pressure field using computational fluid dynamics and optimized the design of the Webster nozzle. Grinding experiments show that the improved nozzle can improve the surface roughness of AISI D2 tool steel and the life of the grinding wheel. Balan et al. [210] found through numerical simulations that the droplet size decreases with an increase in the atomization pressure. The numerical simulation results are in agreement with the existing empirical models and experimental measurements. Medium-diameter droplets with a high atomization pressure can penetrate the high-pressure gas barrier layer and effectively lubricate the grinding zone. Park et al. [211] studied the change law of the particle size and distribution of MQL droplets with the nozzle distance and air pressure through a wavelet transform. The results show that the higher the nozzle pressure is, the more droplets are provided. However, with an increase in the nozzle distance, the obtained droplet size is smaller, and the deposited droplet on the surface is smaller. Maruda et al. [212] believed that a larger atomization cone angle would prevent droplet interaction in air, thus ensuring a smaller droplet diameter. Jia et al. [213] found through hydrodynamic analysis that the peak jet velocity of the MQL nozzle increased with an increase in air pressure and gas−liquid ratio and decreased with an increase in nozzle diameter. Emami et al. [214] found that the droplet size in the pneumatic atomization of MQL is affected by the flow rate of the lubricating medium, gas flow rate, and physical properties of the lubricant used. By increasing the atomized gas pressure, the gas velocity increased exponentially. As the flow rate of compressed air increased, the droplet size at the nozzle outlet decreased. Moreover, an increase in the flow rate of the lubricating medium led to an increase in the droplet size. Images captured by high-speed cameras also show that a low gas flow rate leads to a larger droplet size, whereas a high gas flow rate leads to a smaller droplet size, a higher jet velocity, and a large increase in the droplet number. Sai et al. [215] found that the average and median diameters of droplets decreased significantly with an increase in atomized air pressure. From the perspective of the noise reduction mechanism, Zhu et al. [216] analyzed the influence of factors such as the jet velocity, gas−liquid velocity ratio, and azimuth measurement on noise. In aerodynamic atomization, a higher atomization pressure is typically used to improve the atomization performance, including decreasing the droplet size and increasing the droplet velocity, thus improving the droplet infiltration performance and interface friction. However, with an increase in the atomization pressure, the uniformity of the droplet spectrum, surface energy and infiltration characteristics of the droplet, and movement trajectory of the droplet cannot be controlled actively and effectively. A large number of inhalable droplet particles are produced in the process of atomization, and small droplet particles are easily dispersed under the disturbance of high-speed airflow.

For electrostatic atomization, the droplet size is reduced, and the ability to enter the processing area is improved. Shah et al. [78] observed the best tribological and machining properties at 20 kV in the voltage range of 0–25 kV. Compared with the traditional MQL condition, the tool wear under the electrostatic atomization MQL condition was reduced by 38%. Electrostatic atomization MQL technology improves the atomization quality and enhances the penetration ability of droplets into the cutting zone. According to the analysis, at a voltage of 20 kV, small-diameter oil droplets were generated, which may improve the heat removal efficiency. Moreover, smaller droplets can penetrate the gap between the tool and workpiece and provide better lubrication. Lee et al. [69] believed that diamond nanofluid droplets could be injected into the grinding wheel–workpiece contact area more effectively and stably through electrostatic atomization, which improves the workpiece surface roughness. The existence of an electrostatic field causes the lubricating medium to produce an electric wetting effect in the cutting zone. Feng et al. [217] found that electroosmosis has a significant effect on the penetration of cutting fluid in the tool-chip contact zone, which complements and perfects the capillary penetration of the cutting fluid during machining. In the processes of friction and separation, the radial electric field established by the triboelectrification electrostatic potential on the chip and rake face excites the initially escaped low-energy electrons, causing an electron avalanche and microplasma emission, which induces charged particle emission. The polarity of the net charged particles escaping outward from the capillary slit is negative, forming a self-excited axial electric field pointing to the inside of the capillary region. As shown in Fig. 27, the electric field can trigger electroosmosis of the liquid in the capillary. Jia et al. [218, 219] also found that charged soybean oil produces an electrowetting effect in a microchannel in the grinding zone. The migration activity of the MQL medium in the grinding zone and the lubrication effect of the grinding wheel–workpiece contact interface were improved. Furthermore, electrostatic atomization was observed to result in the formation of a metal oxide layer that positively altered the friction behavior in the cutting zone. Brittle metal oxides have been reported to improve wear and abrasion resistance by acting as a lubricant layer between the sliding surfaces [220].

With regard to ultrasonic atomization MQL technology, Jun et al. [221] found that under a low feed rate, ultrasonic

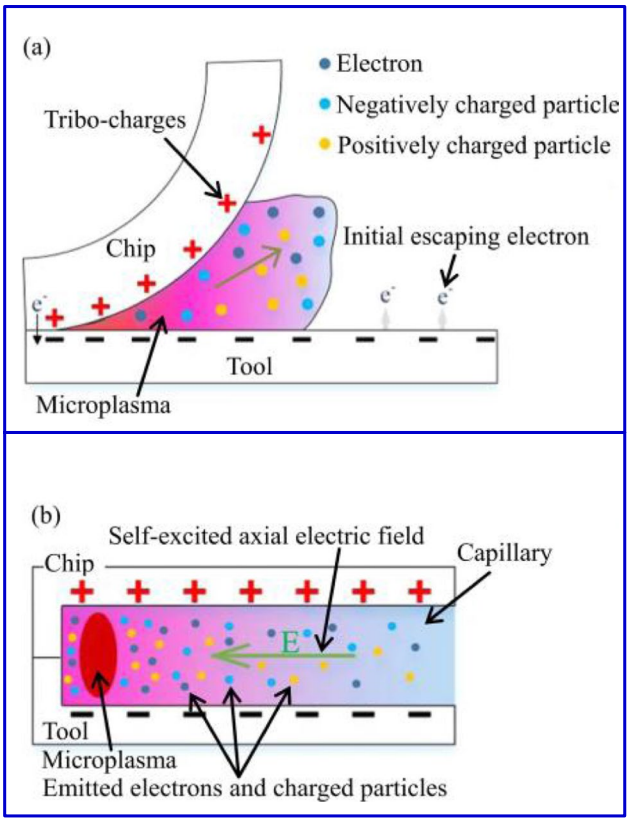

Fig. 27 Effect of electricity on capillary infiltration [217]

atomization MQL technology could significantly improve tool life. This is because plowing/friction is dominant under this condition. Nath et al. [222] found that evenly distributed droplets could form a uniform liquid film during processing. A larger spray distance can reduce the COF at the cutting interface and improve the tool life and surface quality during machining. Hoyne et al. [223] showed that during the machining of titanium alloy, the lubricant produced by ultrasonic atomization MQL could effectively penetrate the tool-chip interface and improve the COF. Hoyne et al. [224] also established a three-dimensional fluid lubrication film analytical model for an ultrasonic atomization MQL system based on Navier−Stokes equations. Hadad et al. [86] developed an ultrasonic atomizing MQL nozzle that utilized the Venturi effect to generate primary atomization and enhanced secondary atomization by high-frequency vibration on the resonant surface of the nozzle tip. Therefore, compared with the traditional pneumatic atomization MQL system, lubrication medium microdroplets have smaller particle sizes and more uniform distributions. Lefebure et al. [87] conducted a study on the atomization performance of biodegradable biolubricants by using ultrasonic atomization MQL. The results show that the size distribution of ultrasonic atomized droplets is affected by the mesh size, driving voltage, and lubricant viscosity. The increase in voltage is beneficial for decreasing the droplet size. At low voltages, viscosity had little effect on the average droplet diameter. However, at high voltages, there is a clear positive correlation. The droplet size greatly increases with an increase in the diameter of the vibrating mesh. Ultrasonic atomization enhances the crushing behavior in the conventional pneumatic atomization process and improves the homogeneity of the droplet size. The three-dimensional fluid lubrication film model established by Hoyne et al. [224] optimizes the ultrasonic atomization MQL process parameters. Lefebure et al. [87] promoted ultrasonic atomization of biological lubricants with higher viscosities.

3.2 Turning

3.2.1 Devices

For the research and development of a new turning process, Li et al. [225] developed an electrostatic atomization NMQL controllable jet-turning system. The system includes an adjustable multinegative power supply, which has a plurality of negative terminals of different voltages and at least one positive terminal interface. Each negative terminal interface works independently of the other. The internal cooling turning tool was equipped with a built-in integrated nozzle and external integrated nozzle. Two nozzles were distributed near the turning tool to provide a lubricating medium. Controllable distribution was realized in the process of spraying, which improved the uniformity of the droplet spectrum, deposition efficiency, and effective utilization of the liquid, controlled the movement law of the droplet, and reduced environmental pollution. Guo et al. [226] developed a magnetic field-assisted turning processing device. The energized coil generates a magnetic field under the energized state during cutting, which can send magnetic nanoparticles to the microtexture. To prevent derivative cutting of the microtextured tool during the cutting process, the residual chips in the grooves were discharged in time. The service life of the microtextured tool was extended, and the surface quality of the workpiece was improved. As shown in Fig. 28, this system was used in a subsequent study [73]. Li et al. [227] developed an intelligent working system for an electrocard-assisted internal cold-textured tool and NMQL. The design of a steerable internal cooling nozzle with an atomization effect was realized, and a precise and controllable supply of trace lubricating liquid was realized. Heat accumulation during the cutting process was reduced by the application of electric card materials.

For the research and development of the following nozzle system for turning processing, Sui et al. [228, 229] designed an intelligent nozzle system for MQL of an NC horizontal lathe. The lateral moving part is composed of an L-shaped fixed bracket and lead screw system. The stepper motor

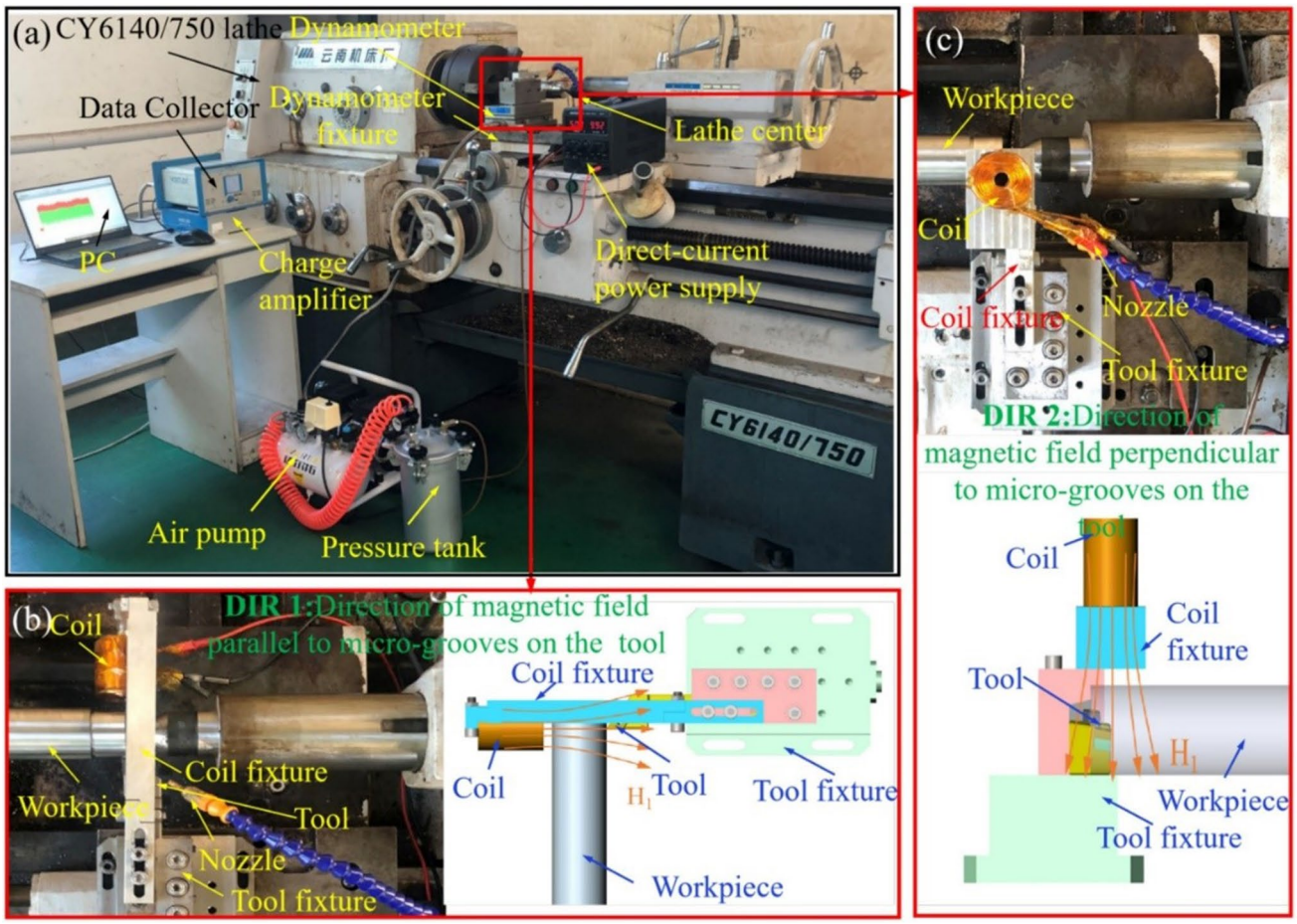

Fig. 28 Magnetic field-assisted MQL processing system [73]

provided the power required for the lateral movement of the lead screw. The longitudinal expansion part is composed of a barrel-fixed outer frame and a lead screw system. The moving part was composed of a power lead screw and three auxiliary sliding rods. The rotating part was driven by a motor or cylinder.

3.2.2 Characteristics

1. Distribution of the flow field

Shen et al. [230] found that in the turning of MQL, workpiece rotation generated negative pressure in the flank face-workpiece wedge area, which was conducive to the entry of the lubricating medium. The atomizing nozzle changes the distribution of the flow field, forming a compound distribution of the negative pressure and pressurization zone. Optimization of the nozzle pose can reduce the influence of the pressurization zone and improve the wettability of the lubricating medium. Chen et al. [231] found that although the airflow could not directly enter the cutting area owing to the blockage of chips, the airflow flow could still be observed from the velocity vector diagram. Air flowed from both sides of the chip to the cutting area. As shown in Fig. 29, there was a high-pressure zone of over 5000 Pa in the cutting zone. The high-pressure zone caused a sharp drop in airflow velocity in the cutting zone. Two vortices were observed. One vortex was generated in the cut zone, and another vortex was generated around the low-pressure zone. These eddies can enhance the heat exchange between the cutting zone and atmosphere. High-speed oil droplets were located at the center of the spray area. The low-speed jet is mostly located at the edge of the spray zone. This is because the oil droplets are slowed by the surrounding air as they leave the sprayer. The droplet near the edge of the spray zone exchanges kinetic energy with the static ambient air, and the droplet velocity decreases rapidly. Therefore, the velocity distribution of the droplet decreased from the center to the edge. Meanwhile, the velocity of the droplet is out of sync with that of the air stream. Droplet inertia is greater than that of air, which causes the velocity of the droplet to decrease less than that of air. The largest droplet was mainly concentrated at the center of the spray zone, and the smallest

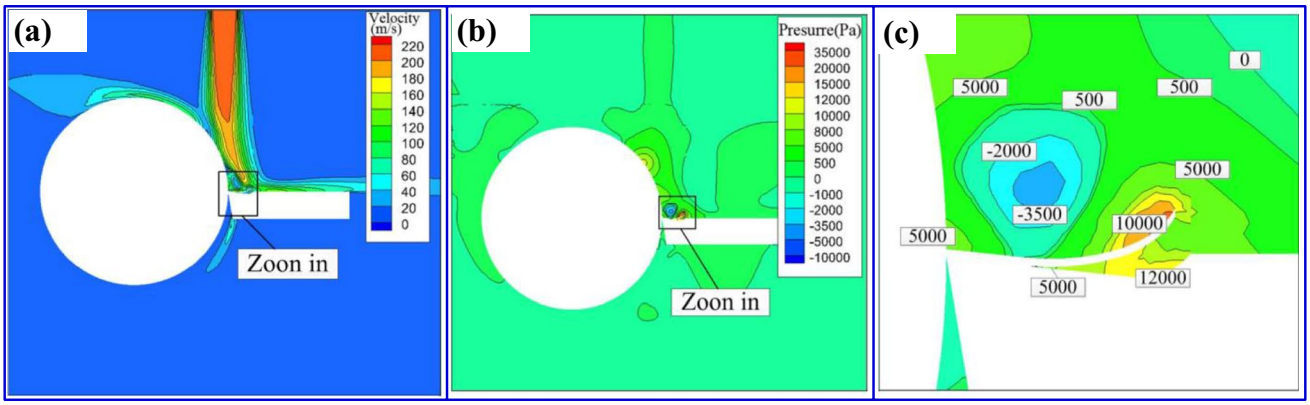

Fig. 29 The flow field of turning [231]

droplet was distributed near the edge of the spray zone. This is because the larger the diameter is, the larger the inertia, and the smaller the transverse fluctuation velocity. Therefore, large droplets do not spread to the edge, and the center of the spray zone is the area with the highest density of large droplets. The droplets entering the cutting area are all large droplets; therefore, these droplets splash when they impact the cutting area boundary. Because of chip obstruction, the oil droplets do not directly enter the cutting area. However, oil droplets could still penetrate the cutting zone through the capillary mesh after the first or second impact. Capillary permeation is the main method for forming a friction interfacial film between a tool and workpiece.

2. Lubricant infiltration

Turning is a type of continuous cutting that is primarily used in the processing of rotary parts. Continuous cutting refers to cutting where the cutting edge is always in contact with the workpiece during the cutting process. As shown in Fig. 30, for continuous cutting, there is a lubrication exclusion zone at the tool-chip interface. It can be seen from the stress distribution between the front cutter face and chip that there is a certain contact length, and the tool and chip are in

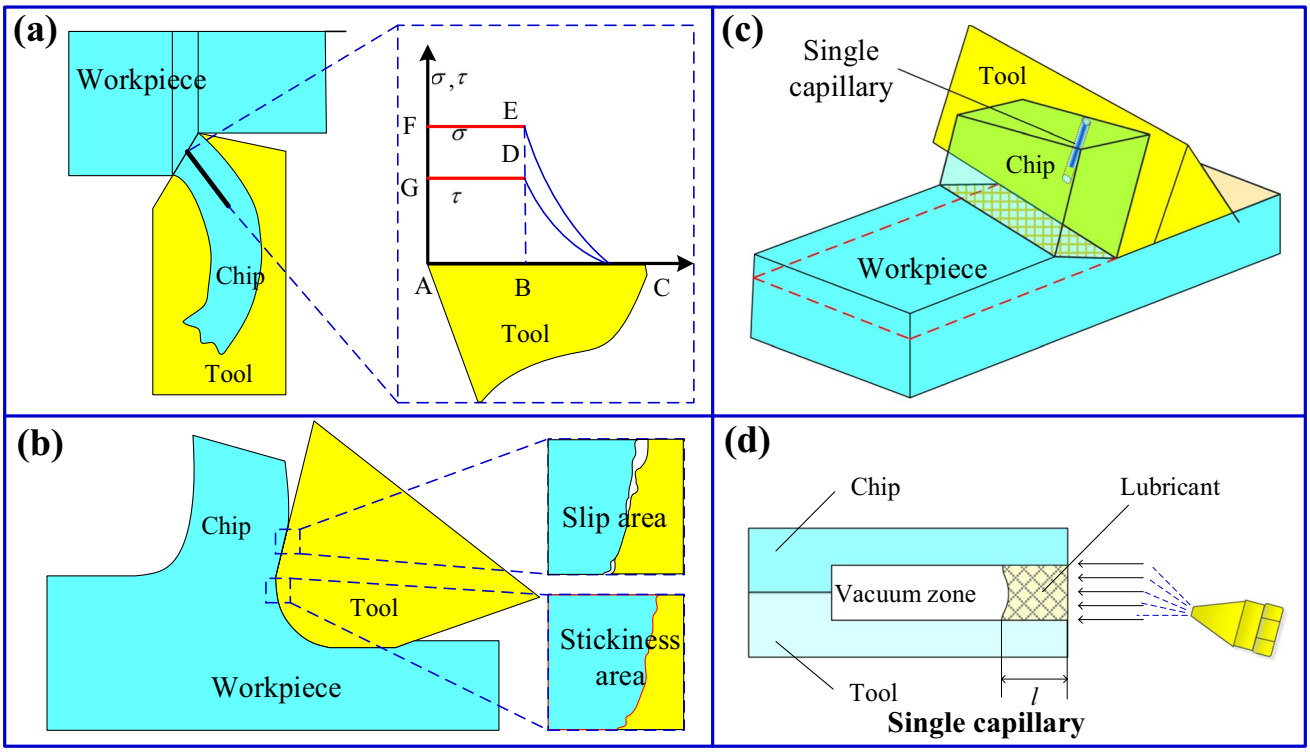

Fig. 30 Capillary infiltration of continuous cutting

constant intense contact [232]. Therefore, from a technical point of view, continuous contact friction at high temperature, high pressure, and high speed causes workpiece surface adhesion/tool wear. Therefore, there are manufacturing cost, manufacturing cycle, and manufacturing precision problems in production. In continuous cutting, the fluid performance of the lubricant is the main consideration, and droplet wetting, spreading, and transport are very important. How to achieve lubrication in the tool-chip contact area must always be considered by scholars. The research results of Das et al. showed that the viscosity of lubricating media was ranked as Al_2O_3 nanofluid, Fe_2O_3 nanofluid, and CuO nanofluid. However, the results show that CuO nanofluids exhibit the best behavior, followed by Fe_2O_3 nanofluids and Al_2O_3 nanofluids. This is because CuO nanofluids have the lowest surface tension. A low viscosity and surface tension are conducive to liquid transport and penetration. Singh et al. [117] developed a hybrid nanofluid with improved thermal and tribological properties by mixing Al_2O_3-based nanofluids with graphene nanosheets at volume concentrations of 0.25, 0.75, and 1.25 vol %. The thermal conductivity of the hybrid nanofluid was lower than that of its components, and the viscosity was between those of their components. However, tribological tests confirmed that the hybrid nanofluids produced the least wear. The hybrid nanofluid exhibited better wettability results compared with Al_2O_3-based nanofluids and base fluids. The turning of AISI 304 steel using MQL technology clearly showed that the mixing of graphene and Al_2O_3 enhanced the performance of the mixed nanofluids.

For the process of the cutting fluid penetrating the cutting zone, it is widely considered that there are a large number of capillaries between the tool and chip in the cutting process. The cutting fluid permeated the cutting zone through these capillaries**.** Generally, the capillary between the tool chip and tool workpiece penetrated by the cutting fluid can be divided into three stages [233]: (1) liquid-phase infiltration, (2) droplet evaporation, and (3) gas-phase filling. The state of the cutting fluid and filling time of the capillary were different at each stage. In the first stage, a vacuum inside a single capillary tube was used. Therefore, the liquid phase penetrated the capillaries. In the second stage, owing to the conduction of cutting heat, after the cutting fluid penetrates a section of the capillary, the penetrated droplets absorb the cutting heat and increase its internal energy. The pressure rose rapidly, reaching more than 100 MPa instantaneously. The interior resembles a sudden "explosion," turning into steam. After "explosion," the steam will fill the inside of the capillary tube. Simultaneously, the cutting fluid at the opening of the capillary is ejected, which hinders further development of the cutting fluid. In the third stage, when the capillary was filled with the gas phase, the cutting fluid completely transformed into the gas phase after absorbing the cutting heat and continued to fill the capillary in the gas phase state. The interface state is often a boundary lubrication; the lubricant is adsorbed on the solid surface, forming a solid boundary lubrication layer. The boundary lubrication layer has a certain ability to support the load. The capillary interaction in the tool-chip contact zone directly affects the friction on the front tool surface and subsequently affects the friction angle and shear angle. Thus, the mechanical behavior of the material removal changed. Moreover, the generation of heat was inhibited because of the reduction in friction.

To solve this bottleneck, the contact state of tool chips can be changed by introducing ultrasonic vibrations or textured tools. For example, Yan et al. [234] introduced the ultrasonic vibration MQL process, which exhibited lower cutting forces and tool wear rates owing to the combined advantages of lubrication and vibration. Moreover, the tool-chip contact length of the new process was shorter, and the chip shape and surface integrity were better. Furthermore, a mathematical model for predicting the lubrication permeation length based on capillary rise theory was established. This model was used to study the effects of different parameters on lubrication in vibration-assisted machining. It was shown that lubrication during vibration-assisted machining can provide better cutting performance. Hao et al. [235] constructed a new technique using the composite hydrophilic/hydrophobic wettability of textured surfaces to improve the friction resistance of cutting tools. The results show that compared with nontextured tools and microgroove-textured tools, textured PCD tools with hydrophilic/hydrophobic wettability reduce cutting forces, average COF, and cutting tool wear. The new tool has the effect of regulating the movement of the cutting fluid toward the tool-chip interface, which can further improve cutting performance and reduce tool wear. Table 2 shows the turning processes for the different materials.

Table 2 Literature on NMQL turning

Materials	References
Aluminum alloys	[142] [182]
General carbon steel	[91] [108] [236]
Stainless steel	[66] [118] [119] [122] [138] [181] [237] [238]
Hardened steel	[47] [48] [49] [117] [120] [173] [239] [240] [241] [242] [243] [244] [245] [246] [247] [248]
Superalloy	[58] [110] [140] [249] [250] [251] [252] [253] [254] [255] [256] [257] [258] [259] [260]
Titanium alloy	[89] [261] [262] [263]

3.3 Milling

3.3.1 Devices

For the research and development of new processes, Li et al. [264] developed a milling system and method under various lubrication conditions. The system uses a tool to mill the workpiece, a force measuring system to measure the milling force, a tool changing system to replace the tool, and a tool library to store the tool. Different cutting tools can be selected according to the different processing conditions. The optimal angle difference of the tool with an unequal helical angle is selected according to different conditions, including dry cutting, flooding lubrication, MQL, or NMQL, and the optimal tool is selected according to different cutting parameters to obtain the minimum milling force. Moreover, Li et al. [265] developed a tool device and tool system for assisting chip breaking under different lubrication conditions. This solves the problem of the long chip affecting the surface quality of the workpiece in the existing technology and has the beneficial effect of chip realization. As shown in Fig. 31, Zhang et al. [266] analyzed the machining performance of three internally cooled milling cutters under low-temperature MQL conditions. The experimental results show that the double straight channel milling cutter has the best performance in prolonging tool life and reducing cutting force.

The research and development of controllable jet nozzle followers has been widely conducted in the field of milling. Goldman et al. [267] invented a lubricant nozzle positioning system and a method that uses a C-shaped arm element to connect the nozzle to the locator and compensate for the load. The change in the nozzle position with the machining parameters was realized by driving the positioner in a pneumatic manner. Peter [268] developed a nozzle-positioning device using MQL. The pneumatic muscle movement drives the cable and connecting rod to move to realize the change in nozzle position. Yuan et al. [269] developed a nozzle positioning system. Accurate positioning of the nozzle can be achieved by adjusting the position of the fixed arm relative to the circumferential ring slide, the angle and length of the first telescopic arm relative to the fixed arm, and the length and angle of the second telescopic arm relative to the first telescopic arm. Moreover, by using a circumferential single degree-of-freedom revolute joint and locking element, nozzle vibration and displacement can be effectively avoided. Wu et al. [270] invented an MQL multidegree-of-freedom intelligent sprinkler system based on a CNC milling machine, which realized lateral and longitudinal movement through a lead screw guide mechanism and nozzle jet angle adjustment through a gear ring gear mechanism. Cao et al. [271] developed a programmable MQL injection angle phase adjustment device and an application method that controlled the injection angle phase adjustment of the nozzle through the synchronization belt. Zhao et al. [272] invented a manipulator used in external cold MQL, including a suspension structure, manipulator arm, controller, and oil mist-generating device. The suspension structure was used to connect the manipulator with the frame, and the free end of the manipulator was provided with a nozzle. The oil-mist generating device is connected to the nozzle, and the controller can control the movement of the manipulator to

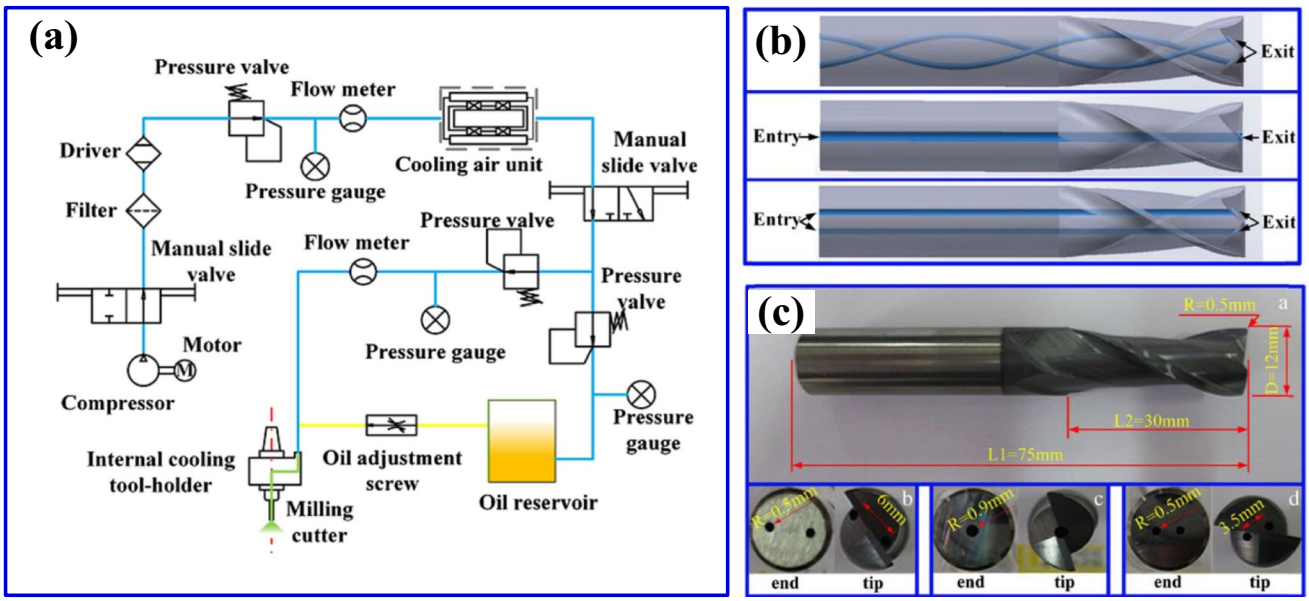

Fig. 31 Cryogenic MQL system [266]

make the nozzle spray the oil mist into the processing area. Wu et al. [273] developed a precision jet-lubrication device suitable for MQL milling. A cooling ring is set at the lower end of the tool spindle, and its lower end is connected with a nozzle. The cooling ring was connected to the headstock by a large ball screw mechanism to adjust the height of the nozzle.

3.3.2 Characteristics

1. Distribution of the flow field

Duchosal et al. [274] obtained this conclusion in milling, and the nozzle incidence angle did not change with the rotational speed. Duan et al. [275] revealed the influence law of milling tool speed, spiral angle, and diameter on the flow field distribution in MQL milling. The numerical analysis results show that the flow field around the rotary milling tool mainly includes inlet flow, circumferential flow, return flow, radial flow, and gas barrier. The flow field distribution in cavity milling was studied based on a dynamic analysis of the flow field in face milling. Flow field distribution models of square, round, quadrangle, and irregular cavities were established and verified experimentally. The results indicate that the speed of the milling cutter affects the target distance of the nozzle, the spiral angle mainly affects the incidence angle, and the diameter of the milling cutter does not affect the relative position of the nozzle. Moreover, the cavity shape has little effect on the flow field distribution. The incidence angle of the nozzle is only related to the spiral angle of the milling cutter, and the spiral angle of the milling cutter and shape of the cavity do not affect the elevation angle. An elevation angle of 60°–65° was conducive to the transfer of the cutting fluid. The shape of the cavity did not affect the velocity and pressure of the flow field. The multiparameter contribution rate was analyzed. The distance contribution rate was 62.5%, followed by an incidence angle of 31.2% and an elevation angle of 6%. Du et al. [276] analyzed the effects of different spraying distances and angles on the infiltration process and tool temperature. The results show that the spray distance has a significant effect on jet divergence, and the optimal cutting distance can effectively avoid underlubrication or overlubrication. Spraying along the cutting direction promotes lubricant accessibility and a greater concentration of droplets in the cutting area, particularly late in the cutting process, resulting in increased penetration, reduced friction, and improved heat dissipation. Figure 32 indicates that when the nozzle is set at cutting-in, a large number of MQL droplets are distributed around the tool at the beginning of cutting (30°), and the droplets are mainly distributed in the tool flank zone. The nozzle was set at the cutting point, and the tool easily obtained more MQL droplets in the middle stage of cutting (60°). When the nozzle is set at the cut-out, the droplets in the postcutting stage (90°) are well focused on the tool surface, especially the rake face, and the contact zone is widespread. In addition, a sufficient number of droplets also reach the tool surface in the middle stage of cutting (60°) and at the beginning of cutting (30°).

2. Lubricant infiltration

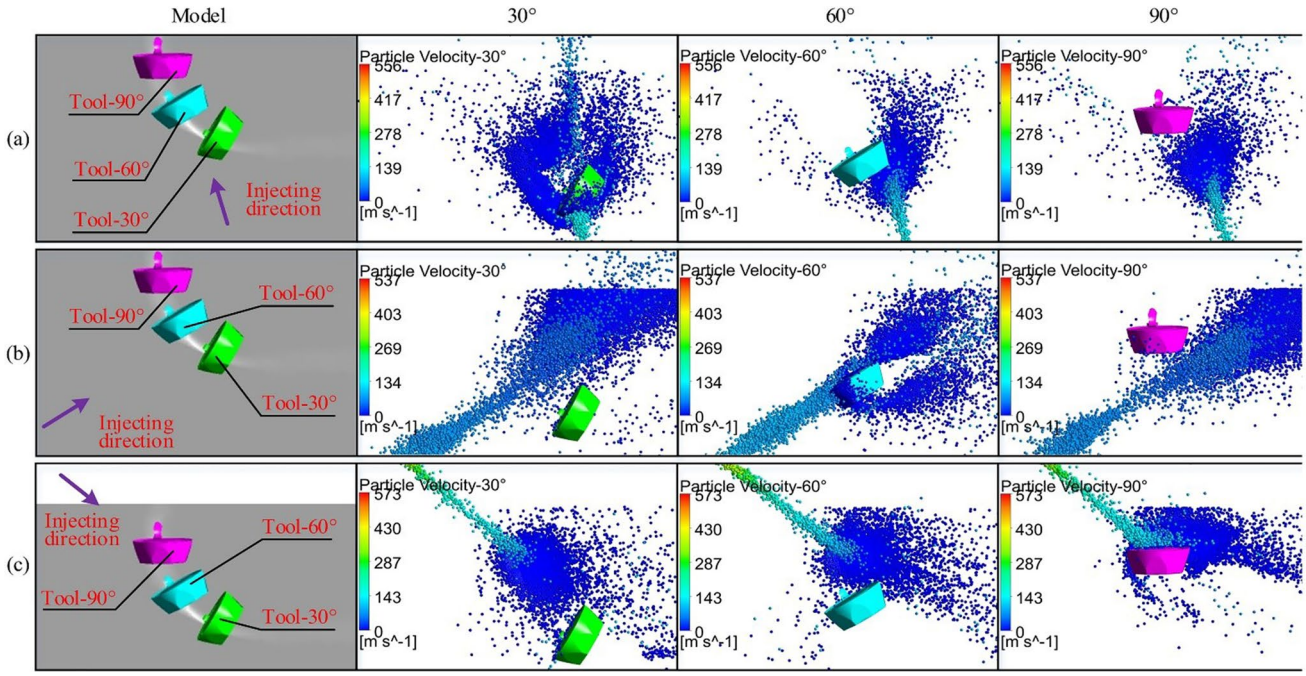

Fig. 32 Droplet distribution behavior at different cutting stages [276]

Milling belongs to intermittent cutting; the tool and workpiece in the cutting process are not in continuous contact, and the actual cutting area changes at any time. Therefore, the milling force fluctuation, impact, and vibration are large, and the smoothness is poor. During the cutting process, the lubricant can be effectively supplied to the friction interface between the tool and chip during the time gap between the tool and chip contact. Therefore, the viscosity and heat-transfer properties of the lubricant must be considered.

As shown in Fig. 33, for a single tool insert, the two wedge-shaped friction pairs of the rake face chip and flank face workpiece do not always exist but appear and disappear at a certain frequency [277]. According to Cui et al. [278], compared to turning, the wetting boundary of nanofluids is essentially changed. The infiltration of a single edge in a very short time is not conducive to membrane formation. The strength of the lubricant film is challenged because of its high-frequency impact. Huang et al. [279] believed that nanoparticles can form continuous films on the friction surface by penetrating the milling cutter/workpiece interface. The wear resistance and load-bearing capacity of the base oil can be improved to reduce the shear stress at the milling cutter/workpiece interface, thereby reducing the COF of the cutting fluid and tool wear. Alberts et al. [280] found that when graphite nanoparticles are added as the cutting fluid, the tangential force of the cutting force and cutting energy consumption are significantly reduced. An experimental study conducted by Yin et al. [52] on Ti-6Al-4 V milling showed that Al_2O_3 nanoparticles exhibited higher hardness, which was conducive to reducing the milling force. SiO_2 nanofluids exhibit a high viscosity and can improve the surface quality of the workpiece. Therefore, it can be inferred that the bearing capacity of nanoparticles and oil film strength of nanofluids are important characteristics in milling. Table 3 lists the milling processes of the different materials.

Table 3 Literature on NMQL milling

Materials	References
Aluminum alloys	[68] [74] [124] [275] [281] [282]
General carbon steel	[106] [166]
Stainless steel	[72] [76] [283] [284] [285] [286]
Hardened steel	[184] [287] [288] [289] [290]
Superalloy	[123] [183] [291] [292] [293]
Titanium alloy	[50] [51] [52] [107] [294] [295] [296]

3.4 Grinding

3.4.1 Devices

Li et al. [297] developed an oil-film formation process for a magnetic nanoparticle jet coupled with a magnetic workbench. The magnetic nanoparticle fluid is transmitted to the nozzle to form a lubricating film on the workpiece surface of the magnetic table to achieve maximum cooling and lubrication of the grinding process area. Li et al. [298] also developed an MQL grinding device that combined the electrostatic atomization of nanofluids with heat pipes. The combined electrostatic atomization nozzles were connected to the liquid and gas supply systems of the nanoparticles. The nanofluid was atomized using an electrostatic atomization combination nozzle and sprayed into the grinding area to absorb heat in the grinding area. The electrothermal film material absorbed heat in the grinding zone through the electric heating effect. After leaving the grinding zone, the absorbed heat is dissipated by the heat-pipe grinding wheel to form the Carnot cycle. Liu et al. [299] developed a supersonic nozzle eddy current control cooling system coupled with an NMQL system. The cryogenic gas generator uses a supersonic nozzle to improve the nozzle exit speed of the vortex tube. The flow path of the vortex tube nozzle was set to different streamline lines to improve the eddy strength of the gas at the vortex tube nozzle and the degree of energy

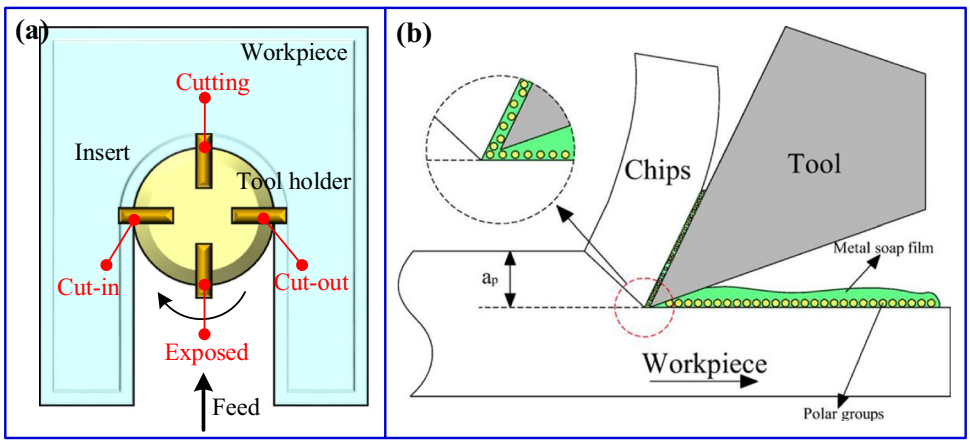

Fig. 33 Machining mechanism of milling [106]

separation. The cooling efficiency of the vortex tube and heat pipe was improved by the heat transfer enhancement. In another invention [300], an expander cooled the compressed gas passing through an approximate isentropic expansion to form cryogenic cool air. As shown in Fig. 34, Gao et al. [301] developed a multiangle two-dimensional ultrasonic vibration-assisted NMQL grinding device. The pumping effect of ultrasonic vibration was used to inject nanofluid into the interface between the grinding wheel and workpiece. Technology integration is beneficial for the permeation state transformation of microdroplets.

Research and development of a nozzle-following device for the grinding process is limited. Shi et al. [302] proposed a grinding wheel structure with a spray-cooling effect based on the principle of centrifugal atomization. The simulation and experimental results show that the new grinding wheel can significantly reduce the grinding temperature of difficult-to-cut materials with low energy consumption. Reishauer [303] developed a process to monitor the position of a grinder coolant nozzle and evaluated the grinding performance by monitoring the power consumption changes of the grinder spindle drive. When the spindle power exceeds the expectation, the nozzle rotates along the hinge or translates along the slider, and the optimal position is determined through the cycle test.

3.4.2 Characteristics

1. Distribution of the flow field

Stachursk et al. [304] simulated the flow-field distribution in the hob grinding zone. The results show that reducing the nozzle angle increases the gas flow at the hob-grinding-wheel contact interface. Emami et al. [214] also believed that in the grinding process of MQL, the air barrier layer on the grinding wheel surface has an entry flow, which is conducive to the MQL medium entering the grinding wheel–workpiece contact area. Through fluid dynamics analysis, Zhang et al. [305] found that there was a boundary in the wedge-shaped zone between the grinding wheel and workpiece and that the boundary was an entry flow, which was conducive to the entry of lubricating media. As shown in Fig. 35, the return flow was not conducive to the entry of the lubricating medium. When the nozzle sprays the grinding fluid into the wedge area, the spraying direction should be maintained above the boundary line as far as possible, which is conducive to the injection of grinding fluid in the wedge clearance. The results indicate that when the nozzle shaft and workpiece surface form a certain angle (15°–20°), the grinding fluid easily enters the wedge clearance.

2. Lubricant infiltration

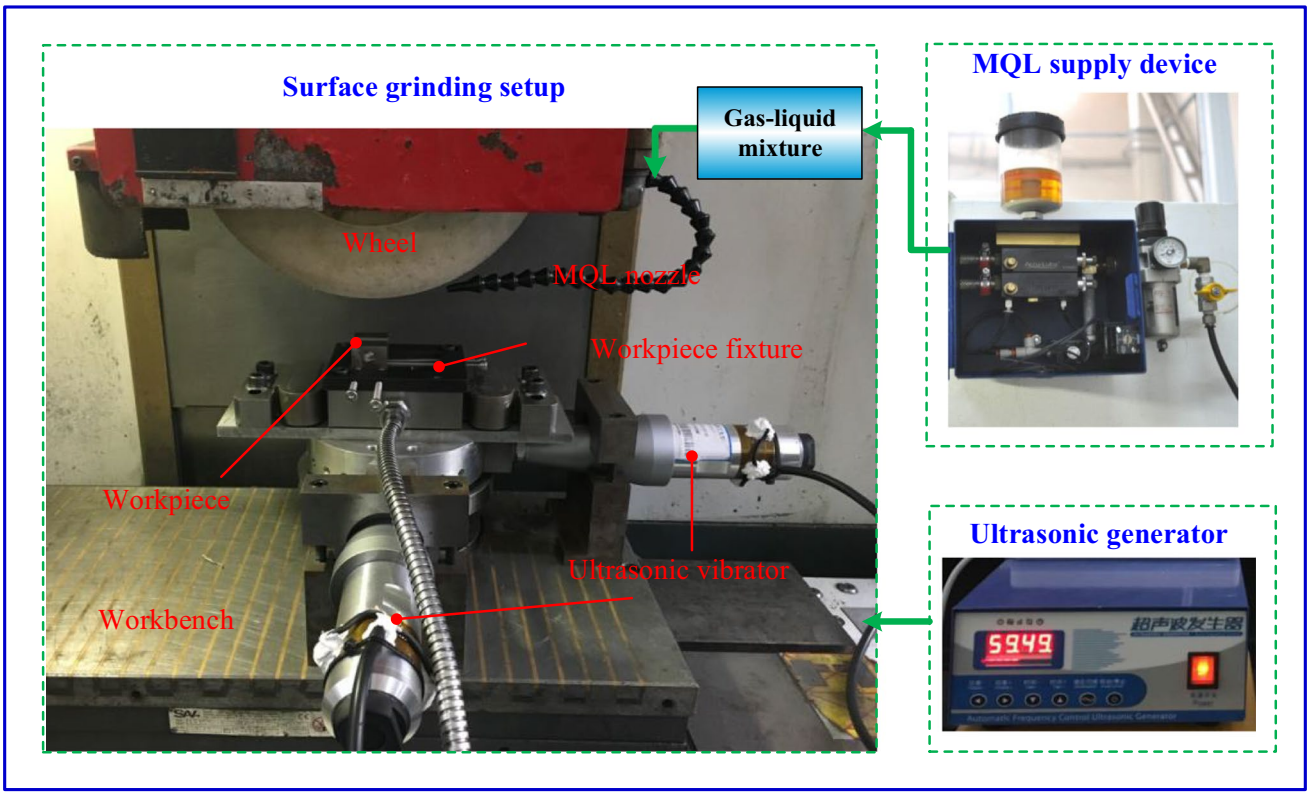

Fig. 34 Multiangle two-dimensional ultrasonic vibration-assisted NMQL grinding device [301]

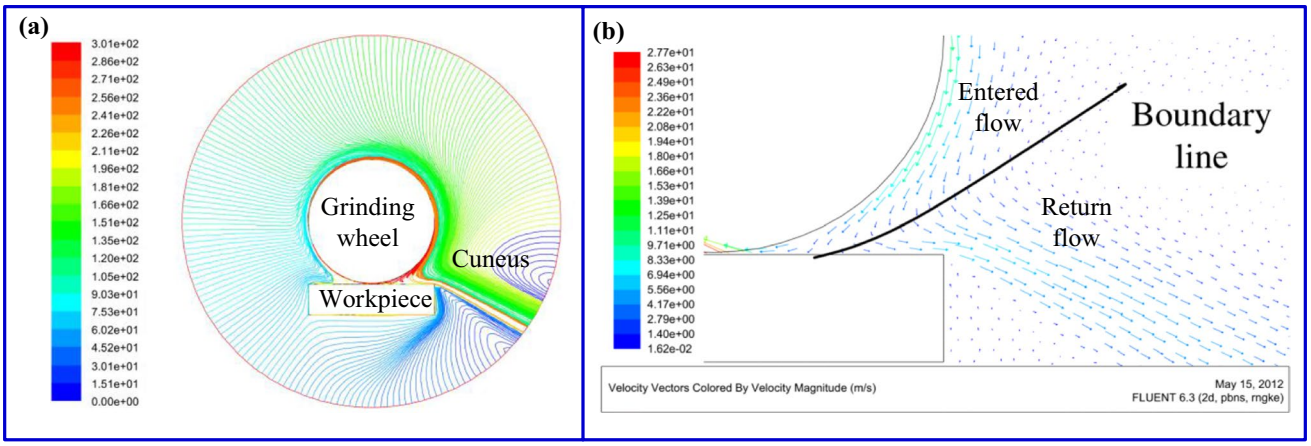

Fig. 35 The flow field of grinding [305]

Grinding is a basic form of machining. The final accuracy and surface quality of most parts are guaranteed through the grinding process. The most remarkable characteristics of the grinding process are the high circumferential speed of the grinding wheel and the high specific energy [306–308]. Grinding is different from milling and turning because the negative rake angle of the abrasive particles and the radius of the cutting edge are larger. Consequently, material removal is more difficult and consumes more energy [309]. Friction and plowing cause the grinding process to produce greater heat flux. Paradoxically, grinding is a surface integrity-oriented process. Therefore, the technical bottleneck in heat dissipation is the primary technical bottleneck in grinding. Because grinding is different from other machining forms, the contact time between each abrasive particle and workpiece is very short under the action of the high circumferential speed of the grinding wheel. Meanwhile, the volume of the grinding chips was very small, and the heat removed by the grinding chips was very small. The high energy density in the grinding zone significantly affects the surface quality and performance of the workpiece. In particular, when the grinding zone temperature exceeds a critical value, it can cause thermal damage to the surface of the workpiece (surface oxidation, burns, residual tensile stress, and cracks). Meanwhile, the grinding performance and machining accuracy of the grinding wheel are reduced. With the accumulation of heat on the workpiece surface, the dimensional accuracy and shape accuracy are out of tolerance owing to grinding heat. Generally, grinding is the final process of the parts. The grinding technology and processes determine the final precision and surface quality of the parts. Therefore, effective measures must be taken to reduce or even eliminate the influence of grinding heat on workpiece machining accuracy and surface quality.

The influence of the fluid on the heat dissipation was twofold. First, the strong heat transfer characteristics of nanofluids improve the heat dissipation performance. On the other hand, the antiwear and antifriction effects of the nanofluid reduce the heat flux of the heat source at the frictional interface. As shown in Fig. 36, with the help of self-diffusion osmosis, the nanofluids can form a lubricating film with a larger coverage and stronger friction and wear resistance. The lubricating film was more easily combined with the surface of the friction pair and improved the stability of the oil film. Cui et al. [278] considered the removal behavior of the material and concluded that the lubrication film on the workpiece surface could play a greater role in the sliding and plowing stages. During grinding, the machining trajectory of the latter abrasive was based on that of the former abrasive. This implies that the surface to be machined by the latter abrasive is a new surface machined by the former abrasive. Because the former abrasive forms a stable lubrication film on the workpiece surface after cutting, the latter abrasive benefits from the stable lubrication film in a good lubrication state. Consequently, the friction heat during the sliding and plowing phases was significantly reduced. Zhang et al. [88] found that a grinding wheel was beneficial to the filtration and film-forming processes. Capillary and microchannel networks were formed during grinding because of the pores on the grinding wheel surface. Lubricant penetration has sufficient space and power owing to the dynamic pump effect. Moreover, lubricants can be stored in pores and filled at any time. Thus, a sufficient amount of nanolubricant is rolled into the film repeatedly during repeated cutting of the abrasive.

For the selection of nanofluids, Wang et al. [310] found that different workpiece materials exhibit different removal mechanisms. Owing to the brittleness removal mechanism of Ni-based alloys, the chip is C-type. The chip of 45 steel is curled into long stripes owing to the plastic removal mechanism. Meanwhile, a large amount of grinding energy was consumed during the removal process. Therefore, plastic

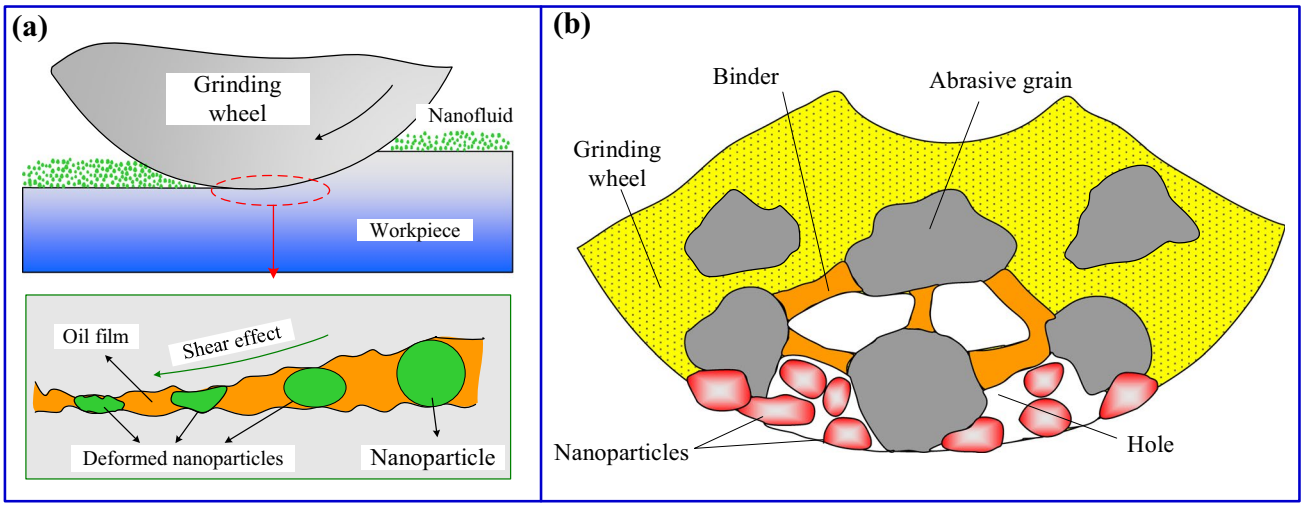

Fig. 36 Mechanism of grinding

Table 4 Literature on NMQL grinding

Materials	References
General carbon steel	[95] [96] [310] [311]
Stainless steel	[171] [312]
Hardened steel	[82] [179] [313]
Superalloy	[53] [57] [83] [104] [125] [126] [310] [314] [315]
Titanium alloy	[69] [154] [155] [170] [316] [317] [318] [319]
Composites	[320] [321] [322] [323]
Ceramics	[324] [325] [326] [327] [328]
Cemented carbide	[169] [172] [329] [330]

removal consumes more energy than brittle removal. Nodular cast iron is shaped like a short block of broken chips. The material removal process affected the surface quality to some extent, and the surface quality obtained by this material was worse than that of 45 steel. The application of different NMQL methods has a significant influence on the grinding characteristics of different materials, such as the force ratio, specific grinding energy, G ratio, and surface roughness. The MoS_2 NMQL is suitable for processing soft medium carbon steel, such as 45 steel, whereas the Al_2O_3 nanofluid is suitable for processing high-strength and hard materials, such as nickel-based alloys. Table 4 shows the grinding processes for the different materials.

4 Conclusions and prospects

4.1 Conclusions

The current study covers the latest research on the application of nanofluids in the field of mechanical manufacturing. First, the preparation, fluid, thermal, and tribological properties of nanofluids are disclosed. In addition, innovative equipment for nanofluid supply is reviewed, and the atomization mechanism under different boundary conditions is analyzed. The technical problems of the parameterized controllable power supply system were solved. Furthermore, the properties of the nanofluids in turning, milling, and grinding are discussed. The mapping relationship between the nanofluid parameters and the processing properties was clarified. The flow field distribution and lubricant wetting behavior under different tool workpiece boundaries were revealed. The point-by-point conclusions of this study are as follows.

1. The hard phase or layered lubrication structure can be selected based on the interface load. The base oil can select water- or vegetable oil-based fluids according to the guidance of processing cooling and lubrication. A two-step method is recommended to prepare nanofluids in the manufacturing process because the equipment used in the one-step method is expensive and difficult to operate. The stability of nanofluids is an important bottleneck to further improve the machining performance. For example, in the turning process of AISI 304 steel with MoO_3/water nanofluids, the average cutting force and tool wear were significantly reduced by 32.05% and 53%, respectively, when 0.45 vol % SPAN20 surfactant was added. The mapping relationship between the concentration of nanofluid and machining performance was

clearly defined. Owing to the instability of nanofluids, there is a certain concentration that causes the nanofluids to exhibit the best performance. The stability of mixed nanofluids is better than that of single nanofluids. The influence of thermal and fluid properties on the machining performance of the nanofluids was revealed. The mechanism of action of hybrid nanofluids at the friction interface requires further exploration. Stability is a key factor that affects the performance of nanofluids. Mechanical/ultrasonic treatments and dispersants should be performed before use.

2. Adding nanoparticles to the base fluid increased the dynamic viscosity of the nanofluid and led to an improvement in the lubricating performance. Owing to inertia, the droplets continue to flow forward after entering the tool–workpiece interface. High-viscosity fluids have poor fluidity and short flow distances, and it is difficult for them to penetrate the gap in the cutting area. In addition, a higher viscosity index value is ideal because it ensures stable lubrication within the operating-temperature range. A small surface tension can penetrate numerous capillaries in the tool chip contact area and form a lubricating film during the machining process. Meanwhile, the smaller the surface tension, the more easily the droplets are broken, and the utilization rate, migration, and permeability of the lubricant are further improved. Moreover, a small contact angle represents a large penetration area, which expands the thermal boundary layer and improves the heat transfer performance. For boiling heat transfer, the small surface tension of nanofluids implies that the binding force of bubble formation and expansion is weak. The presence of more bubbles and the high activity of boiling heat transfer will help achieve excellent performance.
3. Nanofluids are high-performance cooling lubrication media with a cutting-fluid reduction supply. The friction of the interface is improved; for example, in the friction and wear tests, the COF of the Jatropha curcas oil-based Al_2O_3 nanofluid was reduced by 85% compared with the dry condition. The tool life has been significantly improved; for example, cutting fluid based on Al_2O_3 nanoparticles has improved the tool life by nearly 177–230% in hard milling. The heat transfer performance was significantly improved; for example, the addition of CNT nanoparticles increased the CHTC of normal saline by 145.06%.
4. Electrostatic atomization and ultrasonic atomization improved the size distribution of the nanofluid droplets and the uniformity of the droplet size. The development of composite efficiency enhancement processes, such as texture tools, cryogenic medium, and ultrasonic vibration-assisted processing, enriches NMQL process technology. This provides a technical guarantee of clean precision manufacturing. The parametric intelligent feeding device and the subsequent nozzle system will further the application of nanofluids in the field of intelligent manufacturing.
5. The wettability of nanofluids should be considered during turning because of the continuous contact of the tool chip. Owing to the impact load of high frequency in milling, the oil film strength and extrusion resistance of nanofluids must be considered. Owing to the high material removal energy, the friction reduction and thermal properties of nanofluids in the grinding zone must be considered simultaneously.

4.2 Prospects

1. Lubricants should develop additives with excellent comprehensive performance and environmental friendliness by combining anti-wear, friction-reduction, and oxidation resistance. The synergistic effect of the modification and addition of antioxidants is expected to be an effective method for enhancing the oxidation stability of vegetable oils. Nanofluids based on vegetable oil have excellent lubrication and cooling effects, but the multimapping law of the process parameters under various working conditions is still unclear.
2. Studies on the synergistic technology of nanofluids combined with texture tools, ultrasonic vibration, and cryogenic cooling media have been carried out. In the future, scholars should jointly promote extensive and in-depth research. The parameterized modeling of composite enhancement processes and their compatibility with traditional processing models must be evaluated.
3. Integrated communication with machine tools to extract processing parameters, adaptive adjustment equipment for nanofluid supply parameters, and atomization parameters must be widely promoted. The manufacturing and application of intelligent supply devices will further promote the construction of intelligent factories. This is what current international organizations and policies advocate.
4. It is recommended that new research and application associations be established to promote the application and development of nanofluids in machining. Parameter database construction standards must be drafted and evaluated by experts and scholars in the industry, as well as major customers of application scenarios. Quantitative evaluation indicators based on the demand for carbon reduction and energy conservation must also be unified.

Author contribution Xiaoming Wang: investigation, writing (original draft), and writing (review and editing). Yuxiang Song: writing (review and editing). Changhe Li: technical and material support; instructional support, and writing (review). Yanbin Zhang: formal analysis, validation, and writing (review and editing). Hafiz Muhammad Ali: modify paper, formal analysis. Shubham Sharma: modify paper, formal analysis. Runze Li: formal analysis, validation. Min Yang: formal analysis, validation. Teng Gao: modify paper, formal analysis. Mingzheng Liu: formal analysis, validation. Xin Cui: formal analysis, validation. Zafar Said: statistical analysis, validation. Zongming Zhou: formal analysis, validation.

Funding This study was financially supported by the National Natural Science Foundation of China (Grant Nos. 51975305, 51905289, 52105457, and 52105264), National Key Research and Development Plan (2020YFB2010500), Key Projects of Shandong Natural Science Foundation of China (Grant Nos. ZR2020KE027, ZR2020ME158, and ZR2021QE116), Major Science and Technology Innovation Engineering Projects of Shandong Province (Grant No. 2019JZZY020111), and Source Innovation Project of Qingdao West Coast New Area (Grant Nos. 2020–97 and 2020–98).

Data availability Data sharing is not applicable to this article.

Code availability Code availability is not applicable to this article.

Declarations

Ethics approval We declare that the papers we submitted are my research work under the guidance of the instructor and research results we have obtained. We confirm that this article has not been published previously and is not being submitted for publication elsewhere. We have not considered elsewhere except *The International Journal of Advanced Manufacturing Technology*. We confirm that this article has had the full consent of all authors. If this article was accepted, we confirm that it will not be published elsewhere in the same form, in English or in any other language, without the written consent of the publisher.

Consent to participate Consent to participate is not applicable to this article.

Consent for publication The authors declare that they participated in this paper willingly and the authors declare to consent to the publication of this paper.

Conflict of interest The authors declare no conflict of interest.

References

1. Hassan F, Jamil F, Hussain A, Ali HM, Janjua MM, Khushnood S, Farhan M, Altaf K, Said Z, Li CH (2022) Recent advancements in latent heat phase change materials and their applications for thermal energy storage and buildings: A state of the art review. SusTain Energy Techn 49:101646
2. Tripathi V, Chattopadhyaya S, Mukhopadhyay AK, Sharma S, Li CH, Di Bona G (2022) A sustainable methodology using lean and smart manufacturing for the cleaner production of shop floor management in industry 4.0. Mathematics 10(3):347
3. Jha K, Tyagi YK, Kumar R, Sharma S, Huzaifah MRM, Li CH, Ilyas RA, Dwivedi SP, Saxena A, Pramanik A (2021) Assessment of dimensional stability, biodegradability, and fracture energy of bio-composites reinforced with novel pine cone. Polymers 13(19):3260
4. Mia M, Gupta MK, Singh G, Krolczyk G, Pimenov DY (2018) An approach to cleaner production for machining hardened steel using different cooling-lubrication conditions. J Clean Prod 187:1069–1081
5. Ejaz A, Babar H, Ali HM, Jamil F, Janjua MM, Fattah IMR, Said Z, Li CH (2021) Concentrated photovoltaics as light harvesters: outlook, recent progress, and challenges. SusTain Energy Techn 46:101199
6. Gao T, Zhang YB, Li CH, Wang YQ, Chen Y, An QL, Zhang S, Li HN, Cao HJ, Ali HM, Zhou ZM, Sharma S (2022) Fiber-reinforced composites in milling and grinding: machining bottlenecks and advanced strategies. Front Mech Eng 17(2):24
7. Liu MZ, Li CH, Zhang YB, An QL, Yang M, Gao T, Mao C, Liu B, Cao HJ, Xu XF, Said Z, Debnath S, Jamil M, Ali HM, Sharma S (2021) Cryogenic minimum quantity lubrication machining: from mechanism to application. Front Mech Eng 16(4):649–697
8. Sarikaya M, Gupta MK, Tomaz I, Danish M, Mia M, Rubaiee S, Jamil M, Pimenov DY, Khanna N (2021) Cooling techniques to improve the machinability and sustainability of light-weight alloys: a state-of-the-art review. J Manuf Process 62:179–201
9. Li RZ, Du ZD, Qian XJ, Li Y, Martinez-Camarillo JC, Jiang LM, Humayun MS, Chen ZP, Zhou QF (2021) High resolution optical coherence elastography of retina under prosthetic electrode. Quant Imaging Med Surg 11(3):918–927
10. Debnath S, Reddy MM, Yi QS (2014) Environmental friendly cutting fluids and cooling techniques in machining: a review. J Clean Prod 83:33–47
11. Krolczyk GM, Maruda RW, Krolczyk JB, Wojciechowski S, Mia M, Nieslony P, Budzik G (2019) Ecological trends in machining as a key factor in sustainable production - A review. J Clean Prod 218:601–615
12. Klocke F, Eisenbltter G (1997) Dry Cutting. CIRP Ann-Manuf Techn 46(2):519–526
13. Zhang S, Li JF, Wang YW (2012) Tool life and cutting forces in end milling Inconel 718 under dry and minimum quantity cooling lubrication cutting conditions. J Clean Prod 32:81–87
14. Zhao XF, Li CH, Yu TB (2022) Effect of B4C on CBN/CuSnTi laser cladding grinding tool. Int J Adv Manuf Technol 119(9–10):6307–6319
15. Liu M, Li C, Zhang Y, Yang M, Gao T, Cui X, Wang X, Xu W, Zhou Z, Liu B, Said Z, Li R, Sharma S (2022) Analysis of grinding mechanics and improved grinding force model based on randomized grain geometric characteristics. Chin J Aeronaut. https://doi.org/10.1016/j.cja.2022.1011.1005
16. Pimenov DY, Mia M, Gupta MK, Machado AR, Tomaz IV, Sarikaya M, Wojciechowski S, Mikolajczyk T, Kaplonek W (2021) Improvement of machinability of Ti and its alloys using cooling-lubrication techniques: a review and future prospect. J Mater Res Technol-Jmr&T 11:719–753
17. Li GX, Chandra S, Rashid RAR, Palanisamy S, Ding SL (2022) Machinability of additively manufactured titanium alloys: A comprehensive review. J Manuf Process 75:72–99
18. Fu Q, Wu SJ, Li CH, Xu JY, Wang DZ (2022) Delamination and chip breaking mechanism of orthogonal cutting CFRP/Ti6Al4V composite. J Manuf Process 73:183–196
19. Gupta MK, Song QH, Liu ZQ, Sarikaya M, Jamil M, Mia M, Khanna N, Krolczyk GM (2021) Experimental characterisation of the performance of hybrid cryo-lubrication assisted turning of Ti-6Al-4V alloy. Tribol Int 153:106582
20. M'Saoubi R, Axinte D, Soo SL, Nobel C, Attia H, Kappmeyer G, Engin S, Sim WM (2015) High performance cutting of advanced aerospace alloys and composite materials. CIRP Ann Manuf Technol 64(2):557–580
21. Chetan GS, Rao PV (2015) Application of sustainable techniques in metal cutting for enhanced machinability: a review. J Clean Prod 100:17–34

22. Pereira O, Rodriguez A, Fernandez-Abia AI, Barreiro J, de Lacalle LNL (2016) Cryogenic and minimum quantity lubrication for an eco-efficiency turning of AISI 304. J Clean Prod 139:440–449
23. Khanna N, Agrawal C, Pimenov DY, Singla AK, Machado AR, da Silva LRR, Gupta MK, Sarikaya M, Krolczyk GM (2021) Review on design and development of cryogenic machining setups for heat resistant alloys and composites. J Manuf Process 68:398–422
24. Akhtar SS (2021) A critical review on self-lubricating ceramic-composite cutting tools. Ceram Int 47(15):20745–20767
25. Sarikaya M, Gullu A (2014) Taguchi design and response surface methodology based analysis of machining parameters in CNC turning under MQL. J Clean Prod 65:604–616
26. Jamil M, Zhao W, He N, Gupta MK, Sarikaya M, Khan AM, Sanjay MR, Siengchin S, Pimenov DY (2021) Sustainable milling of Ti-6Al-4V: a trade-off between energy efficiency, carbon emissions and machining characteristics under MQL and cryogenic environment. J Clean Prod 281:125374
27. Sarikaya M, Gullu A (2015) Multi-response optimization of minimum quantity lubrication parameters using Taguchi-based grey relational analysis in turning of difficult-to-cut alloy Haynes 25. J Clean Prod 91:347–357
28. Gao T, Zhang YB, Li CH, Wang YQ, An QL, Liu B, Said Z, Sharma S (2021) Grindability of carbon fiber reinforced polymer using CNT biological lubricant. Sci Rep 11(1):22535
29. Duan ZJ, Li CH, Ding WF, Zhang YB, Yang M, Gao T, Cao HJ, Xu XF, Wang DZ, Mao C, Li HN, Kumar GM, Said Z, Debnath S, Jamil M, Ali HM (2021) Milling force model for aviation aluminum alloy: academic insight and perspective analysis. Chin J Mech Eng 34(1):18
30. Gao T, Li CH, Yang M, Zhang YB, Jia DZ, Ding WF, Debnath S, Yu TB, Said Z, Wang J (2021) Mechanics analysis and predictive force models for the single-diamond grain grinding of carbon fiber reinforced polymers using CNT nano-lubricant. J Mater Process Technol 290:116976
31. Said Z, Sundar LS, Tiwari AK, Ali HM, Sheikholeslami M, Bellos E, Babar H (2022) Recent advances on the fundamental physical phenomena behind stability, dynamic motion, thermophysical properties, heat transport, applications, and challenges of nanofluids. Phys Rep-Rev Sect Phys Lett 946. https://doi.org/10.1016/j.physrep.2021.1007.1002
32. Said Z, Arora S, Farooq S, Sundar LS, Li CH, Allouhi A (2022) Recent advances on improved optical, thermal, and radiative characteristics of plasmonic nanofluids: academic insights and perspectives. Sol Energy Mater Sol Cells 236:111504
33. Choi SUS, Eastman JA (1995) Enhancing thermal conductivity of fluids with nanoparticles. Argonne National Lab. IL (United States), pp 1–8
34. Khan WA, Pop I (2010) Boundary-layer flow of a nanofluid past a stretching sheet. Int J Heat Mass Transf 53(11–12):2477–2483
35. Duan ZJ, Li CH, Zhang YB, Gao T, Liu X, Li R, Said Z, Debnath S, Sharma S (2022) Mechanical behavior and Semiempirical force model of aerospace aluminum alloy milling using nano biological lubricant. Front Mech Eng https://doi.org/10.1007/s11465-022-0720-4
36. Said Z, Jamei M, Sundar LS, Pandey AK, Allouhi A, Li CH (2022) Thermophysical properties of water, water and ethylene glycol mixture-based nanodiamond + Fe3O4 hybrid nanofluids: an experimental assessment and application of data-driven approaches. J Mol Liq 347:117944
37. Tarafdar A, Sirohi R, Negi T, Singh S, Badgujar PC, Shahi NC, Kumar S, Sim SJ, Pandey A (2021) Nanofluid research advances: preparation, characteristics and applications in food processing. Food Res Int 150:110751
38. Sharma AK, Tiwari AK, Dixit AR (2016) Effects of minimum quantity lubrication (MQL) in machining processes using conventional and nanofluid based cutting fluids: A comprehensive review. J Clean Prod 127:1–18
39. Sharma P, Said Z, Kumar A, Nizetic S, Pandey A, Hoang AT, Huang ZH, Afzal A, Li CH, Le AT, Nguyen XP, Tran VD (2022) Recent advances in machine learning research for nanofluid-based heat transfer in renewable energy system. Energy Fuels 36(13):6626–6658
40. Xu WH, Li CH, Zhang YB, Ali HM, Sharma S, Li RZ, Yang M, Gao T, Liu MZ, Wang XM, Said Z, Liu X, Zhou ZM (2022) Electrostatic atomization minimum quantity lubrication machining: from mechanism to application. Int J Extreme Manuf 4(4):042003
41. Anqi AE, Li CH, Dhahad HA, Sharma K, Attia E, Abdelrahman A, Mohammed AG, Alamri S, Rajhi AA (2022) Effect of combined air cooling and nano enhanced phase change materials on thermal management of lithium-ion batteries. J Energy Storage 52:104906
42. Ghodbane M, Said Z, Tiwari AK, Sundar LS, Li CH, Boumeddane B (2022) 4E (energy, exergy, economic and environmental) investigation of LFR using MXene based silicone oil nanofluids. SusTain Energy Techn 49:101715
43. Wang XM, Li CH, Zhang YB, Ali HM, Sharma S, Li RZ, Yang M, Said Z, Liu X (2022) Tribology of enhanced turning using biolubricants: A comparative assessment. Tribol Int 174:107766
44. Tang LZ, Zhang YB, Li CH, Zhou ZM, Nie XL, Chen Y, Cao HJ, Liu B, Zhang NQ, Said Z, Debnath S, Jamil M, Ali HM, Sharma S (2022) Biological stability of water-based cutting fluids: progress and application. Chin J Mech Eng 35(1):3
45. Shen B, Shih AJ, Tung SC (2008) Application of nanofluids in minimum quantity lubrication grinding. Tribol Trans 51(6):730–737
46. Cui X, Li CH, Zhang YB, Jia DZ, Zhao YJ, Li RZ, Cao HJ (2019) Tribological properties under the grinding wheel and workpiece interface by using graphene nanofluid lubricant. Int J Adv Manuf Technol 104(9–12):3943–3958
47. Das A, Patel SK, Das SR (2019) Performance comparison of vegetable oil based nanofluids towards machinability improvement in hard turning of HSLA steel using minimum quantity lubrication. Mech Ind 20(5):506
48. Das A, Patel SK, Arakha M, Dey A, Biswal BB (2021) Processing of hardened steel by MQL technique using nano cutting fluids. Mater Manuf Process 36(3):316–328
49. Kumar R, Sahoo AK, Mishra PC, Das RK (2020) Influence of Al2O3 and TiO2 nanofluid on hard turning performance. Int J Adv Manuf Technol 106(5–6):2265–2280
50. Bai XF, Li CH, Dong L, Yin QA (2019) Experimental evaluation of the lubrication performances of different nanofluids for minimum quantity lubrication (MQL) in milling Ti-6Al-4V. Int J Adv Manuf Technol 101(9–12):2621–2632
51. Songmei Y, Xuebo H, Guangyuan Z, Amin M (2017) A novel approach of applying copper nanoparticles in minimum quantity lubrication for milling of Ti-6Al-4V. Adv Prod Eng Manage 12(2):139–150
52. Yin QA, Li CH, Dong L, Bai XF, Zhang YB, Yang M, Jia DZ, Hou YL, Liu YH, Li RZ (2018) Effects of the physicochemical properties of different nanoparticles on lubrication performance and experimental evaluation in the NMQL milling of Ti-6Al-4V. Int J Adv Manuf Technol 99(9–12):3091–3109
53. Li BK, Li CH, Zhang YB, Wang YG, Jia DZ, Yang M, Zhang NQ, Wu QD, Han ZG, Sun K (2017) Heat transfer performance of MQL grinding with different nanofluids for Ni-based alloys using vegetable oil. J Clean Prod 154:1–11

54. Lee PH, Nam JS, Li C, Lee SW (2012) An experimental study on micro-grinding process with nanofluid minimum quantity lubrication (MQL). Int J Precis Eng Man 13(3):331–338
55. Ni J, Cui Z, Wu C, Sun JB, Zhou JH (2021) Evaluation of MQL broaching AISI 1045 steel with sesame oil containing nanoparticles under best concentration. J Clean Prod 320:128888
56. Pal A, Chatha SS, Sidhu HS (2022) Assessing the lubrication performance of various vegetable oil-based nano-cutting fluids via eco-friendly MQL technique in drilling of AISI 321 stainless steel. J Braz Soc Mech Sci 44(4):148
57. Virdi RL, Chatha SS, Singh H (2020) Machining performance of Inconel-718 alloy under the influence of nanoparticles based minimum quantity lubrication grinding. J Manuf Process 59:355–365
58. Musavi SH, Davoodi B, Niknam SA (2019) Effects of reinforced nanoparticles with surfactant on surface quality and chip formation morphology in MQL-turning of superalloys. J Manuf Process 40:128–139
59. Tevet O, Von-Huth P, Popovitz-Biro R, Rosentsveig R, Wagner HD, Tenne R (2011) Friction mechanism of individual multilayered nanoparticles. Proc Natl Acad Sci USA 108(50):19901–19906
60. Fan XQ, Li W, Fu HM, Zhu MH, Wang LP, Cai ZB, Liu JH, Li H (2017) Probing the function of solid nanoparticle structure under boundary lubrication. Acs Sustain Chem Eng 5(5):4223–4233
61. Kao MJ, Lin CR (2009) Evaluating the role of spherical titanium oxide nanoparticles in reducing friction between two pieces of cast iron. J Alloy Compd 483(1–2):456–459
62. Wang XM, Li CH, Zhang YB, Ding WF, Yang M, Gao T, Cao HJ, Xu XF, Wang DZ, Said Z, Debnath S, Jamil M, Ali HM (2020) Vegetable oil-based nanofluid minimum quantity lubrication turning: academic review and perspectives. J Manuf Process 59:76–97
63. Said Z, Saidur R, Rahim NA (2016) Energy and exergy analysis of a flat plate solar collector using different sizes of aluminium oxide based nanofluid. J Clean Prod 133:518–530
64. Yang M, Li CH, Zhang YB, Jia DZ, Zhang XP, Hou YL, Shen B, Li RZ (2018) Microscale bone grinding temperature by dynamic heat flux in nanoparticle jet mist cooling with different particle sizes. Mater Manuf Process 33(1):58–68
65. Khajehzadeh M, Moradpour J, Razfar MR (2019) Influence of nanolubricant particles' size on flank wear in hard turning. Mater Manuf Process 34(5):494–501
66. Dubey V, Sharma AK, Pimenov DY (2022) Prediction of surface roughness using machine learning approach in MQL turning of AISI 304 steel by varying nanoparticle size in the cutting fluid. Lubricants 10(5):81
67. Mao C, Zhang J, Huang Y, Zou HF, Huang XM, Zhou ZX (2013) Investigation on the effect of nanofluid parameters on MQL grinding. Mater Manuf Process 28(4):436–442
68. Yuan SM, Hou XB, Wang L, Chen BC (2018) Experimental Investigation on the compatibility of nanoparticles with vegetable oils for nanofluid minimum quantity lubrication machining. Tribol Lett 66(3):106
69. Lee PH, Kim JW, Lee SW (2018) Experimental characterization on eco-friendly micro-grinding process of titanium alloy using air flow assisted electrospray lubrication with nanofluid. J Clean Prod 201:452–462
70. Huang W, Shen C, Liao SJ, Wang XL (2011) Study on the ferrofluid lubrication with an external magnetic field. Tribol Lett 41(1):145–151
71. Xu MC, Dai QW, Huang W, Wang XL (2020) Using magnetic fluids to improve the behavior of ball bearings under starved lubrication. Tribol Int 141:105950
72. Lv T, Xu XF, Yu AB, Niu CC, Hu XD (2021) Ambient air quantity and cutting performances of water-based Fe3O4 nanofluid in magnetic minimum quantity lubrication. Int J Adv Manuf Technol 115(5–6):1711–1722
73. Guo XH, Huang Q, Wang CD, Liu TS, Zhang YP, He HD, Zhang KD (2022) Effect of magnetic field on cutting performance of micro-textured tools under Fe3O4 nanofluid lubrication condition. J Mater Process Technol 299:117382
74. Najiha MS, Rahman MM, Yusoff AR (2015) Flank wear characterization in aluminum alloy (6061 T6) with nanofluid minimum quantity lubrication environment using an uncoated carbide tool. J Manuf Sci E-T ASME 137(6):061004
75. Lv T, Xu XF, Yu AB, Hu XD (2021) Oil mist concentration and machining characteristics of SiO2 water-based nano-lubricants in electrostatic minimum quantity lubrication-EMQL milling. J Mater Process Technol 290:116964
76. Xu XF, Lv T, Luan ZQ, Zhao YY, Wang MH, Hu XD (2019) Capillary penetration mechanism and oil mist concentration of Al2O3 nanoparticle fluids in electrostatic minimum quantity lubrication (EMQL) milling. Int J Adv Manuf Technol 104(5–8):1937–1951
77. Bartolomeis AD, Newman ST, Shokrani A (2020) Initial investigation on surface integrity when machining Inconel 718 with conventional and electrostatic lubrication. Procedia CIRP 87:65–70
78. Shah P, Gadkari A, Sharma A, Shokrani A, Khanna N (2021) Comparison of machining performance under MQL and ultrahigh voltage EMQL conditions based on tribological properties. Tribol Int 153:106595
79. Jia DZ, Zhang YB, Li CH, Yang M, Gao T, Said Z, Sharma S (2022) Lubrication-enhanced mechanisms of titanium alloy grinding using lecithin biolubricant. Tribol Int 169:107461
80. Lv T, Huang SQ, Liu ET, Ma YL, Xu XF (2018) Tribological and machining characteristics of an electrostatic minimum quantity lubrication (EMQL) technology using graphene nano-lubricants as cutting fluids. J Manuf Process 34:225–237
81. Shokrani A, Betts J, Jawahir IS (2022) Improved performance and surface integrity in finish machining of Inconel 718 with electrically charged tungsten disulphide MQL. CIRP Ann-Manuf Techn 71:109–112
82. Huang WT, Liu WS, Tsai JT, Chou JH (2018) Multiple quality characteristics of nanofluid/ultrasonic atomization minimum quality lubrication for grinding hardened mold steel. IEEE Trans Autom Sci Eng 15(3):1065–1077
83. Huang WT, Tsai JT, Hsu CAF, Ho WH, Chou JH (2022) Multiple performance characteristics in the application of taguchi fuzzy method in nanofluid/ultrasonic atomization minimum quantity lubrication for grinding Inconel 718 Alloys. Int J Fuzzy Syst 24(1):294–309
84. Huang WT, Chou FI, Tsai JT, Lin TW, Chou JH (2020) Optimal design of parameters for the nanofluid/ultrasonic atomization minimal quantity lubrication in a micromilling process. IEEE Trans Industr Inf 16(8):5202–5212
85. Huang WT, Chou FI, Tsai JT, Chou JH (2020) Application of graphene nanofluid/ultrasonic atomization MQL system in micromilling and development of optimal predictive model for SKH-9 high-speed steel using fuzzy-logic-based multi-objective design. Int J Fuzzy Syst 22(7):2101–2118
86. Hadad M, Beigi M (2021) A novel approach to improve environmentally friendly machining processes using ultrasonic nozzle-minimum quantity lubrication system. Int J Adv Manuf Technol 114(3–4):741–756
87. Lefebure A, Shim D (2021) Ultrasonic atomization of highly viscous biodegradable oils for MQL applications. J Mech Sci Technol 35(12):5503–5516

88. Zhang YB, Li HN, Li CH, Huang CZ, Ali HM, Xu XF, Mao C, Ding WF, Cui X, Yang M, Yu TBA, Jamil M, Gupta MK, Jia DZ, Said Z (2022) Nano-enhanced biolubricant in sustainable manufacturing: From processability to mechanisms. Friction 10(6):803–841
89. Gaurav G, Sharma A, Dangayach GS, Meena ML (2020) Assessment of jojoba as a pure and nano-fluid base oil in minimum quantity lubrication (MQL) hard-turning of Ti-6Al-4V: A step towards sustainable machining. J Clean Prod 272:122553
90. Padmini R, Krishna PV, Rao GKM (2016) Effectiveness of vegetable oil based nanofluids as potential cutting fluids in turning AISI 1040 steel. Tribol Int 94:490–501
91. Su Y, Gong L, Li B, Liu ZQ, Chen DD (2016) Performance evaluation of nanofluid MQL with vegetable-based oil and ester oil as base fluids in turning. Int J Adv Manuf Technol 83(9–12):2083–2089
92. Yin QA, Li CH, Dong L, Bai XF, Zhang YB, Yang M, Jia DZ, Li RZ, Liu ZQ (2021) Effects of physicochemical properties of different base oils on friction coefficient and surface roughness in MQL milling AISI 1045. Int J Pr Eng Man-GT 8(6):1629–1647
93. Bai XF, Zhou FM, Li CH, Dong L, Lv XJ, Yin QG (2020) Physicochemical properties of degradable vegetable-based oils on minimum quantity lubrication milling. Int J Adv Manuf Technol 106(9–10):4143–4155
94. Dong L, Li CH, Zhou FM, Bai XF, Gao W, Duan ZJ, Li XP, Lv XJ, Zhang FB (2021) Temperature of the 45 steel in the minimum quantity lubricant milling with different biolubricants. Int J Adv Manuf Technol 113(9–10):2779–2790
95. Zhang YB, Li CH, Jia DZ, Zhang DK, Zhang XW (2015) Experimental evaluation of MoS2 nanoparticles in jet MQL grinding with different types of vegetable oil as base oil. J Clean Prod 87:930–940
96. Zhang YB, Li CH, Yang M, Jia DZ, Wang YG, Li BK, Hou YL, Zhang NQ, Wu QD (2016) Experimental evaluation of cooling performance by friction coefficient and specific friction energy in nanofluid minimum quantity lubrication grinding with different types of vegetable oil. J Clean Prod 139:685–705
97. Wang YG, Li CH, Zhang YB, Yang M, Li BK, Jia DZ, Hou YL, Mao C (2016) Experimental evaluation of the lubrication properties of the wheel/workpiece interface in minimum quantity lubrication (MQL) grinding using different types of vegetable oils. J Clean Prod 127:487–499
98. Guo SM, Li CH, Zhang YB, Wang YG, Li BK, Yang M, Zhang XP, Liu GT (2017) Experimental evaluation of the lubrication performance of mixtures of castor oil with other vegetable oils in MQL grinding of nickel-based alloy. J Clean Prod 140:1060–1076
99. Guo SM, Li CH, Zhang YB, Yang M, Jia DZ, Zhang XP, Liu GT, Li RZ, Bing ZR, Ji HJ (2018) Analysis of volume ratio of castor/soybean oil mixture on minimum quantity lubrication grinding performance and microstructure evaluation by fractal dimension. Ind Crops Prod 111:494–505
100. Mcnutt J, He Q (2016) Development of biolubricants from vegetable oils via chemical modification. J Ind Eng Chem 36:1–12
101. Kivak T, Sarikaya M, Yildirim CV, Sirin S (2020) Study on turning performance of PVD TiN coated Al2O3+TiCN ceramic tool under cutting fluid reinforced by nano-sized solid particles. J Manuf Process 56:522–539
102. Talib N, Sasahara H, Rahim EA (2017) Evaluation of modified jatropha-based oil with hexagonal boron nitride particle as a biolubricant in orthogonal cutting process. Int J Adv Manuf Technol 92(1–4):371–391
103. Li BK, Li CH, Zhang YB, Wang YG, Yang M, Jia DZ, Zhang NQ, Wu QD (2017) Effect of the physical properties of different vegetable oil-based nanofluids on MQLC grinding temperature of Ni-based alloy. Int J Adv Manuf Technol 89(9–12):3459–3474
104. Zhang YB, Li CH, Jia DZ, Li BK, Wang YG, Yang M, Hou YL, Zhang XW (2016) Experimental study on the effect of nanoparticle concentration on the lubricating property of nanofluids for MQL grinding of Ni-based alloy. J Mater Process Technol 232:100–115
105. Sen B, Mia M, Gupta MK, Rahman MA, Mandal UK, Mondal SP (2019) Influence of Al2O3 and palm oil-mixed nano-fluid on machining performances of Inconel-690: IF-THEN rules-based FIS model in eco-benign milling. Int J Adv Manuf Technol 103(9–12):3389–3403
106. Duan ZJ, Yin QG, Li CH, Dong L, Bai XF, Zhang YB, Yang M, Jia DZ, Li RZ, Liu ZQ (2020) Milling force and surface morphology of 45 steel under different Al2O3 nanofluid concentrations. Int J Adv Manuf Technol 107(3–4):1277–1296
107. Roushan A, Rao US, Patra K, Sahoo P (2022) Performance evaluation of tool coatings and nanofluid MQL on the micromachinability of Ti-6Al-4V. J Manuf Process 73:595–610
108. Amrita M, Srikant RR, Sitaramaraju AV, Prasad MMS, Krishna PV (2013) Experimental investigations on influence of mist cooling using nanofluids on machining parameters in turning AISI 1040 steel. P I Mech Eng J-J Eng 227(12):1334–1346
109. Hegab H, Umer U, Deiab I, Kishawy H (2018) Performance evaluation of Ti-6Al-4V machining using nano-cutting fluids under minimum quantity lubrication. Int J Adv Manuf Technol 95(9–12):4229–4241
110. Yildirim CV, Sarikaya M, Kivak T, Sirin S (2019) The effect of addition of hBN nanoparticles to nanofluid-MQL on tool wear patterns, tool life, roughness and temperature in turning of Ni-based Inconel 625. Tribol Int 134:443–456
111. Talib N, Rahim EA (2018) Performance of modified jatropha oil in combination with hexagonal boron nitride particles as a bio-based lubricant for green machining. Tribol Int 118:89–104
112. Rapeti P, Pasam VK, Gurram KMR, Revuru RS (2018) Performance evaluation of vegetable oil based nano cutting fluids in machining using grey relational analysis—a step towards sustainable manufacturing. J Clean Prod 172:2862–2875
113. Pavani PNL, Rao RP, Srikiran S (2015) Performance evaluation and optimization of nano boric acid powder weight percentage mixed with vegetable oil using the Taguchi approach. J Mech Sci Technol 29(11):4877–4883
114. Rahman SS, Ashraf MZI, Amin AKMN, Bashar MS, Ashik MFK, Kamruzzaman M (2019) Tuning nanofluids for improved lubrication performance in turning biomedical grade titanium alloy. J Clean Prod 206:180–196
115. Said Z, Cakmak NK, Sharma P, Sundar LS, Inayat A, Keklikcioglu O, Li CH (2022) Synthesis, stability, density, viscosity of ethylene glycol-based ternary hybrid nanofluids: experimental investigations and model -prediction using modern machine learning techniques. Powder Technol 400:117190
116. Said Z, Sharma P, Sundar LS, Li CH, Tran DC, Pham NDK, Nguyen XP (2022) Improving the thermal efficiency of a solar flat plate collector using MWCNT-Fe3O4/water hybrid nanofluids and ensemble machine learning. Case Stud Therm Eng 40:102448
117. Singh RK, Sharma AK, Dixit AR, Tiwari AK, Pramanik A, Mandal A (2017) Performance evaluation of alumina-graphene hybrid nano-cutting fluid in hard turning. J Clean Prod 162:830–845
118. Sharma AK, Singh RK, Dixit AR, Tiwari AK (2017) Novel uses of alumina-MoS2 hybrid nanoparticle enriched cutting fluid in hard turning of AISI 304 steel. J Manuf Process 30:467–482
119. Sharma AK, Tiwari AK, Dixit AR, Singh RK (2020) Measurement of machining forces and surface roughness in turning of AISI 304 steel using alumina-MWCNT hybrid nanoparticles enriched cutting fluid. Measurement 150:107078

120. Junankar AA, Yashpal Y, Purohit JK (2022) Experimental investigation to study the effect of synthesized and characterized monotype and hybrid nanofluids in minimum quantity lubrication assisted turning of bearing steel. P I Mech Eng J-J Eng 236(9):1794–1813
121. Thakur A, Manna A, Samir S (2020) Experimental investigation of nanofluids in minimum quantity lubrication during turning of EN-24 steel. P I Mech Eng J-J Eng 234(5):712–729
122. Dubey V, Sharma AK, Vats P, Pimenov DY, Giasin K, Chuchala D (2021) Study of a multicriterion decision-making approach to the MQL turning of AISI 304 steel using hybrid nanocutting fluid. Materials 14(23):7207
123. Sirin S, Kivak T (2021) Effects of hybrid nanofluids on machining performance in MQL-milling of Inconel X-750 superalloy. J Manuf Process 70:163–176
124. Safiei W, Rahman MM, Yusoff AR, Arifin MN, Tasnim W (2021) Effects of SiO2-Al2O3-ZrO2 Tri-hybrid nanofluids on surface roughness and cutting temperature in end milling process of aluminum alloy 6061–T6 using uncoated and coated cutting inserts with minimal quantity lubricant method. Arab J Sci Eng 46(8):7699–7718
125. Zhang XP, Li CH, Zhang YB, Jia DZ, Li BK, Wang YG, Yang M, Hou YL, Zhang XW (2016) Performances of Al2O3/SiC hybrid nanofluids in minimum-quantity lubrication grinding. Int J Adv Manuf Technol 86(9–12):3427–3441
126. Zhang XP, Li CH, Zhang YB, Wang YG, Li BK, Yang M, Guo SM, Liu GT, Zhang NQ (2017) Lubricating property of MQL grinding of Al2O3/SiC mixed nanofluid with different particle sizes and microtopography analysis by cross-correlation. Precis Eng 47:532–545
127. Noroozi M, Radiman S, Zakaria A (2014) Influence of sonication on the stability and thermal properties of Al2O3 nanofluids. J Nanomater 2014:612417
128. Mondragon R, Julia JE, Barba A, Jarque JC (2012) Characterization of silica-water nanofluids dispersed with an ultrasound probe: a study of their physical properties and stability. Powder Technol 224:138–146
129. Mahbubul IM, Saidur R, Amalina MA, Elcioglu EB, Okutucu-Ozyurt T (2015) Effective ultrasonication process for better colloidal dispersion of nanofluid. Ultrason Sonochem 26:361–369
130. Mao C, Zou HF, Zhou X, Huang Y, Gan HY, Zhou ZX (2014) Analysis of suspension stability for nanofluid applied in minimum quantity lubricant grinding. Int J Adv Manuf Technol 71(9–12):2073–2081
131. Gajrani KK, Suvin PS, Kailas SV, Sankar MR (2019) Thermal, rheological, wettability and hard machining performance of MoS2 and CaF2 based minimum quantity hybrid nano-green cutting fluids. J Mater Process Technol 266:125–139
132. Shabgard M, Seyedzavvar M, Abbasi H (2017) Investigation into features of graphite nanofluid synthesized using electro discharge process. Int J Adv Manuf Technol 90(5–8):1203–1216
133. Shukla R, Tiwari AK, Agarawal S (2022) Effects of surfactant and MoO3 nanofluid on tribological and machining characteristics in minimum quantity lubrication (MQL)-turning of AISI 304 steel. Proceedings of the Institution of Mechanical Engineers Part E-Journal of Process Mechanical Engineering:09544089221105928
134. Behera BC, Chetan SD, Ghosh S, Rao PV (2017) Spreadability studies of metal working fluids on tool surface and its impact on minimum amount cooling and lubrication turning. J Mater Process Technol 244:1–16
135. Amrita M, Kamesh B, Srikant RR, Prithiviraajan RN, Reddy KS (2019) Thermal enhancement of graphene dispersed emulsifier cutting fluid with different surfactants. Mater Res Express 6(12):125030
136. Gao T, Li CH, Zhang YB, Yang M, Jia DZ, Jin T, Hou YL, Li RZ (2019) Dispersing mechanism and tribological performance of vegetable oil-based CNT nanofluids with different surfactants. Tribol Int 131:51–63
137. Sirin E, Kivak T, Yildirim CV (2021) Effects of mono/hybrid nanofluid strategies and surfactants on machining performance in the drilling of Hastelloy X. Tribol Int 157:106894
138. Das A, Pradhan O, Patel SK, Das SR, Biswal BB (2019) Performance appraisal of various nanofluids during hard machining of AISI 4340 steel. J Manuf Process 46:248–270
139. Nwoguh TO, Okafor AC, Onyishi HA (2021) Enhancement of viscosity and thermal conductivity of soybean vegetable oil using nanoparticles to form nanofluids for minimum quantity lubrication machining of difficult-to-cut metals. Int J Adv Manuf Technol 113(11–12):3377–3388
140. Bertolini R, Ghiotti A, Bruschi S (2021) Graphene nanoplatelets as additives to MQL for improving tool life in machining Inconel 718 alloy. Wear 476:203656
141. Das SK, Putra N, Roetzel W (2003) Pool boiling characteristics of nano-fluids. Int J Heat Mass Transf 46(5):851–862
142. Wang XM, Li CH, Zhang YB, Said Z, Debnath S, Sharma S, Yang M, Gao T (2022) Influence of texture shape and arrangement on nanofluid minimum quantity lubrication turning. Int J Adv Manuf Technol 119(1–2):631–646
143. Zhang YB, Li CH, Jia DZ, Zhang DK, Zhang XW (2015) Experimental evaluation of the lubrication performance of MoS2/CNT nanofluid for minimal quantity lubrication in Ni-based alloy grinding. Int J Mach Tools Manuf 99:19–33
144. Li CH, Li JY, Wang S, Zhang Q (2013) Modeling and numerical simulation of the grinding temperature field with nanoparticle jet of MQL. Adv Mech Eng 986984
145. Hayat MA, Ali HM, Janjua MM, Pao W, Li CH, Alizadeh M (2020) Phase change material/heat pipe and Copper foam-based heat sinks for thermal management of electronic systems. J Energy Storage 32:101971
146. Said Z, Sundar LS, Rezk H, Nassef AM, Chakraborty S, Li CH (2021) Thermophysical properties using ND/water nanofluids: an experimental study, ANFIS-based model and optimization. J Mol Liq 330:115659
147. Said Z, Sharma P, Sundar LS, Afzal A, Li CH (2021) Synthesis, stability, thermophysical properties and AI approach for predictive modelling of Fe3O4 coated MWCNT hybrid nanofluids. J Mol Liq 340:117291
148. Yang M, Li CH, Zhang YB, Wang YG, Li BK, Jia DZ, Hou YL, Li RZ (2017) Research on microscale skull grinding temperature field under different cooling conditions. Appl Therm Eng 126:525–537
149. Mao C, Zou HF, Huang Y, Li YF, Zhou ZX (2013) Analysis of heat transfer coefficient on workpiece surface during minimum quantity lubricant grinding. Int J Adv Manuf Technol 66(1–4):363–370
150. Cui X, Li CH, Zhang YB, Said Z, Debnath S, Sharma S, Ali HM, Yang M, Gao T, Li RZ (2022) Grindability of titanium alloy using cryogenic nanolubricant minimum quantity lubrication. J Manuf Process 80:273–286
151. Shen B, Shih AJ, Xiao GX (2011) A Heat Transfer Model Based on Finite Difference Method for Grinding. J Manuf Sci E-T ASME 133(3):031001
152. Hadad M, Sadeghi B (2012) Thermal analysis of minimum quantity lubrication-MQL grinding process. Int J Mach Tools Manuf 63:1–15
153. Yang M, Li CH, Luo L, Li RZ, Long YZ (2021) Predictive model of convective heat transfer coefficient in bone

micro-grinding using nanofluid aerosol cooling. Int Commun Heat Mass Transf 125:105317
154. Zhang JC, Li CH, Zhang YB, Yang M, Jia DZ, Hou YL, Li RZ (2018) Temperature field model and experimental verification on cryogenic air nanofluid minimum quantity lubrication grinding. Int J Adv Manuf Technol 97(1–4):209–228
155. Zhang JC, Wu WT, Li CH, Yang M, Zhang YB, Jia DZ, Hou YL, Li RZ, Cao HJ, Ali HM (2021) Convective heat transfer coefficient model under nanofluid minimum quantity lubrication coupled with cryogenic air grinding Ti-6Al-4V. Int J Pr Eng Man-GT 8(4):1113–1135
156. Kumar R, Ranjan N, Kumar V, Kumar R, Chohan JS, Yadav A, Piyush SS, Prakash C, Singh S, Li CH (2022) Characterization of friction stir-welded polylactic acid/aluminum composite primed through fused filament fabrication. J Mater Eng Perform 31(3):2391–2409
157. Khare JM, Dahiya S, Gangil B, Ranakoti L, Sharma S, Huzaifah MRM, Ilyas RA, Dwivedi SP, Chattopadhyaya S, Kilinc HC, Li CH (2021) Comparative analysis of erosive wear behaviour of epoxy, polyester and vinyl esters based thermosetting polymer composites for human prosthetic applications using taguchi design. Polymers 13(20):3607
158. Cui X, Li CH, Zhang YB, Ding WF, An QL, Li HN, Said Z, Sharma S, Li R, Debnath S (2022) A comparative assessment of force, temperature and wheel wear in sustainable grinding aerospace alloy using bio-lubricant. Front Mech Eng 18(1):3
159. Liu M, Li C, Cao H, Zhang S, Chen Y, Liu B, Zhang N, Zhou Z (2022) Research progresses and applications of CMQL machining technology. China Mech Eng 33(5):529–550
160. Yang YY, Yang M, Li CH, Said Z, Ali HM, Sharma S (2022) Machinability of ultrasonic vibration assisted micro-grinding in biological bone using nanolubricant. Front Mech Eng https://doi.org/10.1007/s11465-022-0717-z
161. Mao C, Huang Y, Zhou X, Gan H, Zhang J, Zhou ZX (2014) The tribological properties of nanofluid used in minimum quantity lubrication grinding. Int J Adv Manuf Technol 71(5–8):1221–1228
162. Akincioglu S, Sirin S (2021) Evaluation of the tribological performance of the green hBN nanofluid on the friction characteristics of AISI 316L stainless steel. Ind Lubr Tribol 73(9):1176–1186
163. Kumar AS, Deb S, Paul S (2020) Tribological characteristics and micromilling performance of nanoparticle enhanced water based cutting fluids in minimum quantity lubrication. J Manuf Process 56:766–776
164. Singh R, Sharma V (2022) Experimental investigations into tribological and machining characteristics of Al2O3 and ZrO dispersed Jatropha oil-based nanofluids. J Braz Soc Mech Sci 44(8):345
165. Kulandaivel A, Kumar S (2020) Effect of magneto rheological minimum quantity lubrication on machinability, wettability and tribological behavior in turning of Monel K500 alloy. Mach Sci Technol 24(5):810–836
166. Yin QA, Li CH, Zhang YB, Yang M, Jia DZ, Hou YL, Li RZ, Dong L (2018) Spectral analysis and power spectral density evaluation in Al2O3 nanofluid minimum quantity lubrication milling of 45 steel. Int J Adv Manuf Technol 97(1–4):129–145
167. Li CH, Zhang DK, Jia DZ, Wang S, Hou YL (2015) Experimental evaluation on tribological properties of nano-particle jet MQL grinding. Int J Surf Sci Eng 9(2–3):159–175
168. Jia DZ, Li CH, Zhang DK, Zhang YB, Zhang XW (2014) Experimental verification of nanoparticle jet minimum quantity lubrication effectiveness in grinding. J Nanopart Res 16(12):2758
169. Wu WT, Li CH, Yang M, Zhang YB, Jia DZ, Hou YL, Li RZ, Cao HJ, Han ZG (2019) Specific energy and G ratio of grinding cemented carbide under different cooling and lubrication conditions. Int J Adv Manuf Technol 105(1–4):67–82
170. Singh H, Sharma VS, Dogra M (2020) Exploration of graphene assisted vegetables oil based minimum quantity lubrication for surface grinding of TI-6AL-4V-ELI. Tribol Int 144:106113
171. Pal A, Chatha SS, Singh K (2020) Performance evaluation of minimum quantity lubrication technique in grinding of AISI 202 stainless steel using nano-MoS(2)with vegetable-based cutting fluid. Int J Adv Manuf Technol 110(1–2):125–137
172. Zhang ZC, Sui MH, Li CH, Zhou ZM, Liu B, Chen Y, Said Z, Debnath S, Sharma S (2022) Residual stress of grinding cemented carbide using MoS2 nano-lubricant. Int J Adv Manuf Technol 119(9–10):5671–5685
173. Guo YH, Cui XB, Guo JX (2020) Biomimetic integration of MQL and tool surface microstructure in intermittent machining. Int J Adv Manuf Technol 111(7–8):1847–1861
174. Cao Y, Zhu YJ, Ding WF, Qiu YT, Wang LF, Xu JH (2022) Vibration coupling effects and machining behavior of ultrasonic vibration plate device for creep-feed grinding of Inconel 718 nickel-based superalloy. Chin J Aeronaut 35(2):332–345
175. Kuang WJ, Miao Q, Ding WF, Zhao YJ, Zhao B, Wen XB, Li SP (2022) Fretting wear behaviour of machined layer of nickel-based superalloy produced by creep-feed profile grinding. Chin J Aeronaut 35(10):401–411
176. Cao Y, Yin JF, Ding WF, Xu JH (2021) Alumina abrasive wheel wear in ultrasonic vibration-assisted creep-feed grinding of Inconel 718 nickel-based superalloy. J Mater Process Technol 297:117241
177. Li RZ, Qian XJ, Gong C, Liu Y, Zhang JH, Xu B, Humayun MS, Zhou QF (2022) Simultaneous assessment of the whole eye biomechanics using high frequency ultrasonic elastography. Invest Ophthalmol Vis Sci 63(7):1–8
178. Cao Y, Ding WF, Zhao BA, Wen XB, Li SP, Wang JZ (2022) Effect of intermittent cutting behavior on the ultrasonic vibration-assisted grinding performance of Inconel718 nickel-based superalloy. Precis Eng 78:248–260
179. Rabiei F, Rahimi AR, Hadad MJ (2017) Performance improvement of eco-friendly MQL technique by using hybrid nanofluid and ultrasonic-assisted grinding. Int J Adv Manuf Technol 93(1–4):1001–1015
180. Behera BC, Ghosh S, Rao PV (2018) Modeling of cutting force in MQL machining environment considering chip tool contact friction. Tribol Int 117:283–295
181. Nunez D, Arroba C, Vaca H, Perez C, Morales C (2019) Spray lubrication in turning processes, effects on productivity and quality. Dyna 94(5):561–567
182. Yucel A, Yildirim CV, Sarikaya M, Sirin S, Kivak T, Gupta MK, Tomaz IV (2021) Influence of MoS2 based nanofluid-MQL on tribological and machining characteristics in turning of AA 2024 T3 aluminum alloy. J Mater Res Technol-Jmr&T 15:1688–1704
183. Gunan F, Kivak T, Yildirim CV, Sarikaya M (2020) Performance evaluation of MQL with AL(2)O(3) mixed nanofluids prepared at different concentrations in milling of Hastelloy C276 alloy. J Mater Res Technol-Jmr&T 9(5):10386–10400
184. Minh DT, The LT, Bao NT (2017) Performance of Al2O3 nanofluids in minimum quantity lubrication in hard milling of 60Si(2)Mn steel using cemented carbide tools. Adv Mech Eng 9(7):1687814017710618
185. Bangma TJ (2019) Minimum quantity lubrication system with air blow off. United States of America: US10259088, 2019–04–16
186. Li CH, Wu XF, Zhang NQ, Zhang YB, Wu QD, Cao HJ, Gao T, Yang M, Lu BH, Yang YY, Cui X, Zhao XF, Liu MZ, Jia DZ, Zhang XW, Ma H (2022) Internal cooling/external cooling-switching milling minimum-quantity-lubrication intelligent

nozzle system and method. The People's Republic of China: US20220143769, 2022–05–12
187. Guo SM, LI CH, Lu BH, Cao HJ, Zhang YB, Yang M, Zhang NQ, Wu QD (2017) High-speed milling micro lubrication liquid supply nozzle structure and separation and recovery mechanism and system. The People's Republic of China: CN106392764, 2017–02–15
188. Yang M, LI CH, Zhang YB, Li BK, Wang YG, Guo SM (2015) Electrostatic atomization inner-cooled grinding head. The People's Republic of China: CN105147356, 2015–12–16
189. Jia DZ, Zhao HY, Yang M, Wang XM, Cui X, Gao T, Wu WT, LI CH, Cao HJ, Han ZG, Zhang NQ (2019) Electrostatic nozzle and controllable jet flow minimal quantity lubrication grinding system. The People's Republic of China: CN209615205, 2019–11–12
190. SU Y, Zhao ZC, Chen DD, Liu ZQ, Li B, Cao H, Gong Y (2014) Cutting method and device capable of controlling spraying of nanometer fluid droplets. The People's Republic of China: CN104029079, 2014–09–10
191. Xu XF, Lv T, Huang SQ, Hu XD, Ma YL (2018) Charged aerosol U-shaped nozzle. The People's Republic of China: CN108247135, 2018–07–06
192. Xu XF, Hu XD, Feng BH, Zhao YY, Lv T (2019) Electrostatic minimum quantity lubrication device. The People's Republic of China: CN209793270, 2019–12–17
193. Yang M, Ma H, LI CH, Zhou ZM, Li M, Wu XF, Zhang NQ, Liu B, Cao HJ (2022) Multi-energy-field driven electrostatic atomization trace lubricant conveying device. The People's Republic of China: CN114012498, 2022–02–08
194. Yang M, Li CH, Li RZ, Yang YL, Hou YL, Jia DZ, Zhang YB, Zhang XW (2018) Neurosurgical ultrasonic focusing assisted three-stage atomization cooling and postoperative wound film forming device. The People's Republic of China: CN107789030, 2018–03–13
195. Li H, Ren K, Yin Z, Zhao JJ, Cao ZY, Lv ZQ (2015) The vibration characteristics and design of ultrasonic atomization system based on longitudinal-flexural vibration conversion. J Vib Eng 28(3):462–469
196. Cao Y, Li H, Ren K, Liu SJ, Wang ZW (2018) Research on heat transfer performances of spherical focused ultrasoundassisted ultrasonic atomizing cooling system. China Mech Eng 29(11):1279–1284
197. Zhao B, Yue YS, Ding WF, Wu BF, Xu JH, Fu YC, Yin JF, Qian N (2022) Ultrasonic vibration atomization rotary jet cooling device and operation process thereof. The People's Republic of China: CN113977344, 2022–01–28
198. Wang XM, Li CH, Zhang YB, Yang M, Zhou ZM, Chen Y, Liu B, Wang DZ (2022) Research progress on key technology of enabled atomization and supply system of minimum quantity lubrication. Surf Technol 51(9):1–14
199. Ni CB, Zhu LD (2020) Investigation on machining characteristics of TC4 alloy by simultaneous application of ultrasonic vibration assisted milling (UVAM) and economical-environmental MQL technology. J Mater Process Technol 278:116518
200. Kapoor SG, Nath C (2014) Atomizing-based cutting fluid delivery system method. United States of America: US20140353406, 2017–12–04
201. Xiong WQ (2012) Minimal quantity lubrication (MQL) supply system for processing of outer-cooling type high-speed machine tool and inner-cooling type high-speed machine tool. The People's Republic of China: CN102528550, 2012–07–04
202. Xiong WQ, Gong L, Zhang YS, Wang CY (2017) High-pressure pneumatic pulse type micro lubricating oil spray supplying system. The People's Republic of China: CN106838590, 2017–06–13
203. Yao YQ (2020) MQL electric control closed-loop precision adjustable micro pump. The People's Republic of China: CN211176254, 2020–08–04
204. Yuan SM, Hou XB (2017) Lubricating system with trace amount. The People's Republic of China: CN206802727, 2017–12–26
205. LI CH, Zhang YB, Jia DZ, Yang M, Zhang RZ, Zhang NQ, J HJ, Zhao R, Hou YL, Wu QD (2021) Continuous feeding precise micro-lubricating pump which supports different lubrication working conditions. Commonwealth of Australia: AU2018352789, 2021–01–21
206. Jochen R, Aldo DN, Stefano D (2011) Minimal quantity lubricating system. PCT: WO2011134776, 2011–11–03
207. Abd Rahim E, Dorairaju H (2018) Evaluation of mist flow characteristic and performance in Minimum Quantity Lubrication (MQL) machining. Measurement 123:213–225
208. Obikawa T, Asano Y, Kamata Y (2009) Computer fluid dynamics analysis for efficient spraying of oil mist in finish-turning of Inconel 718. Int J Mach Tools Manuf 49(12–13):971–978
209. Alberdi R, Sanchez JA, Pombo I, Ortega N, Izquierdo B, Plaza S, Barrenetxea D (2011) Strategies for optimal use of fluids in grinding. Int J Mach Tools Manuf 51(6):491–499
210. Balan ASS, Kullarwar T, Vijayaraghavan L, Krishnamurthy R (2017) Computational fluid dynamics analysis of MQL spray parameters and its influence on superalloy grinding. Mach Sci Technol 21(4):603–616
211. Park KH, Olortegui-Yume J, Yoon MC, Kwon P (2010) A study on droplets and their distribution for minimum quantity lubrication (MQL). Int J Mach Tools Manuf 50(9):824–833
212. Maruda RW, Krolczyk GM, Feldshtein E, Pusavec F, Szydlowski M, Legutko S, Sobczak-Kupiec A (2016) A study on droplets sizes, their distribution and heat exchange for minimum quantity cooling lubrication (MQCL). Int J Mach Tools Manuf 100:81–92
213. Jia DZ, Li CH, Zhang YB, Zhang DK, Zhang XW (2015) Numerical simulation and experimental research about downstream flow field of atomizing nozzle in nanoparticle jet MQL grinding. Modular Machine Tool Automatic Manuf Tech 09:5–9
214. Emami M, Sadeghi MH, Sarhan AAD (2013) Investigating the effects of liquid atomization and delivery parameters of minimum quantity lubrication on the grinding process of Al2O3 engineering ceramics. J Manuf Process 15(3):374–388
215. Sai SS, ManojKumar K, Ghosh A (2015) Assessment of spray quality from an external mix nozzle and its impact on SQL grinding performance. Int J Mach Tools Manuf 89:132–141
216. Zhu GY, Yuan SM, Kong XY, Zhang C, Chen BC (2020) Flow and aeroacoustic characteristics evaluation of microjet noise reduction concept in the nozzle design for minimum quantity lubrication. J Sound Vib 488:115638
217. Feng BH, Luan ZQ, Zhang RC, Xia Y, Yao WQ, Liu JW, Ma YL, Hu XD, Xu XF (2022) Effect of electroosmosis on lubricant penetration at the tool-chip interface. J Mater Process Technol 307:117653
218. Jia DZ, Li CH, Zhang YB, Yang M, Cao HJ, Liu B, Zhou ZM (2022) Grinding performance and surface morphology evaluation of titanium alloy using electric traction bio micro lubricant. J Mech Eng 58(5):198–211
219. Jia D, Zhang N, Liu B, Zhou Z, Wang X, Zhang Y, Mao C, Li C (2021) Particle size distribution characteristics of electrostatic minimum quantity lubrication and grinding surface quality evaluation. Diamond Abrasives Eng 41(3):89–95
220. Xie GX, Guo D, Luo JB (2015) Lubrication under charged conditions. Tribol Int 84:22–35
221. Jun MBG, Joshi SS, Devor RE, Kapoor SG (2008) An experimental evaluation of an atomization-based cutting fluid application system for micromachining. J Manuf Sci E-T ASME 130(3):031118

222. Nath C, Kapoor SG, Srivastava AK, Iverson J (2014) Study of droplet spray behavior of an atomization-based cutting fluid spray system for machining titanium alloys. J Manuf Sci E-T ASME 136(2):021004
223. Hoyne AC, Nath C, Kapoor SG (2015) On cutting temperature measurement during titanium machining with an atomization-based cutting fluid spray system. J Manuf Sci E-T ASME 137(2):024502
224. Hoyne AC, Nath C, Kapoor SG (2013) Characterization of fluid film produced by an atomization-based cutting fluid spray system during machining. J Manuf Sci E-T ASME 135(5):051006
225. LI CH, Zhang YB, Jia DZ, Zhang DK (2014) Nanofluid minimum quantity lubrication electrostatic atomization controllable jet flow turning system. The People's Republic of China: CN104209806, 2014–12–17
226. Guo XH, Huang Q, Zhang KD, Zhang L, Zhang YP (2020) Turning device assisted by magnetic field. The People's Republic of China: CN211727522, 2020–10–23
227. Li CH, Wang XM, Luo L, Cao HJ, Lu BH, Li RZ, Zhang YB, Luo HM, Diao YC, Xu HZ, Jia DZ, Yang M, Hou YL (2019) Electric card auxiliary inner-cooling texture turning tool and nano fluid micro-lubrication intelligent working system. The People's Republic of China: CN110116223, 2019–08–13
228. Sui MH, Li CH, Wu WT, Cao HJ, Ji HJ, Zhang NQ, Wu QD, Gao T, Zhang YB, Yang M, Jia DZ, Hou YL, Li RZ (2019) Numerical control horizontal lathe minimal quantity lubrication intelligent spray head system based on three-axis parallel platform. The People's Republic of China: CN209110704, 2019–07–16
229. Sui MH, Wu WT, Li CH, Li RZ, Gao T, Zhang YB, Yang M, Jia DZ, Yin QA, Zhang XY, Hou YL (2020) Numerical control horizontal lathe minimal quantity lubrication intelligent spray head system based on six-axis linkage platform. The People's Republic of China: CN211805123, 2020–10–30
230. Shen Y, Pei H, Wang G (2012) The numerical simulation and flow field analysis of MQL cylindrical turning. Machinery Design Manuf (08):208–210
231. Chen M, Jiang L, Shi B, Liu Z, An Q (2012) CFD analysis on the flow field of minimum quantity lubrication during external thread turning materials Science. Forum 723:113–118
232. Hosokawa A, Kosugi K, Ueda T (2022) Turning characteristics of titanium alloy Ti-6Al-4V with high-pressure cutting fluid. CIRP Ann-Manuf Techn 71:81–84
233. Godlevski VA, Volkov AV, Latyshev VN, Maurin LN (2010) Description of the lubricating action of the tribo-active components of cutting fluids. Lubr Sci 11(1):51–62
234. Yan LT, Zhang QJ, Yu JZ (2018) Analytical models for oil penetration and experimental study on vibration assisted machining with minimum quantity lubrication. Int J Mech Sci 148:374–382
235. Hao XQ, Cui W, Li L, Li HL, Khan AM, He N (2018) Cutting performance of textured polycrystalline diamond tools with composite lyophilic/lyophobic wettabilities. J Mater Process Technol 260:1–8
236. Abbas AT, Benyahia F, El Rayes MM, Pruncu C, Taha MA, Hegab H (2019) Towards optimization of machining performance and sustainability aspects when turning AISI 1045 steel under different cooling and lubrication strategies. Materials 12(18):3023
237. Singh T, Dureja JS, Dogra M, Bhatti MS (2019) Multi-response optimization in environment friendly turning of AISI 304 austenitic stainless steel. Multidiscip Model Mater Struct 15(3):538–558
238. Karimpour H, Abedini V, Hajialimohamadi A (2022) Effects of process parameters on machining forces and surface roughness during turning 304L steel using SiO2 nanofluid. Proceedings of the Institution of Mechanical Engineers Part E-Journal of Process Mechanical Engineering:09544089221089140
239. Cui XB, Li YH, Guo JX, Ming PM (2021) Analysis of a sustainable MQL machining process combining modified waste cooking oil and multifunctional biomimetic microstructure. Sustain Mater Techno 29:e00311
240. Khan AM, Gupta MK, Hegab H, Jamil M, Mia M, He N, Song QH, Liu ZQ, Pruncu CI (2020) Energy-based cost integrated modelling and sustainability assessment of Al-GnP hybrid nanofluid assisted turning of AISI52100 steel. J Clean Prod 257:120502
241. Anandan V, Babu MN, Sezhian MV, Yildirim CV, Babu MD (2021) Influence of graphene nanofluid on various environmental factors during turning of M42 steel. J Manuf Process 68:90–103
242. Yildirim CV (2020) Investigation of hard turning performance of eco-friendly cooling strategies: cryogenic cooling and nanofluid based MQL. Tribol Int 144:106127
243. Das A, Patel SK, Biswal BB, Sahoo N, Pradhan A (2020) Performance evaluation of various cutting fluids using MQL technique in hard turning of AISI 4340 alloy steel. Measurement 150:107079
244. Duc TM, Long TT, Chien TQ (2019) Performance evaluation of MQL parameters using Al2O3 and MoS2 nanofluids in hard turning 90CrSi Steel. Lubricants 7(5):40
245. Das A, Patel SK, Biswal BB, Das SR (2020) Performance evaluation of aluminium oxide nano particles in cutting fluid with minimum quantity lubrication technique in turning of hardened AISI 4340 alloy steel. Scientia Iranica 27(6):2838–2852
246. Dash L, Padhan S, Das SR (2020) Design optimization for analysis of surface integrity and chip morphology in hard turning. Struct Eng Mech 76(5):561–578
247. Ibrahim AMM, Omer MAE, Das SR, Li W, Alsoufi MS, Elsheikh A (2022) Evaluating the effect of minimum quantity lubrication during hard turning of AISI D3 steel using vegetable oil enriched with nano-additives. Alex Eng J 61(12):10925–10938
248. Cui XB, Guo YH, Guo JX, Ming PM (2020) Bio-inspired design of cleaner interrupted turning and its effects on specific cutting energy and harmful gas emission. J Clean Prod 271:122354
249. Ramanan KV, Babu SR, Jebaraj M, Ross KNS (2021) Face turning of Incoloy 800 under MQL and nano-MQL environments. Mater Manuf Process 36(15):1769–1780
250. Mane PA, Kallol AN, Doiphode RL, Manjunath GA, Saleh B, Abbas M, Saleel CA, Alarifi IM (2022) Inconel 718 turning process parameters optimization with MQL nanofluid based on CuO nanoparticles. J Nanomater 2022:1408529
251. Rakesh PR, Chakradhar D (2022) Investigation on the effect of graphene nano-cutting fluid minimum quantity lubrication on the machining performance of Inconel 625. Arab J Sci Eng 47(7):8469–8483
252. Pandey K, Datta S, Roy T (2022) Machinability of Inconel 825 under nano-Al2O3 based nanofluid minimum quantity lubrication. Sadhana-Acad Proc Eng Sci 47(3):127
253. Sarikaya M, Sirin S, Yildirim CV, Kivak T, Gupta MK (2021) Performance evaluation of whisker-reinforced ceramic tools under nano-sized solid lubricants assisted MQL turning of Co-based Haynes 25 superalloy. Ceram Int 47(11):15542–15560
254. Gong L, Bertolini R, Bruschi S, Ghiotti A, He N (2022) Surface integrity evaluation when turning Inconel 718 alloy using sustainable lubricating-cooling approaches. Int J Pr Eng Man-GT 9(1):25–42
255. Sirin S (2022) Investigation of the performance of cermet tools in the turning of Haynes 25 superalloy under gaseous N2 and hybrid nanofluid cutting environments. J Manuf Process 76:428–443
256. Musavi SH, Davoodi B, Niknam SA (2021) Eco-green machining of superalloy A286: assessment of tool wear morphology

and surface topology. Proc Inst Mech Eng Part B-J Eng Manuf 235(9):1412–1424
257. Behera BC, Alemayehu H, Ghosh S, Rao PV (2017) A comparative study of recent lubri-coolant strategies for turning of Ni-based superalloy. J Manuf Process 30:541–552
258. Hegab H, Salem A, Rahnamayan S, Kishawy HA (2021) Analysis, modeling, and multi-objective optimization of machining Inconel 718 with nano-additives based minimum quantity coolant. Appl Soft Comput 108:107416
259. Gupta MK, Song QH, Liu ZQ, Sarikaya M, Jamil M, Mia M, Singla AK, Khan AM, Khanna N, Pimenov DY (2021) Environment and economic burden of sustainable cooling/lubrication methods in machining of Inconel-800. J Clean Prod 287:125074
260. Yildirim CV (2019) Experimental comparison of the performance of nanofluids, cryogenic and hybrid cooling in turning of Inconel 625. Tribol Int 137:366–378
261. Nguyen D, Lee PH, Guo Y, Park KH, Kwon P (2019) Wear performance evaluation of minimum quantity lubrication with exfoliated graphite nanoplatelets in turning titanium alloy. J Manuf Sci E-T ASME 141(8):081006
262. Anandan V, Babu MN, Muthukrishnan N, Babu MD (2020) Performance of silver nanofluids with minimum quantity lubrication in turning on titanium: a phase to green manufacturing. J Braz Soc Mech Sci 42(4):198
263. Khan AM, Anwar S, Jamil M, Nasr MM, Gupta MK, Saleh M, Ahmad S, Mia M (2021) Energy, environmental, economic, and technological analysis of Al-GnP nanofluid- and cryogenic LN2-assisted sustainable machining of Ti-6Al-4V Alloy. Metals 11(1):88
264. LI CH, Zhang YB, Cao HJ, Duan ZJ, Mao C, Ding WF, Zhang NQ, Bai XF, Sui MH, Liu YH, Wu WT, Gao T, Yang M, Jia DZ, Li RZ, Hou YL (2020) Milling system and method under different lubrication conditions. United States of America: US20200164447, 2020–05–28
265. LI CH, Yin QA, Cao HJ, Ding WF, Zhang NQ, Liu YH, Bai XF, Dong L, Duan ZJ, Sui MH, Wu WT, Gao T, Yang M, Jia DZ, Li RZ, Hou YL (2020) Milling tool device for auxiliary chip breaking and tool system for auxiliary chip breaking under different lubricating conditions. United States of America: US20200164475, 2020–05–28
266. Zhang CL, Zhang S, Yan XF, Zhang Q (2016) Effects of internal cooling channel structures on cutting forces and tool life in side milling of H13 steel under cryogenic minimum quantity lubrication condition. Int J Adv Manuf Technol 83(5–8):975–984
267. Goldman F, Chambers RV, Clippard WL III, Henn SM, Otto WE (1995) Lubricant nozzle positioning system and method. Europe: EP0679971, 1995–11–02
268. Hahnemann P (2000) Positioniereinheit für Minimalmengenschmierdüsen. Germany: DE000029915499U1, 2000–01–05
269. Yuan SM, Chen BC, Zhu GY (2017) Spray nozzle positioning system and machine tool. The People's Republic of China: CN107020542, 2017–08–08
270. Wu WT, Li CH, Li RZ, Sui MH, Gao T, Zhang YB, Yang M, Jia DZ, Yin QA, Zhang XY, Hou YL (2019) Minimal quantity lubrication multi freedom intelligence spray nozzle system based on numerically controlled fraise machine. The People's Republic of China: CN208773153, 2019–04–23
271. Cao HJ, Chen RH, Ju WJ, Song Y, Li BJ, Xia R(2020) Programmable minimum quantity lubrication jet angle phase adjusting device and using method thereof. The People's Republic of China: CN108115462, 2020–05–01
272. Zhao W, Yu ZY, Zhang ZD, Chen L, Yu M, Zhang K, Wan H, Du L, Jiang W, Wu NH (2019) Outer cooling type miniature lubrication manipulator, machine tool and lubrication method. The People's Republic of China: CN109648396, 2019–04–19
273. Wu YP, Chen Y, Bai YX, Cheng ZG (2021) Precise spraying lubrication device suitable for MQL milling. The People's Republic of China: CN112720051, 2021–04–30
274. Duchosal A, Serra R, Leroy R (2014) Numerical study of the inner canalization geometry optimization in a milling tool used in micro quantity lubrication. Mech Ind 15(5):435–442
275. Duan ZJ, Li CH, Zhang YB, Dong L, Bai XF, Yang M, Jia DZ, Li RZ, Cao HJ, Xu XF (2021) Milling surface roughness for 7050 aluminum alloy cavity influenced by nozzle position of nanofluid minimum quantity lubrication. Chin J Aeronaut 34(6):33–53
276. Du FL, He L, Zhou T, Tian PF, Zou ZC, Zhou XR (2022) Analysis of droplet characteristics and cooling lubrication effects in MQL milling of 316L stainless steel. J Mater Res Technol-Jmr&T 19:4832–4856
277. Yang YY, Gong YD, Li CH, Wen XL, Sun JY (2021) Mechanical performance of 316 L stainless steel by hybrid directed energy deposition and thermal milling process. J Mater Process Technol 291:117023
278. Cui X, Li CH, Ding WF, Chen Y, Mao C, Xu XF, Liu B, Wang DZ, Li HN, Zhang YB, Said Z, Debnath S, Jamil M, Ali HM, Sharma S (2022) Minimum quantity lubrication machining of aeronautical materials using carbon group nanolubricant: from mechanisms to application. Chin J Aeronaut 35(11):85–112
279. Huang HD, Tu JP, Gan LP, Li CZ (2006) An investigation on tribological properties of graphite nanosheets as oil additive. Wear 261(2):140–144
280. Alberts M, Kalaitzidou K, Melkote S (2009) An investigation of graphite nanoplatelets as lubricant in grinding. Int J Mach Tools Manuf 49(12–13):966–970
281. Kumar A, Shrama AK, Gupta TVK, Katiyar JK (2022) Influence of hexagonal boron nitride additive nanocutting fluid on the machining of AA6061-T6 alloy using minimum quality lubrication. Proceedings of the Institution of Mechanical Engineers Part E-Journal of Process Mechanical Engineering. 09544089221110980
282. Najiha MS, Rahman MM, Kadirgama K (2016) Performance of water-based TiO2 nanofluid during the minimum quantity lubrication machining of aluminium alloy, AA6061-T6. J Clean Prod 135:1623–1636
283. Uysal A (2018) Effects of nano graphene particles on surface roughness and cutting temperature during MQL milling of AISI 430 stainless steel. Materials Testing 60(5):533–537
284. Uysal A (2017) Surface roughness in nanofluid minimum quantity lubrication milling of AISI 430 ferritic stainless steel. J Test Eval 45(3):933–939
285. Uysal A (2016) Investigation of flank wear in MQL milling of ferritic stainless steel by using nano graphene reinforced vegetable cutting fluid. Ind Lubr Tribol 68(4):446–451
286. Singh P, Dureja JS, Singh H, Bhatti MS (2019) Performance evaluation of coated carbide tool during face milling of AISI 304 under different cutting environments. Mater Res Express 6(5):056546
287. Duc TM, Tuan NM, Long TT, Ngoc TB (2022) Machining feasibility and Sustainability study associated with air pressure, air flow rate, and nanoparticle concentration in Nanofluid minimum quantity lubrication-assisted hard milling process of 60Si2Mn steel. Proc Inst Mech Eng Part C-J Mech Eng Sci 236(23):11256–11269
288. Dong PQ, Duc TM, Long TT (2019) Performance evaluation of MQCL hard milling of SKD 11 tool steel using MoS2 nanofluid. Metals 9(6):658
289. Vu NC, Dang XP, Huang SC (2021) Multi-objective optimization of hard milling process of AISI H13 in terms of productivity, quality, and cutting energy under nanofluid minimum quantity lubrication condition. Meas Control 54(5–6):820–834

290. Khan AM, Jamil M, UlHaq A, Hussain S, Meng LH, He N (2019) Sustainable machining. Modeling and optimization of temperature and surface roughness in the milling of AISI D2 steel. Ind Lubr Tribol 71(2):267–277
291. Barewar SD, Kotwani A, Chougule SS, Unune DR (2021) Investigating a novel Ag/ZnO based hybrid nanofluid for sustainable machining of inconel 718 under nanofluid based minimum quantity lubrication. J Manuf Process 66:313–324
292. Hsiao TC, Vu NC, Tsai MC, Dang XP, Huang SC (2021) Modeling and optimization of machining parameters in milling of INCONEL-800 super alloy considering energy, productivity, and quality using nanoparticle suspended lubrication. Meas Control 54(5–6):880–894
293. Sirin S, Sarikaya M, Yildirim CV, Kivak T (2021) Machinability performance of nickel alloy X-750 with SiAlON ceramic cutting tool under dry, MQL and hBN mixed nanofluid-MQL. Tribol Int 153:106673
294. Nithiyanandam M, Rahamathullah I, Raj RA (2022) Optimization of process parameters in micro milling of Ti4Al4Mo2Sn using nano Al2O3 additives based minimum quantity cooling lubrication. Bull Chem Soc Ethiop 36(2):339–351
295. Edelbi A, Kumar R, Sahoo AK, Pandey A (2022) Comparative machining performance investigation of dual-nozzle MQL-assisted ZnO and Al2O3 nanofluids in face milling of Ti-3Al-2.5V alloys. Arab J Sci Eng. https://doi.org/10.1007/s13369-13022-07072-13361
296. Kim WY, Senguttuvan S, Kim SH, Lee SW, Kim SM (2021) Numerical study of flow and thermal characteristics in titanium alloy milling with hybrid nanofluid minimum quantity lubrication and cryogenic nitrogen cooling. Int J Heat Mass Transf 170:121005
297. LI CH, Jia DZ, Wang S, Zhang Q (2013) Magnetic nanoparticle jet flow and magnetic force working table coupling oil film forming process and device. The People's Republic of China: CN103192323, 2013–07–10
298. LI CH, Li BK, Wang YG, Yang M, Zhang YB (2018) Minimal quantity lubrication grinding device integrating nanofluid electrostatic atomization with electrocaloric heat pipe. United States of America: US9925638, 2018–03–27
299. Liu GT, LI CH, Zhai MG, Cao HJ, Zhang YB, Yang M, Zhang XP, Wang YG, Zhang NQ (2017) Supersonic flow nozzle vortex tube refrigerating and nanofluid minimum quantity lubrication coupling supply system. The People's Republic of China: CN106737203, 2017–05–31
300. Liu GT, LI CH, Cao HJ, Zhang YB, Yang M, Zhang XP, Zhang NQ, Wu QD (2017) Expansion machine refrigeration subcooling and nano particle jet flow minimal quantity lubrication supply system. The People's Republic of China: CN106584279, 2017–04–26
301. Gao T, Zhang XP, Li CH, Zhang YB, Yang M, Jia DZ, Ji HJ, Zhao YJ, Li RZ, Yao P, Zhu LD (2020) Surface morphology evaluation of multi-angle 2D ultrasonic vibration integrated with nanofluid minimum quantity lubrication grinding. J Manuf Process 51:44–61
302. Shi CF, Li X, Chen ZT (2014) Design and experimental study of a micro-groove grinding wheel with spray cooling effect. Chin J Aeronaut 27(2):407–412
303. Gretler M, Peiffer K (2008) Process for monitoring the setting of the coolant nozzle of a grinding machine. USA: US7452261, 2008–11–18
304. Stachurski W, Sawicki J, Krupanek K, Nadolny K (2021) Application of numerical simulation to determine ability of air used in MQL method to clean grinding wheel active surface during sharpening of hob cutters. Int J Pr Eng Man-GT 8(4):1095–1112
305. Zhang YB, Li CH, Zhang Q, Jia DZ, Wang S, Zhang DK, Mao C (2016) Improvement of useful flow rate of grinding fluid with simulation schemes. Int J Adv Manuf Technol 84(9–12):2113–2126
306. Huang B, Zhang Y, Wang X, Chen Y, Cao H, Liu B, Nie X, Li C (2021) Experimental evaluation of wear Mechanism and grinding performance of SG wheel in machining nickel-based alloy GH4169. Surf Technol 50(12):62–70
307. Shi Z, Guo S, Liu H, Li C, Zhang Y, Yang M, Chen Y, Liu B, Zhou Z, Nie X (2021) Experimental evaluation of minimum quantity lubrication of biological lubricant on grinding properties of GH4169 nickel-base alloy. Surf Technol 50(12):71–84
308. Gao T, Li C, Zhang Y, Yang M, Cao H, Wang D, Liu X, Zhou Z, Liu B (2022) Mechanical behavior of material removal and predictive force model for CFRP grinding using nano reinforced biological lubricant. J Mech Eng. http://kns.cnki.net/kcms/detail/11.2187.TH.20220927.20220939.20220004.html. Accessed 10 Oct 2022
309. Li BK, Dai CW, Ding WF, Yang CY, Li CH, Kulik O, Shumyacher V (2021) Prediction on grinding force during grinding powder metallurgy nickel-based superalloy FGH96 with electroplated CBN abrasive wheel. Chin J Aeronaut 34(8):65–74
310. Wang YG, Li CH, Zhang YB, Yang M, Li BK, Dong L, Wang J (2018) Processing Characteristics of vegetable oil-based nanofluid MQL for grinding different workpiece materials. Int J Pr Eng Man-GT 5(2):327–339
311. Ni J, Yang YF, Wu C (2019) Assessment of water-based fluids with additives in grinding disc cutting process. J Clean Prod 212:593–601
312. Lee PH, Lee SW, Lim SH, Lee SH, Ko HS, Shin SW (2015) A study on thermal characteristics of micro-scale grinding process using nanofluid minimum quantity lubrication (MQL). Int J Precis Eng Man 16(9):1899–1909
313. Molaie MM, Akbari J, Movahhedy MR (2016) Ultrasonic assisted grinding process with minimum quantity lubrication using oil-based nanofluids. J Clean Prod 129:212–222
314. Wang YG, Li CH, Zhang YB, Yang M, Zhang XP, Zhang NQ, Dai JJ (2017) Experimental evaluation on tribological performance of the wheel/workpiece interface in minimum quantity lubrication grinding with different concentrations of Al2O3 nanofluids. J Clean Prod 142:3571–3583
315. Esmaeili H, Adibi H, Rizvi R, Rezaei SM (2022) Coupled thermo-mechanical analysis and optimization of the grinding process for Inconel 718 superalloy using single grit approach. Tribol Int 171:107530
316. Liu GT, Li CH, Zhang YB, Yang M, Jia DZ, Zhang XP, Guo SM, Li RZ, Zhai H (2018) Process parameter optimization and experimental evaluation for nanofluid MQL in grinding Ti-6Al-4V based on grey relational analysis. Mater Manuf Process 33(9):950–963
317. Zhang JC, Li CH, Zhang YB, Yang M, Jia DZ, Liu GT, Hou YL, Li RZ, Zhang NQ, Wu QD, Cao HJ (2018) Experimental assessment of an environmentally friendly grinding process using nanofluid minimum quantity lubrication with cryogenic air. J Clean Prod 193:236–248
318. Setti D, Sinha MK, Ghosh S, Rao PV (2015) Performance evaluation of Ti-6Al-4V grinding using chip formation and coefficient of friction under the influence of nanofluids. Int J Mach Tools Manuf 88:237–248
319. Ibrahim AMM, Li W, Xiao H, Zeng ZX, Ren YH, Alsoufi MS (2020) Energy conservation and environmental sustainability during grinding operation of Ti-6Al-4V alloys via eco-friendly oil/graphene nano additive and Minimum quantity lubrication. Tribol Int 150:106387
320. Qu SS, Gong YD, Yang YY, Wang WW, Liang CY, Han B (2020) An investigation of carbon nanofluid minimum quantity

lubrication for grinding unidirectional carbon fibre-reinforced ceramic matrix composites. J Clean Prod 249:119353
321. Nandakumar A, Rajmohan T, Vijayabhaskar S (2019) Experimental evaluation of the lubrication performance in MQL grinding of nano SiC reinforced Al matrix composites. SILICON 11(6):2987–2999
322. Qu SS, Yao P, Gong YD, Chu DK, Yang YY, Li CW, Wang ZL, Zhang XP, Hou Y (2022) Environmentally friendly grinding of C/SiCs using carbon nanofluid minimum quantity lubrication technology. J Clean Prod 366:132898
323. Gao T, Li CH, Jia DZ, Zhang YB, Yang M, Wang XM, Cao HJ, Li RZ, Ali HM, Xu XF (2020) Surface morphology assessment of CFRP transverse grinding using CNT nanofluid minimum quantity lubrication. J Clean Prod 277:123328
324. Dambatta YS, Sayuti M, Sarhan AAD, Hamdi M, Manladad SM, Reddy M (2019) Tribological performance of SiO2-based nanofluids in minimum quantity lubrication grinding of Si3N4 ceramic. J Manuf Process 41:135–147
325. Yang M, Li CH, Zhang YB, Jia DZ, Zhang XP, Hou YL, Li RZ, Wang J (2017) Maximum undeformed equivalent chip thickness for ductile-brittle transition of zirconia ceramics under different lubrication conditions. Int J Mach Tools Manuf 122:55–65
326. Choudhary A, Naskar A, Paul S (2018) An investigation on application of nano-fluids in high speed grinding of sintered alumina. J Manuf Process 35:624–633
327. Paul S, Ghosh A (2019) Grinding of WC-Co cermets using hexagonal boron nitride nano-aerosol. Int J Refract Met H 78:264–272
328. Dambatta YS, Sarhan AAD, Sayuti MB, Bin Abd Shukor MH (2019) Fuzzy logic method to investigate grinding of alumina ceramic using minimum quantity lubrication. Int J Appl Ceram Technol 16(4):1668–1683
329. Sui MH, Li CH, Wu WT, Yang M, Ali HM, Zhang YB, Jia DZ, Hou YL, Li RZ, Cao HJ (2021) Temperature of grinding carbide with castor oil-based MoS2 nanofluid minimum quantity lubrication. J Therm Sci Eng Appl 13(5):051001
330. Hosseini SF, Emami M, Sadeghi MH (2018) An experimental investigation on the effects of minimum quantity nano lubricant application in grinding process of Tungsten carbide. J Manuf Process 35:244–253